

Source and magmatic evolution of the Neapolitan
volcanoes through time (Southern Italy)

Dissertation

submitted to

the Mathematic-Scientific Faculties
of the Georg-August-University Göttingen

in partial fulfillment of the requirements

for the doctoral degree (Dr. rer. nat.)

according to the doctoral program

of the Georg-August University School of Science (GAUSS)

presented by

Raffaella Silvia Iovine

from Naples, Italy

Göttingen 2017



Thesis committee:

Supervisor:

Prof. Dr. Gerhard Wörner (GZG, Dep. Geochemistry)

Co-supervisors:

Prof. Dr. Massimo D'Antonio (UNINA, Dep. Geochemistry)

Prof. Dr. Andreas Pack (GZG, Dep. Isotope Geology)

Examination committee:

Prof. Dr. Gerhard Wörner (GZG, Dep. Geochemistry)

Prof. Dr. Massimo D'Antonio (UNINA, Dep. Geochemistry)

Prof. Dr. Andreas Pack (GZG, Dep. Isotope Geology)

Prof. Dr. Sharon Webb (GZG, Dep. Mineralogy)

Prof. Dr. Matthias Willbold (GZG, Dep. Isotope Geology)

Dr. Sara Fanara (GZG, Dep. Mineralogy)

Day of defense:

9 February 2018

Contents

Preface	i
Acknowledgments	ii
Chapter 1 Introduction	1
1.1 Scope and structure of the thesis	1
1.2 Studied volcanic area	3
1.3 Research activity	6
1.4 Author contributions	8
1.5 References	12
Chapter 2 Source and magmatic evolution inferred from geochemical and Sr-O-isotope data on hybrid lavas of Arso, the last eruption at Ischia island (Italy; 1302 AD)	17
Abstract	17
1. Introduction	17
1.1 Geological setting and petrography of Ischia lavas	19
1.1.1 Volcanic history and rocks composition	19
1.1.2 The historic 1302 Arso eruption	19
1.2 Sampling and analytical methods	19
2. Results	21
2.1 Petrography	21
2.2 Mineral chemistry	21
2.3 Major and trace elements composition	22
2.4 $^{87}\text{Sr}/^{86}\text{Sr}$ and $\delta^{18}\text{O}$ isotope data	23
3. Discussion	23
3.1 Mineralogical and isotopic disequilibrium	23
3.2 Fractional crystallization	24
3.3 Mixing processes	25
3.4 Source enrichment and crustal contamination	26
3.5 Implications for the shallow magmatic plumbing system below Ischia	27
4. Conclusions	29
Acknowledgments	29
Appendix A. Supplementary data	29
References	29

Chapter 3 Coupled $\delta^{18}\text{O}$ - $\delta^{17}\text{O}$ and $^{87}\text{Sr}/^{86}\text{Sr}$ isotope compositions suggest a radiogenic and ^{18}O -enriched magma source for Neapolitan volcanoes (Southern Italy) **32**

Abstract	32
1. Introduction	32
2. Geological setting and volcanic history	34
3. Basement underlying the Neapolitan Area	37
4. Samples	39
5. Analytical methods	40
6. Results	42
6.1 $^{87}\text{Sr}/^{86}\text{Sr}$ and $\delta^{18}\text{O}$ isotope data	42
6.2 $\Delta^{17}\text{O}$ variations	44
7. Discussion	45
7.1 Assimilation of silicic Hercynian crust	48
7.2 Assimilation of altered CF pyroclastic rock	50
7.3 Assimilation of Mesozoic carbonate rocks	50
7.4 Source contamination by subducted components	51
7.5 A comparison with Sr-O-isotope relations in magmas from subduction zones worldwide	54
8. Conclusions	55
Acknowledgements	56
References	56

Chapter 4 Timescales of magmatic processes prior to the ~4.7 ka Agnano-Monte Spina eruption (Campi Flegrei caldera, Southern Italy) based on diffusion chronometry from sanidine phenocrysts **65**

Abstract	65
Electronic supplementary material	65
Introduction	65
Geology and eruptive products	67
Volcanic history and petrology	67
The Agnano-Monte Spina eruption	68
Samples and methods	68
Analytical methods	68
Diffusion modeling and parameters	70
Results	71
Composition of the analyzed sanidine phenocrysts	71
Temperature constraints	71
Diffusion times	73
Discussion	73

Conclusions	77
Acknowledgments	77
References	77
Chapter 5 Conclusions	80
5.1 Introduction	80
5.2 Findings	81
5.2.1 Ischia plumbing system	81
5.2.2 Neapolitan magmatic system	81
5.2.3 Magma residence times from diffusion chronometry	82
5.3 Outlook	83
5.4 References	83
Appendix A: Curriculum vitae	xiv
Appendix B: Publications	xvi
Appendix C: Supplementary material	xix

Preface

The dissertation presented here was carried out through an international collaboration between the Department of Geochemistry, University of Göttingen (Göttingen), the Dipartimento di Scienze della Terra, Università di Napoli Federico II (Italy) and Istituto Nazionale di Geofisica e Vulcanologia sezione di Napoli Osservatorio Vesuviano, Naples, Italy. Researchers mostly involved in the collaboration were Prof. Dr. Gerhard Wörner from Göttingen and Prof. Dr. Massimo D'Antonio, Prof. Dr. Lucia Civetta, Prof. Dr. Giovanni Orsi, Dr. Ilenia Arienzo, Dr. Fabio Carmine Mazzeo, Dr. Lorenzo Fedele from Naples. The project start was delayed significantly because the initial project was aimed at analyzing stratigraphically controlled samples from the “ICDP Campi Flegrei (Southern Italy)” drill core, but, for various reasons this drilling project did not start by early 2013 and samples were (and are still) not available. After significant delay, and the written agreement by DFG accepting the changes in the project working plan, the project finally started on 01.01.2014 employing myself from Naples as PhD student in Göttingen, co-supervised by the Italian colleagues. Through these contacts a large set of samples were made available to characterize magma batches and their evolution throughout the entire history of the Campi Flegrei. DFG project (Wo 362/42-1) funded to G.W. was linked to the projects “V2 Precursori di Eruzioni funded to M.D. by the Dipartimento per la Protezione Civile (DPC) – Istituto Nazionale di Geofisica e Vulcanologia (2013–2015), DAAD-MIUR Joint Mobility Program no. 57266092 funded to G.W. and M.D., Ricerca PRIN-COFIN 2008 grant (L.C.), Project V3_3/03 “V3_3_Ischia” 2004–2006 grants (M.D. and G.O.) funded by the Italian DPC and Ricerca Dipartimentale 2016, Dipartimento di Scienze della Terra, dell’Ambiente e delle Risorse, University Federico II, Naples, Italy and therefore was possible to extent our study to the Neapolitan volcanic area including also Procida, Ischia and Somma-Vesuvius samples.

Keywords

Neapolitan Volcanoes; Radiogenic and stable isotopes; $\Delta^{17}\text{O}$ variations; Mantle enrichment; crustal assimilation; Zoned sanidine phenocrysts; Timescales; Diffusion chronometry

Acknowledgments

Thank you so much to everyone who has helped me along my student journey. So many people have been so kind. There are far too many to name but there are some people who I would like to especially thank.

Firstly, I would like to express my sincere gratitude to my supervisor Prof. Gerhard Wörner for raising the funding (DFG project WO 362/42-1) and give me the possibility to work in his group. His patience, encouragement, and immense knowledge were key motivations throughout my PhD; his support helped me in all the time of research and in writing the papers.

My sincere thanks also goes to my co-supervisor Prof. Massimo D'Antonio, for collaboration with the Geoscience Center Göttingen (V2 Precursori di Eruzioni, DAAD-MIUR Joint Mobility Program no. 57266092), for his continuous support during my PhD, availability and constructive suggestions, which were determinant for the work presented in this thesis.

Then, I would like to thank the various funding organizations for giving me the possibility to extend my original topic.

Prof. Andreas Pack is thanked for co-supervising my work and for providing me the possibility to work in the stable isotope lab.

I am grateful to Prof. Lucia Civetta for giving me the chance to come to Germany.

A heartfelt thanks to Dr. Ilenia Arienzo always ready to help for any difficulty with professionalism and affection.

There are not enough words to explain my gratitude to Dr. Fabio Carmine Mazzeo for his patience in supporting me with invaluable suggestions and advice.

I am indebted to all the co-authors of the paper for all the fruitful discussions and for find always time to meet me every time I was going to Naples.

Thank you very much to Dr. Sara Fanara always ready to help and encourage me with affection and generosity.

Dr. Andreas Kronz has been a valuable help during electron microprobe measurements and associated data evaluation. Dr. Klaus Simon is thanked for his helpful and kind support with the ICPMS and related data reduction. Dr. Gerald Hartmann is thanked for conducting TIMS measurements.

Others thanks are to extend to all those who have helped me indirectly: thanks to all friends and colleagues always presents and who have always believed in me.

A special thank goes to my husband Marco who always believed in me (even more than myself); he has suffered my innumerable crises, looking for any manner to make me smile, and especially thanks for coming to Germany with me. At the beginning it was really hard but we made it!! Thanks to my brother Sabatino who for me, many times, had to renounce to his habits..! Thanks little brother.

Many thanks also go to my parents in laws for their love, and for having always encouraged and supported me, and to my sister in law Martina always ready to help me.

Last but certainly not least, I thank my parents. They have always left me the freedom to follow my dreams. They have always believed in me, I would not be here and be what I am without them.

Thanks you all!!!Grazie a tutti!!

1 Introduction

Volcanoes, like earthquakes, are natural phenomena of great destructive potential, which in densely populated areas pose a high risk and affect land use management and urban development. This issue has caused a continuously growing interest in unraveling the processes that trigger eruptions and control eruptive dynamics. This is particularly important for volcanic hazard assessment, especially in those areas where vulnerability has increased through time as a consequence of rapid population expansion. Among them the Neapolitan area (Campania, Southern Italy) laying between two active volcanoes: Vesuvius on the east and Phlegrean Volcanic District (Campi Flegrei, Ischia and Procida islands) on the west. Due to its explosive character, high probability of future eruptions and due to the large population (more than 2.5 million people), the risk and vulnerability from volcanic eruptions in this area are among the highest on Earth. For these reasons, the volcanological history as well as the textural, chemical and physical characteristics of the erupted products have been a matter of extensive scientific studies in the past decades. The understanding of present unrest episodes (gas emissions, seismicity, ground deformation) require the knowledge of past pre-eruptive magmatic processes. In particular the role, mechanisms, and timing of open-system processes (e.g., crustal contamination, magma chamber recharge, volatile exsolution, and magma mingling/mixing) in the magmatic system feeding an active volcano may provide important contributions for volcanic hazards assessment and related risk mitigation. One of the most relevant strategies for the society is the development of an emergency plan that is periodically revised and that includes, prior to an eruption, a massive evacuation of the area that is likely to be affected by pyroclastic flows, lahars, and heavy ash falls (the so-called Red Zone). Thus, a key scientific ingredient for an evacuation to be effective and successful is a reliable forecast of the time evolution of the reactivation of volcanic activity in a so hazardous area such as the Neapolitan one.

1.1 Scope and structure of the thesis

This dissertation is a compilation of two publications and one submitted manuscript, and is addressed to give a contribution in understanding the source(s) and processes operating during the rise and/or stagnation of magmas in the Neapolitan area and their timescales, which are of critical importance for the interpretation of observed variations in the dynamics of the volcanoes. In order to assess these issues, results are combined from 1) bulk and mineral chemistry 2) stable as well as

radiogenic isotopes and 3) Ba diffusion (using diffusion chronometry) in zoned sanidine phenocrysts, by using several analytical and micro-analytical methodologies.

The results of the PhD program have been partially published in three different articles. Each study is here presented as one of the three different chapters 2-4.

In the second chapter I present a petrochemical study of whole rock and separated mineral samples from volcanic products of the 1302 A.D. Arso eruption, at Ischia volcanic island (Gulf of Naples, Southern Italy) to investigate magmatic plumbing system beneath the island and associated magmatic processes. The paper combines geochemical and both radiogenic $^{87}\text{Sr}/^{86}\text{Sr}$ and stable $^{18}\text{O}/^{16}\text{O}$ isotopes to distinguish variable magma sources from assimilation processes as a cause for enriched or crustal signatures in Ischia magmas.

The third chapter follows the idea of the previous one in terms of combining radiogenic and stable isotopes but the aim is to improve our knowledge on the magmatic evolution in the Neapolitan area. The temporal evolution of the system is particular important to assess the present and future changes in the magmatic regime and can only be addressed by the study of a complete sequence of volcanic deposits from its earliest activity to the most recent eruptions. The work introduces triple oxygen isotope studies ($\Delta^{17}\text{O}$), which including the use of both $^{18}\text{O}/^{16}\text{O}$ and $^{17}\text{O}/^{16}\text{O}$ ratios, represent a new way to provide another handle on the long-existing questions related to the sources of volcanic systems, and therefore for the first time, may shed light on the nature of the contaminants (e.g., carbonate assimilation) for the Neapolitan area.

The fourth chapter focuses on timescales of magma mobilization prior to explosive volcanic events at Campi Flegrei caldera and in particular diffusion chronometry has been applied for the first time to sanidine crystals from samples of the ~4.7 ka Agnano-Monte Spina eruption, focusing on the last resorption and crystallization event prior to eruption.

Conclusions of this study and outlook are then presented in chapter five.

All major data, results and conclusions from the project are in the three papers. To avoid repetition, a detail chapter about analytical methods and parameters is omitted.

1.2 Studied volcanic area

The Mediterranean area is one of the most complicated geodynamic settings in the world (e.g., Mazzeo et al., 2014 and references therein) as clearly illustrated by the large variety of igneous rocks. Magmatism on the Italian peninsula is thought to be the result of a complex sequence of tectonic events associated with the collision between Africa and Europe along the southern margin of the Tethys Ocean and subduction of the Ionian oceanic lithosphere (Gvirtzman and Nur, 1999; Faccenna et al., 2007). In particular, the Campanian volcanic area (Southern Italy) has been a site of intense volcanism during Plio-Quaternary times which gave rise to many volcanic centres (Roccamonfina, Campi Flegrei, Ischia, Procida and Vesuvius). Over the past ~40 ka, volcanism has been localized mainly in the Mt. Somma Vesuvius complex and the Phlegrean Volcanic District, that includes the Campi Flegrei caldera as well as the Ischia and Procida islands in the Gulf of Naples (Orsi et al., 1996). All these volcanoes have shown moderately to strongly explosive activity in the recent past.

Procida is a small island situated between the mainland and the larger island of Ischia. Its volcanic history was revisited by De Astis et al. (2004) and Perrotta et al. (2010). They recognized five monogenetic volcanic edifices (Vivara, Terra Murata, Pozzo Vecchio, Fiumicello and Solchiaro; from the oldest to the youngest spanning from ~75 to ~22 ka), whose products are partially intercalated with those of Ischia and Campi Flegrei. Lava xenoliths of high-K basaltic composition occurring in the Solchiaro tuff represent the least-evolved rocks of the whole Phlegrean volcanic district (D'Antonio et al., 1999a). No further volcanic activity has been recorded on the island, where only little seismic activity occurs and no fumaroles are detected.

Ischia is a volcanic island located at the NW corner of the Gulf of Naples. The oldest dated rocks (150 ka old) are poorly exposed along the southern coast of the island. The volcanic products range in composition from shoshonite through latite, to trachyte and phonolite, the latter two being the most abundant. After a long quiescence, the Mt. Epomeo Green Tuff eruption (55 ka) generated the most voluminous pyroclastic deposit of the island, and the caldera collapse that caused the submersion of the central portion of the island (Vezzoli, 1988; Orsi et al., 1991). The last 55 ka of activity on Ischia have been divided into three magmatic cycles based on stratigraphical, geochronological, geochemical, and Sr isotopic data (Brown et al., 2014, and references therein). Deformation, shape, and uplift rate of the Mt. Epomeo resurgent block have affected the distribution of the younger volcanic vents, especially those active in the third and last cycle (10 ka–1302 A.D.), which cluster mostly along the eastern margin of the resurgent block

(Orsi et al., 1991). The Arso eruption, the most widespread effusive eruption on the island in recent times (1302 A.D.), and the Casamicciola earthquakes (1883 and 2017 A.D.) were the latest major volcanic and volcano-tectonic events on Ischia island.

Campi Flegrei is a volcanic field, site of highly explosive volcanism since at least 80 ka (Scarpati et al., 2013), fed by magmas overall ranging from shoshonite to (peralkaline) phonolite in composition. However, more than 99 vol. % of the products are trachytes and phonolites (e.g., D'Antonio et al., 1999b; Pappalardo et al., 1999; Melluso et al., 2012). Orsi et al. (1992, 1996) defined the Campi Flegrei caldera as a “nested” resurgent caldera formed as a consequence of two main collapse events related to the Campanian Ignimbrite (~39 ka; De Vivo et al., 2001; Fedele et al., 2008) and the Neapolitan Yellow Tuff (~15 ka; Deino et al., 2004) eruptions. The Campanian Ignimbrite eruption emplacing at least 300 km³ of trachytic to trachy-phonolitic magma (e.g., Fedele et al., 2007 and references therein), is the largest eruption of the Mediterranean area over the past 200 ka. During the past ~5 kyr, 22 moderately explosive eruptions occurred from vents mostly located in the NE part of the Neapolitan Yellow Tuff caldera: the Agnano-San Vito area (Di Vito et al., 1999, Orsi et al., 2004, 2009). The 12 km² Agnano-San Vito area, including the Astroni, Solfatara and Agnano craters, has been considered as the site of highest probability for future eruptions (Selva et al., 2012). Within this area, the Agnano-Monte Spina eruption (A-MS; ~4.7 ka; de Vita et al., 1999) had a magnitude of 5.3 and has been classified as the only high-magnitude event of the past ~5 kyr at Campi Flegrei caldera (Orsi et al., 2004, 2009). Distribution and thickness of the deposit allowed to estimate the total volume of ejected magma (~0.9 km³ dense rock equivalent; Orsi et al., 2009). The last eruption, the only historical one, occurred in 1538 A.D. after 3 ka of quiescence, and produced the Monte Nuovo tuff cone (Guidoboni and Ciuccarelli, 2011 and references therein). Recent unrest started in the 1950s with low-level seismicity, slow continuous uplift, and changes in the geochemical parameters of fumaroles and thermal springs (e.g., Saccorotti et al., 2007; Del Gaudio et al., 2010; Chiodini et al., 2015; D'Auria et al., 2015).

The *Somma Vesuvius* is a moderate size (1281 m asl) composite central volcano. It consists of an older volcano, Monte Somma, dissected by a summit caldera, and Mount Vesuvius, a recent cone developed within the oldest Somma caldera, and possibly started growing after the 79 A.D. “Pompeii” eruption. The caldera has a complex shape resulting from several collapses, each related to a high-explosive plinian eruption (Cioni et al., 1999). Although the oldest evidence for volcanic activity are lavas and tephra dated at ~370 ka, the present Somma-Vesuvius volcanic complex was

formed just after the emplacement of the Campanian ignimbrite (Brocchini et al., 2001; Di Renzo et al., 2007). The oldest period of activity (39-22 ka), which built up the Mt. Somma stratovolcano, was dominated by lava flow extrusions, prevailing explosive, generally low energy events (Santacroce, 1987; Cioni et al., 1999; Di Renzo et al., 2007; Santacroce et al., 2008). The earliest well-known Plinian eruption, Pomice di Base or Pomice Basali (22.03 ka; Santacroce et al., 2008), determined the beginning of both collapse of the Mt. Somma volcano and formation of the caldera, completed with the 79 A.D. eruption. In the last 22 ka, the Somma Vesuvius volcanic activity was characterized either by long quiescence periods (from few centuries to millennia), interrupted by Plinian or sub-Plinian eruptions, or by periods of open conduit volcanic activity. All plinian eruptions, characterized by vent opening, formed columns up to 30 km high and pyroclastic flow and/or surge deposits reaching distances of over 20 km from the vent (Cioni et al., 2003; Gurioli et al., 2010). These eruptions were accompanied by volcano-tectonic collapses, partial or complete emptying of the feeding, sometimes deeply recharged and zoned, magma chamber and magma/water interaction. Vesuvius main cone mostly formed during the last period of persistent low energy open-conduit activity between 1631 and 1944 (Arrighi et al., 2001). The total volume of erupted magmas has been estimated to be $\sim 300 \text{ km}^3$ (see in Piochi et al., 2005). During open conduit conditions deep, volatile-rich magma batches rise to less than 2 km of depth and mix with the crystal-rich, volatile-poor resident magma, triggering eruptions (Marianelli et al., 1999). Leucite is a typical mineral of Vesuvius; carbonate and skarn lithic clasts are common in the pyroclastic deposits. Since its last eruption in March 1944, Vesuvius has remained dormant and no actual “signs” suggest impending unrest. Volcanic rocks produced at the Mount Somma Vesuvius exhibit variable degrees of silica undersaturation and potassium enrichment and a large range of mineralogical, chemical and isotopic compositions (e.g., Piochi et al., 2006, Di Renzo et al., 2007 and references therein). Particularly, Mt. Somma Vesuvius rocks span from shoshonite to trachy-phonolite, partially overlapping chemical composition of rocks produced at the Campi Flegrei area, and from alkalibasalt to tephrite and phonolite.

Both Phlegrean volcanic district and Somma Vesuvius mafic magmas are generated from lithospheric mantle with MORB affinity and enriched by subduction-related fluids and melts (Mazzeo et al., 2014).

1.3 Research activity

This study provides a multidisciplinary approach, based on separated single minerals from Neapolitan volcanic products aimed to extend the present knowledge on the evolution of the Neapolitan magma source(s). Of particular interest is therefore to study volcanic deposits with tight stratigraphic and thus temporal control through time. In order to achieve the proposed goal, have been carried out the following research activities:

1) A detail geochemical and isotopic ($^{87}\text{Sr}/^{86}\text{Sr}$ and $^{18}\text{O}/^{16}\text{O}$) investigation on phenocrysts of the last eruption occurred on Ischia island (Arso eruption, 1302 A.D.) in order to better understand the geochemical features of the mantle source(s) and the shallow processes that affected the magmas feeding the volcanism at Ischia over the past millennia. Advances in laser fluorination mass spectrometry allow to directly link Sr- and O-isotope measurements for small samples with high analytical precision. Indeed, the combined use of radiogenic ($^{87}\text{Sr}/^{86}\text{Sr}$) and stable isotopes ($^{18}\text{O}/^{16}\text{O}$) allows to discriminate between mantle enrichment and crustal assimilation processes. This activity has provided an improved knowledge of the mixing processes (one of the main trigger mechanisms of Neapolitan eruption) acted in the Ischia plumbing system over the past 3 ka. Results of this study are shown in chapter 2.

2) Isotopic investigations ($^{87}\text{Sr}/^{86}\text{Sr}$ and $^{18}\text{O}/^{16}\text{O}$ - $^{17}\text{O}/^{16}\text{O}$) on handpicked minerals (feldspar, pyroxene, olivine) of pyroclastic products of the Neapolitan volcanic area, aimed at better defining the evolution processes of Neapolitan magmas in a worldwide context, and particularly role and identification of possible assimilants. In this study, have been selected K-trachybasalts of the Solchiaro eruption occurred at Procida island (ca. 20 ka), representing the least evolved and least contaminated magmatic component feeding the Phlegrean Volcanic District activity (D'Antonio et al., 2007), some relevant eruptions occurred at Ischia in the last 10 ka (Vateliero, Cava Nocelle, Arso and Zaro) and in order to cover the entire history of the Campi Flegrei and Somma Vesuvius volcanoes, samples have been selected from all the main periods of activity. Starting from the oldest period, samples from Campi Flegrei have been grouped as follow: 1. Pre Campanian Ignimbrite samples (>39 ka); 2. Campanian Ignimbrite samples (39 ka); 3. Post Campanian Ignimbrite/Pre Neapolitan Yellow Tuff samples (< 39 and > 15 ka); Neapolitan Yellow Tuff samples (15 ka); Post Neapolitan Yellow Tuff samples (<15 ka). For the Somma Vesuvius volcanic complex, samples from three main periods have been selected: 1. Pre caldera activity including lavas older than 22 ka; 2. Caldera-forming phase spanning from 22 ka to 79 A.D.; 3. Post

caldera activity for product younger than 79 A.D. From these samples, minerals have been separated and purified. No such data were available for Procida, Campi Flegrei and Somma Vesuvius samples. From Ischia's volcanic activity a first combination between $^{87}\text{Sr}/^{86}\text{Sr}$ and $^{18}\text{O}/^{16}\text{O}$ has been done by D'Antonio et al. (2013) for latitic magmas of the past 3 kyr (from the Molaro, Vateliero and Cava Nocelle centers). $\Delta^{17}\text{O}$ ratios ($\delta^{18}\text{O}-\delta^{17}\text{O}$) have been analyzed during my PhD for the first time on volcanic samples with the aim to identify with greater certainty the possible assimilants for the Neapolitan magmas. In particular, hoping to solve the fundamental question of whether or not shallow crustal Mesozoic carbonates play a major role in the assimilation process, important issue to better constrain the "shallow" magma reservoirs. Results are presented in chapter 3.

3) Analyses of phenocrysts zonation profiles to assess time scales of magmatic processes at the Campi Flegrei caldera, using Ba diffusion chronometry. Over the past decade, diffusion chronometry in zoned magmatic crystals has become an indispensable tool for recovering the timescales over which magmatic processes occur (e.g., Costa et al., 2008). This method has been successfully used to determine crystal residence timescales and investigate magma recharge rates in various volcanic settings, using Sr, Mg and Li diffusion in plagioclase, Ba diffusion in sanidine, Ni diffusion in olivine and Fe–Mg diffusion in olivine, clinopyroxene and orthopyroxene phenocrysts (e.g. Ginibre et al., 2002; Morgan et al., 2004). Time scales of petrogenetic processes (such as fractional crystallisation, crystal growth and crystal residence times) are critical and important mechanisms for understanding magma emplacement, remobilisation, transport and eruption at active volcanoes as Campi Flegrei are. To this purpose, samples representative of the main eruptive phases of the Agnano-Monte Spina eruption (4.7 ka) have been selected. Feldspar crystals were hand-picked and embedded into epoxy for combined energy-dispersive and wavelength-dispersive electron microprobe analyses. Sanidine crystals from whole rock thin sections were also selected for BaO core-to-rim compositional profiling, focusing on compositional breaks near the crystal rims that possibly record magma mixing processes just prior to eruption. This is the first study at assessing timescales of pre-eruptive processes through diffusion chronometry for the Campi Flegrei products and for the first time have been compared and discussed results from three different analytical techniques: (1) quantitative BaO point-measurements at 10 μm spatial resolution, (2) gray-scale swath profiles from accumulated BSE images and (3) Ba X-ray scans. Results are in chapter 4.

1.4 Author contributions

I collaborated with several researchers (working for institutions in Germany and in Italy). Affiliation of each of the collaborators is reported below. The results of the PhD program have been partially published in two different articles issued in international scientific journals with recognized impact factor. Other results produced during the PhD program have not yet been published in international scientific journal, but are currently submitted to *Lithos* or in preparation for other journals (see Appendix B). I include the two scientific published papers plus the submitted work.

Chapter 2: Source and magmatic evolution inferred from geochemical and Sr-O-isotope data on hybrid lavas of Arso, the last eruption at Ischia island (Italy; 1302 AD).

Raffaella Silvia Iovine^a, Fabio Carmine Mazzeo^b, Ilenia Arienzo^c, Massimo D'Antonio^b, Gerhard Wörner^a, Lucia Civetta^{b,d}, Zeudia Pastore^e, Giovanni Orsi^b

a Geowissenschaftliches Zentrum, Georg-August-Universität, Göttingen, Germany

b Dipartimento di Scienze della Terra, dell'Ambiente e delle Risorse, University Federico II of Naples, Italy

c Istituto Nazionale di Geofisica e Vulcanologia - sezione di Napoli Osservatorio Vesuviano, Naples, Italy

d Istituto Nazionale di Geofisica e Vulcanologia - sezione di Palermo, Italy

e Department of Geology and Mineral Resources Engineering, Norwegian University of Science and Technology, Trondheim, Norway

This chapter was published in the *Journal of Volcanology and Geothermal Research* in 2017.

This study focus on a detail geochemical and isotopic (⁸⁷Sr/⁸⁶Sr and ¹⁸O/¹⁶O) characterization of the last eruptive event occurred at the Ischia island drawing significant conclusions regarding the magmatic plumbing system beneath the island and associated magmatic processes. Chemistry of the mineral phases, and ⁸⁷Sr/⁸⁶Sr and ¹⁸O/¹⁶O values suggest the occurrence of mixing processes between chemically and isotopically distinct batches of magma, and of a possible entrapment of crystals grown during an earlier magmatic phase. Furthermore, magmas extruded during the Arso eruption were affected by crustal contamination as suggested by the detected high oxygen isotope ratios. Samples analyzed in this work were collected during my thesis in Naples and ⁸⁷Sr/⁸⁶Sr isotopic analyses were performed during the thesis although the majority of the interpretation

(geochemistry, O analyses and manuscript writing) has been conducted during my PhD in Göttingen.

In this manuscript, my contribution has been as first author because I executed the analytical work and the writing. All the other coauthors edited and improved the manuscript and in particular:

Dr. Fabio Carmine Mazzeo is the second author because he gave the main contribution to the formulation of the geochemical modeling, improvement of the figures, and he contributed to the interpretation and discussion of the results.

Dr. Ilenia Arienzo supervised and helped me to dissolve the samples for radiogenic analyses and to measure their isotopic composition by thermal ionization mass-spectrometry on a Thermo Finnigan Triton TI instrument and to interpret the results.

Profs. Drs. Massimo D'Antonio, Gerhard Wörner, Lucia Civetta, Giovanni Orsi improved and edited significantly the manuscript and they contributed to the interpretation and discussion of the results.

We were two students working at the Arso samples in Naples: myself and my colleague Zeudia Pastore. Therefore we shared some work.

Chapter 3: Coupled $\delta^{18}\text{O}$ - $\delta^{17}\text{O}$ and $^{87}\text{Sr}/^{86}\text{Sr}$ isotope compositions suggest a radiogenic and ^{18}O -enriched magma source for Neapolitan volcanoes (Southern Italy)

Raffaella Silvia Iovine^{(a,*), Fabio Carmine Mazzeo}^{(b), Gerhard Wörner}^{(a), Carlo Pelullo}^{(b), Gianluca Cirillo}^{(c), Ilenia Arienzo}^{(d), Andreas Pack}^{(a), Massimo D'Antonio}^(b,d)

a Geowissenschaftliches Zentrum, Georg-August-Universität, Göttingen, Germany

b Dipartimento di Scienze della Terra, dell'Ambiente e delle Risorse, University Federico II of Naples, Italy

c Istituto comprensivo Luigi Credaro Livigno Plazal dali Sckòla, 77 - 23030 Livigno, Italy

d Istituto Nazionale di Geofisica e Vulcanologia - sezione di Napoli Osservatorio Vesuviano, Naples, Italy

Chapter 3 is a scientific article currently submitted to *Lithos*.

The rationale of this work is to improve our knowledge on the magmatic evolution in the Neapolitan area by isotopic ($^{87}\text{Sr}/^{86}\text{Sr}$ and $\delta^{18}\text{O}$ - $\delta^{17}\text{O}$) data determined on separated minerals. In particular, to understand the Neapolitan volcanoes in a worldwide context, data have been

compared with published $\delta^{18}\text{O}$ -isotope data from subduction zones worldwide. Sr-O isotope values of Campi Flegrei and Mt. Somma Vesuvius magmas together form one vertical trend in Sr-O isotope space that deviates profoundly from all other subduction-related magmas. Magmatic oxygen isotope ratios recalculated from olivine and clinopyroxene phenocrysts that were in equilibrium with mantle-derived magmas have $\delta^{18}\text{O}$ up to almost 9 ‰ relative to SMOW, compositions that are very different from typical mantle sources. These results suggest that magmas from the Neapolitan volcanoes were derived from 1) a mantle source contaminated by no more than 10% of pelagic sediments and limestone that caused high $\delta^{18}\text{O}$ values but did not significantly affect the Sr-isotope composition, and 2) assimilation of Hercynian crust. Crustal assimilation by carbonates, can be excluded by the lack of a link between isotope data and major and trace element signatures. Assimilation by silicic rocks at deeper crustal levels remains a possibility but is difficult to reconcile with the mafic ($\text{Mg}\# = 70$) nature of host magmas of minerals analyzed. $\Delta^{17}\text{O}$ variations are in agreement with these conclusions.

In this manuscript I prepared the samples for analytical work, performed the oxygen analyses on Procida, partly Ischia and all Campi Flegrei samples and supervised two students from the University of Naples (Cirillo and Perullo) in acquiring oxygen data on minerals belonging to the Somma Vesuvius and Ischia (Zaro eruption) samples. I wrote the manuscript and carried out most of the Sr-isotope measurements.

Dr. Fabio Carmine Mazzeo provided me with some of the samples of this work and in particular those representative of possible contaminants, he improved figures and tables and moreover he has participated to the interpretation and discussion of the results.

Prof. Dr. Gerhard Wörner has contributed to the main idea and structure of this project. He helped in improving the manuscript and to interpret and discuss the results.

Dr. Ilenia Arienzo supervised and performed Sr measurements in Naples. She gave me samples belonging to her previous works and contributed in the interpretation and discussion of the results.

Gianluca Cirillo and Carlo Pelullo acquired the oxygen isotope data under my guidance on samples from Ischia and Somma Vesuvius. They performed Sr isotopic ratios of those samples.

Prof. Dr. Andreas Pack developed the methodology for triple oxygen measurements and helped to acquire the data.

Prof. Dr. Massimo D'Antonio contributed to the interpretation and discussion of the results of this study.

Chapter 4: Timescales of magmatic processes prior to the ~4.7 ka Agnano-Monte Spina eruption (Campi Flegrei caldera, Southern Italy) based on diffusion chronometry from sanidine phenocrysts.

Raffaella Silvia Iovine ^a, Lorenzo Fedele ^b, Fabio Carmine Mazzeo ^b, Ilenia Arienzo ^c, Andrea Cavallo ^d, Gerhard Wörner ^a, Giovanni Orsi ^b, Lucia Civetta ^{b,e}, Massimo D'Antonio ^{b,c}

^a Geowissenschaftliches Zentrum, Georg-August-Universität (GZG), Goldschmidtstrasse 1, 37077 Göttingen, Germany

^b Dipartimento di Scienze della Terra, dell'Ambiente e delle Risorse (DiSTAR), University of Naples Federico II, Largo S.Marcellino 10, 80138 Naples, Italy

^c Istituto Nazionale di Geofisica e Vulcanologia (INGV)–Sezione di Napoli Osservatorio Vesuviano, Via Diocleziano 328, 80124 Naples, Italy

^d Istituto Nazionale di Geofisica e Vulcanologia (INGV)–Sezione Roma1, Via di Vigna Murata 605, 00143 Rome, Italy

^e Istituto Nazionale di Geofisica e Vulcanologia (INGV)–Sezione di Palermo, Via U. La Malfa 153, 90146 Palermo, Italy

This chapter was published in the *Bulletin of Volcanology* in 2017.

This work is a first attempt at assessing timescales of pre-eruptive processes through Ba diffusion chronometry for alkali feldspar phenocrysts from the Agnano Monte Spina eruption occurred ~4.7 ka at the Campi Flegrei caldera. The acquired data suggested that the timescales estimated by diffusion chronology (mostly ≤ 60 years at 930°C) are similar to the inferred time intervals that occurred between eruptions, and thus, the diffusion timescales may represent the reactivation time of a magma that was residing in a shallow reservoir after the influx of a new magma batch that triggered the eruption. The paper compares different methodologies for diffusion time calculations based on quantitative analyses of Ba concentrations, gray-scale swath profiles, and X-ray scans.

In this manuscript, I prepared the mineral sections for the electron microprobe (EMP), I performed the analyses using the three different techniques mentioned above and I gave the main contribution to interpretation and diffusion modeling and wrote only some parts of the paper.

Dr. Lorenzo Fedele is a coauthor of this study because he provided the temperature constraints and he gave a contribution to the interpretation and discussion of the results.

Dr. Fabio Carmine Mazzeo helped me in extrapolating gray-scale swath profiles, in the preparation of the supplementary electronic material and in interpret the results.

Dr. Ilenia Arienzo provided the samples and helped for interpretation of the data.

Dr. Andrea Cavallo obtained additional data using the EMP in Rome.

Prof. Dr. Gerhard Wörner gave the main contribution on the interpretation, discussion and in rewriting the paper.

Profs. Drs. Giovanni Orsi and Lucia Civetta helped to interpret the data.

Prof. Dr. Massimo D'Antonio, the corresponding author of the paper wrote a first draft of the paper and consequently contributed to the interpretation and discussion of the results of this study.

1.5 References

Arrighi S, Principe C, Rosi M (2001) Violent Strombolian and subplinian eruptions at Vesuvius during post-1631 activity. *Bull Volcanol* 63: 126-150.

Brocchini D, Principe C, Castradori D, Laurenzi MA, Gorla L (2001) Quaternary evolution of the southern sector of the Campanian Plain and early Somma-Vesuvius activity: insights from the Trecase 1 well. *Mineral Petrol* 73: 67-91.

Brown RJ, Civetta L, Arienzo I, D'Antonio M, Moretti R, Orsi G, Tomlinson EL, Albert PG, Menzies MA (2014) Geochemical and isotopic insights into the assembly, evolution and disruption of a magmatic plumbing system before and after a cataclysmic caldera-collapse eruption at Ischia volcano (Italy) *Contrib Mineral Petrol* 168: 1-23.

Chiodini G, Vandemeulebrouck J, Caliro S, D'Auria L, De Martino P, Mangiacapra A, Petrillo Z (2015) Evidence of thermal-driven processes triggering the 2005–2014 unrest at Campi Flegrei caldera. *Earth Planet Sci Lett* 414: 58-67.

Cioni R, Santacroce R, Sbrana A (1999) Pyroclastic deposits as a guide for reconstructing the multi-stage evolution of the Somma-Vesuvius caldera. *Bull Volcanol* 60: 207-222.

Cioni R, Longo A, Macedonio G, Santacroce R, Sbrana A, Sulpizio R, Andronico D (2003) Assessing pyroclastic fall hazard through field data and numerical simulations: Example from Vesuvius. *J Geophys Res* 108(B2): 1-11. Doi:10.1029/2001JB000642.

Costa F, Dohmen R, Chakraborty C (2008) Time scales of magmatic processes from modeling the zoning patterns of crystals. *Rev Mineral Geochem* 69: 545–594.

D'Antonio M, Civetta L, Di Girolamo P (1999a) Mantle source heterogeneity in the Campanian region (south Italy) as inferred from geochemical and isotopic features of mafic volcanic rocks with shoshonitic affinity. *Mineral Petrol* 67: 163-192. Doi: 10.1007/BF01161520.

D'Antonio M, Civetta L, Orsi G, Pappalardo L, Piochi M, Carandente A, de Vita S, Di Vito M.A, Isaia R, Southon J (1999b) The present state of the magmatic system of the Campi Flegrei caldera based on the reconstruction of its behaviour in the past 12 ka. *J Volcanol Geotherm Res* 91: 247-268.

D'Antonio M, Tonarini S, Arienzo I, Civetta L, Di Renzo V (2007) Components and processes in the magma genesis of the Phlegrean Volcanic District, southern Italy. *Geol Soc Am* 418: 203–220.

D'Antonio M, Tonarini S, Arienzo I, Civetta L, Dallai L, Moretti R, Orsi G, Andria M, Trecalli A (2013) Mantle and crustal processes in the magmatism of the Campania region: inferences from mineralogy, geochemistry, and Sr–Nd–O isotopes of young hybrid volcanics of the Ischia island (South Italy). *Contrib Mineral Petrol* 165: 1173–1194.

D'Auria L, Pepe S, Castaldo R, Giudicepietro F, Macedonio G, Ricciolino P, Tizzani P, Casu F, Lanari R, Manzo M, Martini M, Sansosti E, Zinno I (2015) Magma injection beneath the urban area of Naples: a new mechanism for the 2012–2013 volcanic unrest at Campi Flegrei caldera. *Sci Rep* 5: 13100. DOI: 10.1038/srep13100.

De Astis G, Pappalardo L, Piochi M (2004) Procida volcanic history: new insights into the evolution of the Phlegrean Volcanic District (Campania region, Italy). *Bull Volcanol* 66: 622-641.

de Vita S, Orsi G, Civetta L, Carandente A, D'Antonio M, Deino A, di Cesare T, Di Vito, MA, Fisher RV, Isaia R, Marotta E, Necco A, Ort M, Pappalardo L, Piochi M, Southon J, (1999) The Agnano-Monte Spina eruption (4100 years BP) in the restless Campi Flegrei caldera (Italy). *J Volcanol Geotherm Res* 91: 269-301.

De Vivo B, Rolandi G, Gans PB, Calvert A, Bohrsen WA, Spera, FJ, Belkin, HE (2001) New constraints on the pyroclastic eruptive history of the Campanian volcanic Plain (Italy). *Mineral Petrol* 73: 47-65.

Deino A, Orsi G, de Vita, S, Piochi M (2004) The age of the Neapolitan Yellow Tuff caldera-forming eruption (Campi Flegrei caldera-Italy) assessed by $^{40}\text{Ar}/^{39}\text{Ar}$ dating method. *J Volcanol Geoth Res* 133: 157-170.

Del Gaudio C, Aquino I, Ricciardi GP, Ricco C, Scandone R (2010) Unrest episodes at Campi Flegrei: a reconstruction of vertical ground movements during 1905–2009. *J Volcanol Geotherm Res* 195: 48–56.

Di Renzo V, Di Vito MA, Arienzo I, Carandente A, Civetta L, D'Antonio M, Giordano F, Orsi G, Tonarini S (2007) Magmatic history of Somma-Vesuvius on the basis of new geochemical and isotopic data from a deep borehole (Camaldoli della Torre). *J Pet* 48: 753–784.

Di Vito MA, Isaia R, Orsi G, Southon J, de Vita S, D'Antonio M, Pappalardo L, Piochi M (1999) Volcanism and deformation in the past 12 ka at the Campi Flegrei caldera (Italy). *J Volcanol Geotherm Res* 91: 221–246.

Faccenna C, Funicello F, Civetta L, D'Antonio M, Moroni M, Piromallo C (2007) Slab distribution, mantle circulation, and the opening of the Tyrrhenian basin. In: Beccaluva, L., et al. (Eds.), *Cenozoic Volcanism in the Mediterranean Area. Geol Soc Am Spec Pap* 418: 153–169.

Fedele FG, Giaccio B, Isaia R, Orsi G, Carroll M, Scaillet, B (2007) The Campanian Ignimbrite Factor: Towards a Reappraisal of the Middle to Upper Palaeolithic “Transition”. In: J. Grattan and R. Torrence (Eds.), *Living Under the Shadow: The Cultural Impacts of Volcanic Eruptions, One World Archaeology Series. 53, Left Coast Press, Walnut Creek, CA: 19-41.*

Fedele L, Scarpati C, Lanphere M, Melluso L, Morra V, Perrotta A, Ricci G (2008) The Breccia Museo formation, Campi Flegrei, southern Italy: geochronology, chemostratigraphy and relationship with the Campanian Ignimbrite eruption. *Bull Volcanol* 70: 1189-1219.

Ginibre C, Kronz A, Wörner G (2002) High-resolution quantitative imaging of plagioclase composition using accumulated backscattered electron images: new constraints on oscillatory zoning. *Contrib Mineral Petrol* 142: 436–448.

Guidoboni E, Ciuccarelli C (2011) The Campi Flegrei caldera: historical revision and new data on seismic crises, bradyseisms, the Monte Nuovo eruption and ensuing earthquakes (twelfth century 1582 ad). *Bull Volcanol* 73: 655-677.

Gurioli L, Sulpizio R, Cioni R, Sbrana A, Santacroce R, Luperini W Andronico D (2010) Pyroclastic flow hazard assessment at Somma-Vesuvius based on the geological record. *Bull Volcanol* 72: 1021-1038.

Gvirtzman Z, Nur A (1999) The formation of Mount Etna as the consequence of slab rollback. *Nature* 401: 782–785.

Marianelli P, Metrich N, Sbrana A (1999), Shallow and deep reservoirs involved in magma supply of the 1944 eruption of Vesuvius, *Bull Volcanol* 61: 48-63.

- Mazzeo FC, D'Antonio M, Arienzo I, Aulinas M, Di Renzo V, Gimén D (2014) Subduction-related enrichment of the Neapolitan volcanoes (Southern Italy) mantle source: New constraints on the characteristics of the slab-derived components. *Chem Geol* 386: 165-183.
- Melluso L, de' Gennaro R, Fedele L, Franciosi L, Morra V (2012) Evidence of crystallization in residual, Cl-F-rich, agpaitic, trachyphonolitic magmas and primitive Mg-rich basalt-trachyphonolite interaction, in the lava domes of the Phlegrean Fields (Italy). *Geol Mag* 149: 532-550.
- Morgan DJ, Blake S, Rogers NW, DeVivo B, Rolandi G, Macdonald R Hawkesworth CJ (2004) Time scales of crystal residence and magma chamber volume from modelling of diffusion profiles in phenocrysts: Vesuvius 1944. *Earth Planet Sci Lett* 222: 933-946.
- Orsi G, Gallo G, Zanchi A (1991) Simple shearing block resurgence in caldera depressions. A model from Pantelleria and Ischia. *J Volcanol Geoth Res* 47: 1-11.
- Orsi G, D'Antonio M, de Vita S, Gallo G (1992) The Neapolitan Yellow Tuff, a large magnitude trachytic phreatoplinian eruption: eruptive dynamics, magma withdrawal and caldera collapse. *J Volcanol Geotherm Res* 53: 275-287.
- Orsi G, de Vita S, Di Vito M (1996) The restless, resurgent Campi Flegrei nested caldera (Italy): constraints on its evolution and configuration. *J Volcanol Geotherm Res* 74: 179-214.
- Orsi G, Di Vito MA, Isaia R (2004) Volcanic hazard assessment at the restless Campi Flegrei caldera. *Bull Volcanol* 66: 514-530. Doi: 10.1007/s00445-003-0336-4.
- Orsi G, Di Vito MA, Selva J, Marzocchi W (2009) Long-term forecast of eruption style and size at Campi Flegrei caldera (Italy). *Earth Planet Sci Lett* 287: 265-276.
- Pappalardo L, Civetta L, D'Antonio M, Deino A, Di Vito M, Orsi G, Carandente A, de Vita S, Isaia R, Piochi M (1999) Chemical and Sr-isotopic evolution of the Phlegrean magmatic system before the Campanian Ignimbrite and the Neapolitan Yellow Tuff eruptions. *J Volcanol Geoth Res* 91: 141-166.
- Perrotta A, Scarpati C, Luongo G, Morra V (2010) Stratigraphy and volcanological evolution of the southwestern sector of Campi Flegrei and Procida Island, Italy. *Geol Soc Am Spec Pap* 464: 171-191.
- Piochi M, Bruno PP, De Astis G (2005) Relative roles of rifting tectonics and magma uprising processes: inferences from geophysical, structural and geochemical data of the Neapolitan volcanic region (southern Italy). *G³* 6(7): 1-25. Doi:10.1029/2004GC000885.
- Piochi M, Ayuso RA, De Vivo B, Somma R (2006) Crustal contamination and crystal entrapment during evolution at Mt. Somma-Vesuvius volcano, Italy: geochemical and Sr isotopic evidence. *Lithos* 86: 303-329.

Saccorotti G, Petrosino S, Bianco F, Castellano M, Galluzzo D, La Rocca M, Del Pezzo E, Zaccarelli L, Cusano P (2007) Seismicity associated with the 2004-2006 renewed ground uplift at Campi Flegrei caldera, Italy. *Phys Earth Planet Inter* 165: 1-28.

Santacroce R ed (1987) Somma-Vesuvius. Somma-Vesuvius, *Quaderni de "La Ricerca Scientifica" CNR* Roma 114(8): 1-251.

Santacroce R, Cioni R, Marianelli P, Sbrana A, Sulpizio R, Zanchetta G, Donahue DJ, Joron JL (2008) Age and whole rock–glass compositions of proximal pyroclastics from the major explosive eruptions of Somma-Vesuvius: A review as a tool for distal tephrostratigraphy. *J Volcanol Geoth Res* 177: 1–18.

Scarpati C, Perrotta A, Lepore S, Calvert A (2013) Eruptive history of Neapolitan volcanoes: constraints from ^{40}Ar – ^{39}Ar dating. *Geol Mag* 150: 412-425.

Selva J, Orsi G, DiVito MA, Marzocchi W, Sandri L (2012) Probability hazard map for future vent opening at the Campi Flegrei caldera, Italy. *Bull Volcanol* 74: 497–510.

Vezzoli L (1988) Island of Ischia. *Quaderni de "La Ricerca Scientifica" CNR* Roma 10: 1-126.



Chapter 2: Source and magmatic evolution inferred from geochemical and Sr-O-isotope data on hybrid lavas of Arso, the last eruption at Ischia island (Italy; 1302 AD)

Raffaella Silvia Iovine ^{a,*}, Fabio Carmine Mazzeo ^b, Ilenia Arienzo ^c, Massimo D'Antonio ^b, Gerhard Wörner ^a, Lucia Civetta ^{b,d}, Zeudia Pastore ^e, Giovanni Orsi ^b

^a Geowissenschaftliches Zentrum, Georg-August-Universität, Göttingen, Germany

^b Dipartimento di Scienze della Terra, dell'Ambiente e delle Risorse, University Federico II of Naples, Italy

^c Istituto Nazionale di Geofisica e Vulcanologia - sezione di Napoli Osservatorio Vesuviano, Naples, Italy

^d Istituto Nazionale di Geofisica e Vulcanologia - sezione di Palermo, Italy

^e Department of Geology and Mineral Resources Engineering, Norwegian University of Science and Technology, Trondheim, Norway

ARTICLE INFO

Article history:

Received 15 April 2016

Received in revised form 22 July 2016

Accepted 4 August 2016

Available online 6 August 2016

Keywords:

Ischia island

Magmatic plumbing system

Radiogenic and stable isotopes

Mingling/mixing

Crustal contamination

ABSTRACT

Geochemical and isotopic ($^{87}\text{Sr}/^{86}\text{Sr}$ and $^{18}\text{O}/^{16}\text{O}$) data have been acquired on whole rock and separated mineral samples from volcanic products of the 1302 AD Arso eruption, Ischia volcanic island (Gulf of Naples, Southern Italy), to investigate magmatic processes. Our results highlight petrographic and isotopic disequilibria between phenocrysts and their host rocks. Similar disequilibria are observed also for more mafic volcanic rocks from Ischia and in the Phlegraean Volcanic District in general. Moreover, $^{87}\text{Sr}/^{86}\text{Sr}$ and $^{18}\text{O}/^{16}\text{O}$ values suggest mixing between chemically and isotopically distinct batches of magma, and crystals cargo from an earlier magmatic phase. The radiogenic Sr isotope composition suggests that the mantle source was enriched by subduction-derived sediments. Furthermore, magmas extruded during the Arso eruption were affected by crustal contamination as suggested by high oxygen isotope ratios. Assimilation and fractional crystallization modelling of the Sr-O isotope compositions indicates that not more than ~7% of granodioritic rocks from the continental crust have been assimilated by a mantle-derived mafic magma. Hence the recent volcanic activity of Ischia has been fed by distinct batches of magma, variably contaminated by continental crust, that mixed during their ascent towards the surface and remobilized phenocrysts left from earlier magmatic phases.

© 2016 Elsevier B.V. All rights reserved.

1. Introduction

Combined radiogenic and stable isotopes have proven to be an invaluable tool in igneous petrology and volcanology to understand magma sources and processes in open magma systems as well as different-scale processes such as mantle enrichment, crustal contamination, and magma mingling/mixing (e.g., James, 1981; Wörner et al., 1985; Taylor and Sheppard, 1986; Ellam and Harmon, 1990; Chalokwu et al., 1999; Wolff et al., 2000; Dallai et al., 2003; Bindeman et al., 2008; Lackey et al., 2008). Understanding past behavior of the magmatic system feeding an active volcano is crucial also for volcanic hazards assessment.

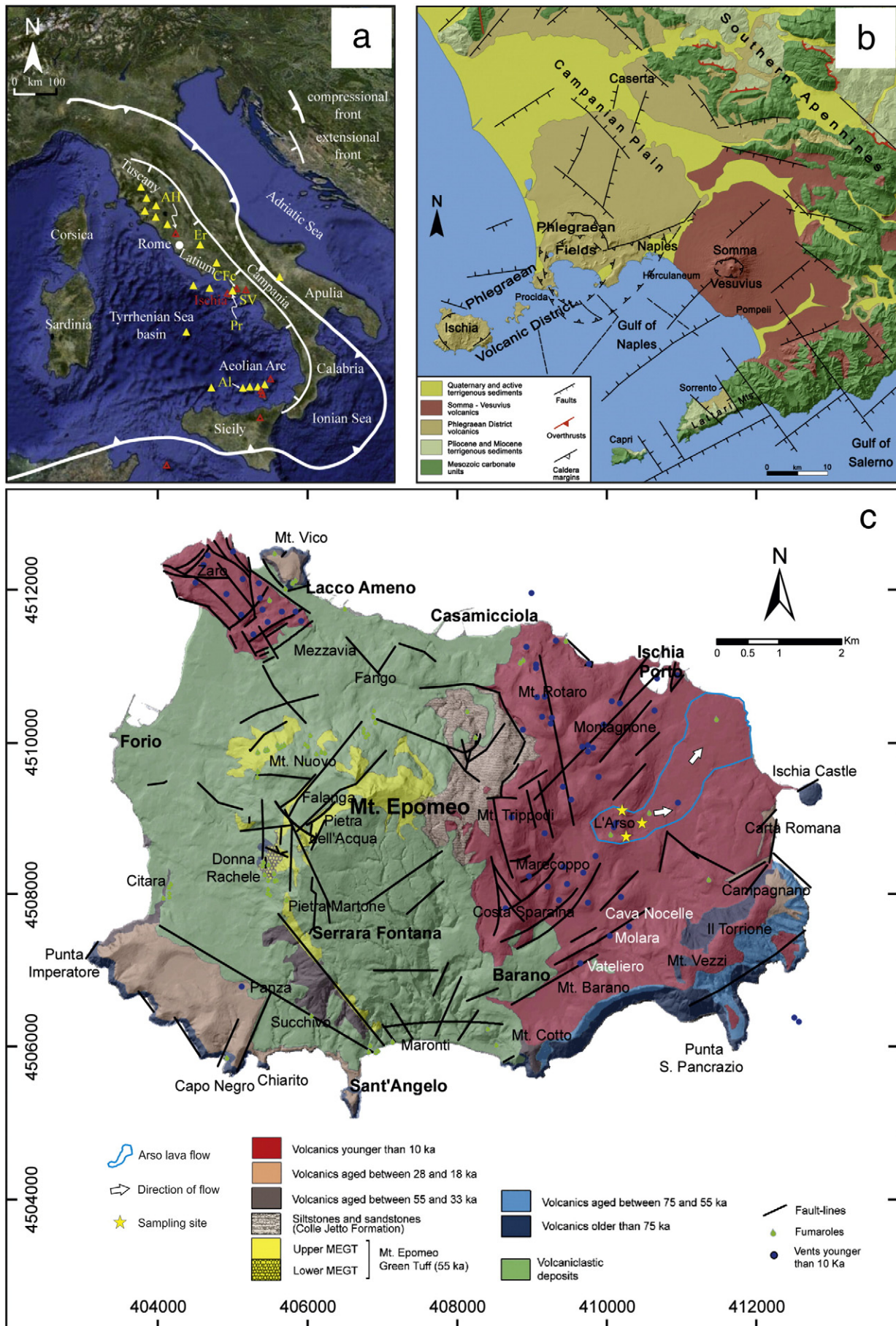
Ischia, an active volcanic island dominated by a resurgent caldera (Orsi et al., 1991) is located in the Gulf of Naples in South Italy, a densely populated area. Together with Campi Flegrei caldera (CFc) and Procida

island (Fig. 1b), Ischia is part of the Phlegraean Volcanic District (PVD; Orsi et al., 1996). Volcanic eruptions have occurred in historical times at both CFc and Ischia with the last events in 1538 AD (Mt. Nuovo eruption) and 1302 AD (Arso eruption), respectively. Because of steep volcano-tectonic flanks, coastal cliffs and intense hydrothermal activity and alteration, Ischia island is prone not only to hazards from renewal of volcanism, but also from gravitational instability (de Vita et al., 2006; Della Seta et al., 2012) and potential tsunamis (Zaniboni et al., 2013). The rationale of this work is to improve our knowledge of the most recent eruption on the island by collecting new geochemical data and putting them into the context of magma evolution in the area. Major, trace element and isotopic ($^{87}\text{Sr}/^{86}\text{Sr}$ and $\delta^{18}\text{O}$) data were determined on separated minerals and whole rocks. Our data are integrated with those of previous studies (Piochi et al., 1999; D'Antonio et al., 2013; Brown et al., 2014) for a better understanding of the geochemical features of the mantle source/s and the shallow processes that affected the magmas feeding the volcanism at Ischia over the past millennia. In particular, we assess the role of source enrichment and continental crustal assimilation processes on the basis of combined O- and Sr-isotope data.

* Corresponding author.

E-mail address: raffaella-silvia.iovine@geo.uni-goettingen.de (R.S. Iovine).

Chapter 2: Source and magmatic evolution inferred from geochemical and Sr-O-isotope data on hybrid lavas of Arso, the last eruption at Ischia island (Italy; 1302 AD)



1.1. Geological setting and petrography of Ischia lavas

Magmatism on the Italian peninsula is the result of the collision between Africa and Europe along the southern margin of the Tethys Ocean and related subduction of the Ionian oceanic lithosphere (Mazzeo et al., 2014 and references therein). Magma ascent from the mantle wedge through the upper crust and the emplacement of magma bodies at large (>8 km) and shallower depths is controlled by the intersection of NE-SW transverse and NW-SE normal regional fault systems (Fig. 1b; Acocella and Funicello, 2006; Moretti et al., 2013 and references therein). The NW-SE trending PVD is a zone of high heat flux (up to 200 mW m⁻²; Piochi et al., 2014) that reflects both the shallow depth of the mantle (around 25 km; Di Stefano et al., 2011) and eruption and related magma storage in the upper crust in the past millennia. Ischia island is the emerged part of a volcanic edifice that rises for over 1000 m from the sea floor in the NW corner of the Gulf of Naples, at a distance of about 30 km from the city of Naples. Roughly rectangular shaped, it measures approximately 9.5 km east to west and 6 km north to south, and has a surface area of ~57 km². Seismic, magnetic, and gravimetric anomalies correlate with the location of the eruptive vents and volcano-tectonic structures of the island (Paoletti et al., 2013; Capuano et al., 2015).

1.1.1. Volcanic history and rocks composition

The volcanic and magmatic history of Ischia (Fig. 1c) has been reconstructed on the basis of stratigraphical, geochronological and petrological data (e.g., Forcella et al., 1981, 1983; Poli et al., 1987, 1989; Rosi et al., 1988; Vezzoli, 1988; Crisci et al., 1989; Civetta et al., 1991; Di Girolamo et al., 1995; Piochi et al., 1999; Brown et al., 2008, 2014; Sbrana et al., 2009; Vezzoli et al., 2009; de Vita et al., 2010; D'Antonio et al., 2013; Moretti et al., 2013; Melluso et al., 2014). Subaerial rocks record volcanic activity that is dominated since 150 ka by the emplacement of compositionally homogeneous alkali-trachytic pyroclastic rocks (Poli et al., 1987, 1989; Vezzoli, 1988). Style, composition and character of (submarine) volcanism pre-dating 150 ka are unknown even though it represents a major portion of the erupted volume at Ischia. Between 150 and 75 ka, trachytic to phonolitic products erupted through vents on a roughly ellipsoidal alignment circumscribing the island. Between 75 and 55 ka, explosive eruptions emplaced a succession of trachyphonolitic pumice fall deposits, block-and-ash-flow deposits and ignimbrites (Brown et al., 2014, and references therein). The rocks are characterized by a wide range of ⁸⁷Sr/⁸⁶Sr but limited ¹⁴³Nd/¹⁴⁴Nd isotope ratios (ca. 0.70650–0.70680 and 0.51253–0.51255, respectively). After a long quiescence the Mt. Epomeo Green Tuff (MEGT) eruption (55 ka) generated the most voluminous pyroclastic deposit of the volcanic field and a caldera collapse that caused the submersion of the central portion of the island (Vezzoli, 1988; Orsi et al., 1991). This is suggested by the occurrence of secondary minerals formed by seawater alteration which gave the tuff its typical green color (Di Napoli et al., 2013, and references therein). After the MEGT event, until ca. 30 ka ago (first post-MEGT cycle), latitic to alkali-trachytic volcanic products characterized by a relatively narrow range of Sr isotopic composition (0.70675–0.70690; D'Antonio et al., 2007; Brown et al., 2014) were erupted. A second post-MEGT cycle (28–18 ka) began with the eruption of the Grotta di Terra shoshonitic center and the onset of resurgence through a simple-shearing mechanism (Orsi et al., 1991). During this cycle a series of alkali-trachytic pyroclastic deposits and small trachytic lava flows was emplaced, that show a gradual increase in Sr-isotope composition with time from ca. 0.70615 up to 0.70650 (Civetta et al.,

1991; D'Antonio et al., 2007). Deformation, shape, and uplift rate of the Mt. Epomeo resurgent block have affected the distribution of the younger volcanic vents, especially those active in the third and last cycle (10 ka–1302 AD) which all cluster along the eastern margin of the resurgent block (Orsi et al., 1991). Volcanism during this cycle of activity was mainly concentrated around 5 ka (de Vita et al., 2010) producing low-magnitude magmatic and phreatomagmatic explosions that generated sequences of scoria-fallout and ash-surge beds, intercalated with subordinate pumice-fallout deposits (de Vita et al., 2010). This last cycle of activity was fed by latitic to phonolitic magmas with a wide range of Sr-isotope compositions (ca. 0.70580–0.70700; D'Antonio et al., 2007, 2013). The alkali-trachytic lavas erupted around 10 ka BP are the least enriched in radiogenic Sr and significantly different from the products erupted at the end of the previous cycle. Petrographic, geochemical and Sr-Nd-O-isotopic characteristics of the latitic magmas of the past 3 kyr (from the Molara, Vateliero and Cava Nocelle centers; Fig. 1c) suggest mingling and mixing processes between magmas with distinct chemical and isotopic composition, and incorporation of crystals inherited from older magma pulses (e.g., Civetta et al., 1991; Di Girolamo et al., 1995; D'Antonio et al., 2013). In agreement with the mixing/mingling hypothesis, H₂O and CO₂ contents in olivine-hosted melt inclusions from the 3 ka latites record entrapment pressures corresponding to crystallization depths ranging from 3 to 18 km (Moretti et al., 2013). The Arso eruption (1302 AD) and the Casamicciola earthquake (1883 AD) were the latest major volcanic and volcano-tectonic events. Ongoing intense fumarolic emissions, sporadic seismicity and ground deformation are clear indicators of the persistent activity of the Ischia magmatic system.

1.1.2. The historic 1302 Arso eruption

Although there is a lot of uncertainty about the date of Arso eruption (Buchner, 1986 and Chiesa et al., 1986), the eruption probably began in January 1302 and lasted about two months. It is the most widespread effusive eruption on the island in recent times. The vent (Fig. 1c) is located at an altitude of about 150 m a.s.l. on the eastern side of Mt. Epomeo in an area characterized by NE-SW and NW-SE fault systems (Di Napoli et al., 2013 and references therein). According to Rittman and Gottini (1980), the eruption began with a phreatomagmatic phase followed by lava extrusion. The products of the initial explosive phase are black scoria of which there are rare and poorly preserved outcrops in the vent area. The lava flows, that reached the sea at Punta Molina (Fig. 1c), are 2.7 km long and 200 m to 1 km wide. They have a thickness of about 30–40 m in the distal part and 4–5 m in the proximal part, and cover an area of about 1.8 km² (Chiesa et al., 1986). The volume of extruded magma has been estimated to be about 0.03 km³ (Chiesa et al., 1986).

1.2. Sampling and analytical methods

Fresh lava and scoria samples (ARS1a lava, ARS4b scoria and ARS5a lava) were collected around the vent area from outcrops that are sparse due to intense vegetation and urbanization (sample locations are indicated in Fig. 1c). Distal products have been already analyzed by Piochi et al. (1999) and were not sampled again. However, the data from this study are included in our discussion.

Lava and scoria samples were crushed to lapilli-size particles through a jaw crusher and an agate mortar respectively and then dried in an oven at about 90 °C for 12 h. About 500 g of crushed sample was sieved using a stack of sieves with meshes ranging from 0.5 to 3 mm, at intervals of

Fig. 1. a) Structures of the subduction-related compression and extension fronts along the Apennines chain (modified after Acocella and Funicello, 2006); red triangles (except Ischia, in yellow) are active volcanoes, green triangles are extinct volcanoes. Pr = Procida; Cfc = Campi Flegrei caldera; SV = Somma-Vesuvius; AH = Alban Hills; Er = Mts. Ernici; b) schematic geological and structural map of the Tyrrhenian margin of the Campania region (modified after Orsi et al., 2003); c) schematic geological map of Ischia showing the outcrop of rocks of different ages on the island, Arso lava flow directions and sample locations are indicated. (c) Redrawn from D'Antonio et al. (2013).

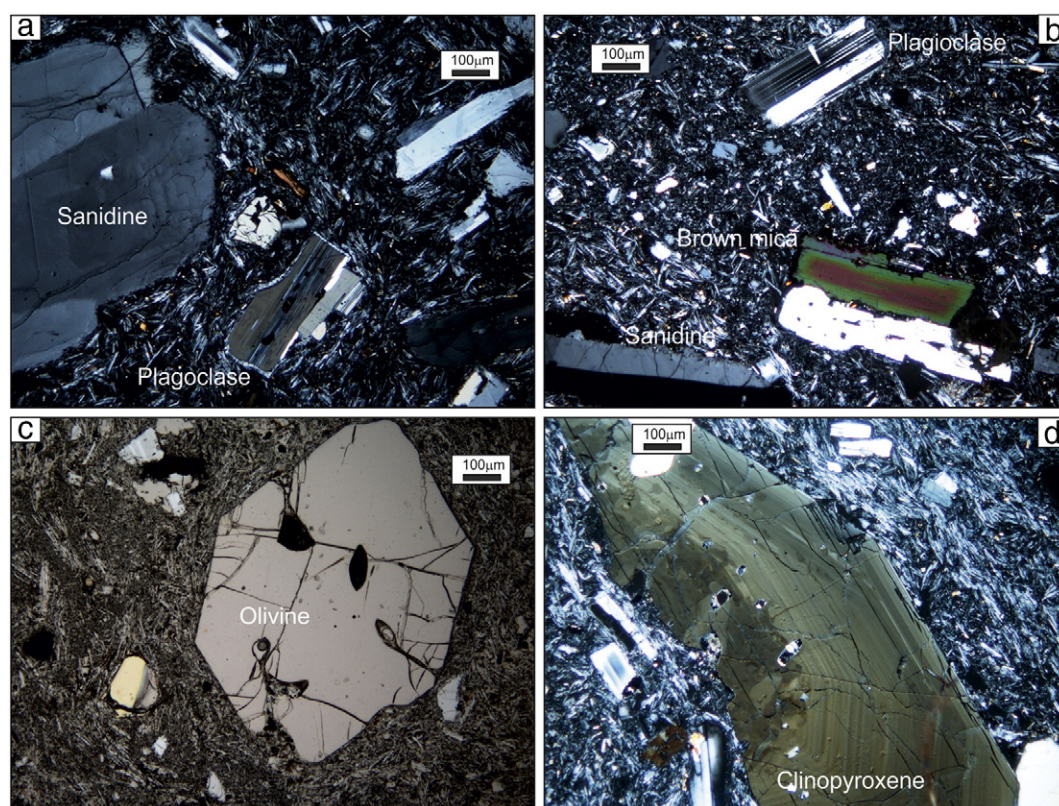


Fig. 2. Texture of representative Arso scoria (a and b) and lava (c and d). The lava samples have porphyritic texture with a trachytic groundmass. Phenocrysts are twinned and zoned euhedral grains of alkali feldspar and plagioclase (a and b). Euhedral olivine with hosted oxides and zoned clinopyroxene are common (c and d). Brown mica occurs as tabular phenocrysts with well-developed cleavage (b).

0.5 mm. The groundmass was separated from the 1.5 to 3 mm fraction by hand-picking under a binocular microscope. Feldspar, olivine and pyroxene phenocrysts sized between 0.5 and 3 mm were also separated. Some large single phenocrysts (~0.02 g) > 1 mm were also analyzed for Sr isotopic composition. Only pure crystals were selected without attached groundmass or mineral inclusions. Pyroxene phenocrysts were distinguished into dark and colorless crystals. After picking, the separated phases were washed in an ultrasonic bath with 7% HF and Milli Q® H₂O in order to remove any potentially remaining groundmass rinds to avoid groundmass contamination during Sr isotopic analyses. Single crystals were hand-picked for δ¹⁸O analyses. Crystals without attached glass were washed in beakers with 5% HF in a sand bath, then rinsed with Milli Q® H₂O, and finally leached with 6 N HCl and washed again with Milli Q® H₂O.

Whole rock samples were prepared and analyzed for major and trace elements at the Georg August Universität, Göttingen (GZG; Germany). For each sample, about 40 g of rock chips were hand-picked to assure that only the freshest pieces were powdered. The samples were washed again with deionized water (to remove the seawater salt) and dried at 120 °C. Sample powders were produced in a low-blank agate planetary ball mill. For each sample two pulverization steps were done with 20 g of material each. The volatile content (LOI) was

measured using standard thermo-gravimetric methods by igniting rock powders at 1100 °C after drying them overnight at 120 °C. Major oxides and some trace elements (Sc, V, Cr, Ni, Rb, Sr, Ba, Y, Zr and Nb) were analyzed on glass-fusion discs by a PANanalytical AXIOS advanced sequential X-Ray Fluorescence spectrometer (XRF). A full trace element spectrum was analyzed by a FISIONS VG PQ STE Inductively Coupled Plasma Mass Spectrometer (ICP-MS). Analytical precision is better than 1% for most XRF major elements, but varies between 1 and 2% for Na, Mg and P. Precision is 10% for most trace elements, 2–5% for rare earth elements (REE) and Y.

Sr and Nd isotopic analyses were performed at the Radiogenic Isotope Laboratory of the Istituto Nazionale di Geofisica e Vulcanologia, sezione di Napoli Osservatorio Vesuviano (INGV-OV) on whole rocks, glasses and separated minerals after dissolution with high-purity HF-HNO₃-HCl mixtures. Sr and Nd were separated from the matrix through conventional ion-exchange procedures described in [Arienzo et al. \(2013\)](#) and measured statically by thermal ionization mass-spectrometry on a Thermo Finnigan Triton TI instrument. During collection of isotopic data, replicate analyses of NIST-SRM 987 (SrCO₃) and La Jolla international reference standards were performed to check for external reproducibility. 2σ_{mean}, i.e. the standard error with N = 180, was better than ±0.000010 for Sr, and ±0.000008 for Nd measurements. The external reproducibility 2σ (where σ is the standard deviation of the standard results, according to [Goldstein et al., 2003](#)), i.e. the mean measured value of ⁸⁷Sr/⁸⁶Sr for the NIST-SRM 987 standard, was 0.710204 ± 0.000015 (2σ, N = 72); that of ¹⁴³Nd/¹⁴⁴Nd for the La Jolla standard was 0.511834 ± 0.000009 (2σ, N = 32). Sr and Nd isotope ratios were normalized to the recommended values of NIST-SRM 987 (⁸⁷Sr/⁸⁶Sr = 0.71025) and La Jolla (¹⁴³Nd/¹⁴⁴Nd = 0.51185) standards, respectively. Sr and Nd blanks were on the order of 0.1 ng during the period of chemistry processing. Measured ⁸⁷Sr/⁸⁶Sr ratios were normalized for within-run isotopic fractionation to ⁸⁶Sr/⁸⁸Sr = 0.1194, and ¹⁴³Nd/¹⁴⁴Nd ratios to ¹⁴⁶Nd/¹⁴⁴Nd = 0.7219.

Table 1
Quantitative mineral assemblage recognized in Arso rocks.

Rocks	Ol	Cpx	Phl	Alk	Plg	Ox
Ars1a	6	11	5	18	15	2
Ars4b	7	9	4	17	16	3
Ars5a	6	12	6	21	13	2

Abbreviations: Ol = olivine; Cpx = clinopyroxene; Phl = Phlogopite; Amph = amphibole; Alk = K-feldspar; Plg = plagioclase; Sod = sodalite; Ox = iron oxide; the modal composition is reported as %.

The chemical composition of minerals was measured using a JEOL JXA-8900R at GZG (Göttingen, Germany) using Wavelength Dispersion Spectrometry (WDS) techniques. The operating conditions are: accelerating voltage of 15 kV, beam current of 15 nA, beam diameter of 10 μm , counting times of 5 s on background and 15 s on peak. The relative standard deviation for the major and minor elements is below 2% and 6% respectively.

The oxygen isotopic composition of ca. 2 mg of feldspar, clinopyroxene and olivine phenocrysts, and powdered bulk rocks was measured at GZG by infrared laser fluorination following the procedure described by Pack et al. (2016). 9 San Carlos olivine (standard) and 9 samples were loaded into an 18-hole Ni metal sampler. The isotope ratios in the extracted O_2 gas were determined using a Thermo MAT253 gas source isotope ratio mass spectrometer in dual inlet mode. Variations in triple oxygen isotope ratios ($^{17}\text{O}/^{16}\text{O}$, $^{18}\text{O}/^{16}\text{O}$) are expressed as the δ notation relative to VSMOW (McKinney et al., 1950). All the measurements have been standard-normalized to the recommended $\delta^{18}\text{O}$ standard value of 5.15‰ of the San Carlos olivine standard. Standards were measured throughout the analyses in order to check systematic daily drifts in mass bias or blank contribution. Each powdered bulk rock were first melted to a sphere with the CO_2 laser under vacuum in order to avoid sputtering and incomplete fluorination of small grains. Based on the standard deviation of the San Carlos standards, the normalization was done simply calculating the average of the measured San Carlos olivine standards as a normalization reference value.

2. Results

2.1. Petrography

The lava samples have a porphyritic texture (Fig. 2). The phenocrysts, in order of decreasing abundance, are: sanidine and plagioclase, clinopyroxene, olivine, magnetite and brown mica often forming agglomerates (Table 1). Groundmass shows a trachytic texture, and consists of microlites of plagioclase (the most abundant phase) and, in subordinate amounts, clinopyroxene, alkali feldspar, magnetite, and rare brown mica. The phenocrysts population of the vesicular scoria sample is similar to that of the dense lava and includes: plagioclase, clinopyroxene, alkali feldspar, olivine, magnetite and brown mica, in order of decreasing abundance. Groundmass shows microlites of predominant clinopyroxenes with subordinate plagioclase and magnetite. In both lava and scoria samples, plagioclase phenocrysts occur as twinned euhedral grains, often zoned and with crystallized inclusions and resorbed edges (Fig. 2a and b). Often plagioclase is included in alkali-feldspar and brown mica phenocrysts. Alkali-feldspar phenocrysts occur as euhedral to subeuhedral phenocrysts with Carlsbad-type twins. They often form the rim on other phenocrysts, mainly plagioclase and clinopyroxene. Olivine is often euhedral in shape (Fig. 2c), but sometimes shows resorbed edges. Crystallized melt inclusions and oxides are generally hosted in olivine crystals. Two types of pyroxene are present in the samples. One type is colorless with no pleochroism, while the other shows light to dark green color with yellowish-brown pleochroism. All clinopyroxene phenocrysts show euhedral to subeuhedral habitus (Fig. 2d) with frequent compositional zonation and crystallized melt inclusions. Brown mica occurs as tabular phenocrysts with well-developed cleavage and often resorbed margins. Fe-oxide minerals occur in minute opaque crystals dispersed in the groundmass.

2.2. Mineral chemistry

The complete dataset of chemical composition of analyzed minerals is reported in the electronic supplementary material.

Olivine has two different compositional populations (Fig. 3a). The most Fe-rich olivines (Fo mol% = 54–61) are found in the groundmass while phenocrysts show the more magnesian compositions with highly variable Fo contents (Fo mol% = 68–83). The Mn concentration is

<0.5 wt.% in phenocrysts but reaches ~2 wt.% in the groundmass. Ca contents in olivine are high in both phenocrysts and matrix, and increase with decreasing Mg (Fig. 3b). The chemical composition of Arso olivines falls within the compositional fields commonly observed in Ischia and Cfc lavas. The most Mg-rich olivine in the Arso products overlap in composition with olivines in mafic rocks of the Solchiaro eruption on Procida (Fig. 3b). Clinopyroxene (Cpx; Fig. 4a), unlike olivine, shows a similar composition in phenocrysts ($\text{Wo}_{51-46}\text{En}_{14-6}\text{Fs}_{46-35}$) and groundmass ($\text{Wo}_{53-47}\text{En}_{15-6}\text{Fs}_{44-33}$). Colorless Cpx are diopside with Mg# ($100 * (\text{Mg}^{2+}/\text{Mg}^{2+} + \text{Fe}^{2+})$) between 89 and 77, while green Cpx are Fe-rich diopside with Mg# ranging between 74 and 61. Both kinds of Cpx show increasing Ti and Al, and constant Ca contents at decreasing Mg# (Fig. 4b–d). Diopside phenocrysts show normal zoning with a more Mg-rich core and Fe-rich rims while light-green Fe-rich diopside crystals show reverse zoning. Cpx chemistry of the Arso products is similar to those found in other Ischia and Cfc volcanic rocks. Plagioclase (Fig. 5) shows a continuous compositional range from almost pure anorthite to oligoclase ($\text{An}_{92.5-27}\text{Ab}_{59-7}\text{Or}_{14-0.5}$). Mainly they show reverse zoning with cores more albitic than their rims but normal zonation is also observed infrequently. Alkali-feldspar (Fig. 5) phenocrysts have a restricted range of $\text{An}_{8.6-3.5}\text{Ab}_{48.3-38.1}\text{Or}_{57.7-43.1}$, while microlites cover a wider compositional range ($\text{An}_{14-4}\text{Ab}_{55.7-52}\text{Or}_{44-32.5}$). Reversely zoned K-feldspar phenocrysts have cores more albitic than their rims. Phlogopite (Fig. 6a) with Mg# ranging from 75 to 52, and TiO_2 and Na_2O contents varying from 4.8 to 7.7 wt.% and 0.5 and 1.9 wt.%, respectively. Its composition is similar to that of phlogopite of other Ischia and Campi Flegrei products. Magnetite is the only Fe-Ti oxide in our samples. Compositions are high in ulvöspinel (25–49 mol%) corresponding to 9–17 wt.% TiO_2 . Groundmass spinels are low in ulvöspinel content (<10 mol%, 1–2 wt.% TiO_2). MnO content is relatively low (<2.5 wt.%) compared to that of spinels of

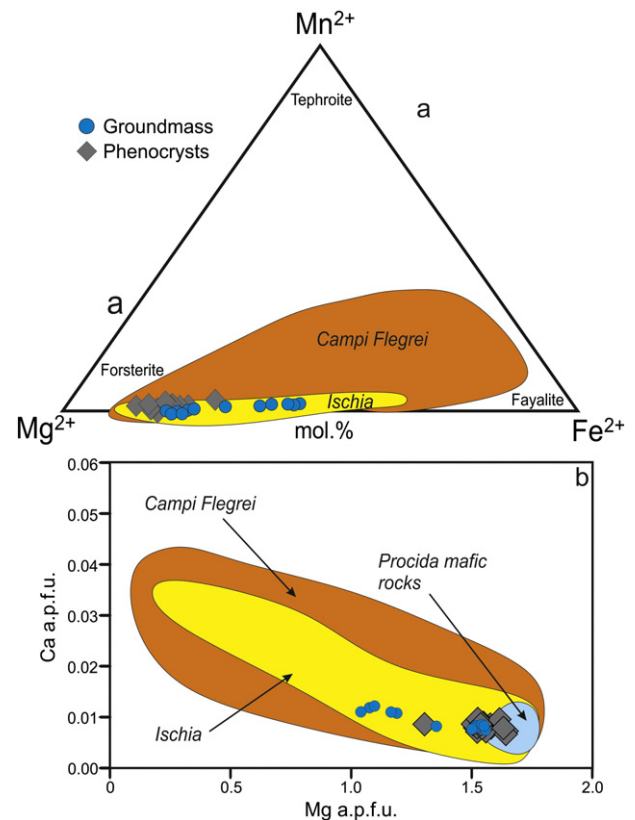


Fig. 3. Classification (a) and Mg vs Ca variation diagram (b) of olivine found in Arso volcanic rocks. Data for the compositional field of minerals for comparison are taken from Melluso et al. (2012, 2014 and references therein).

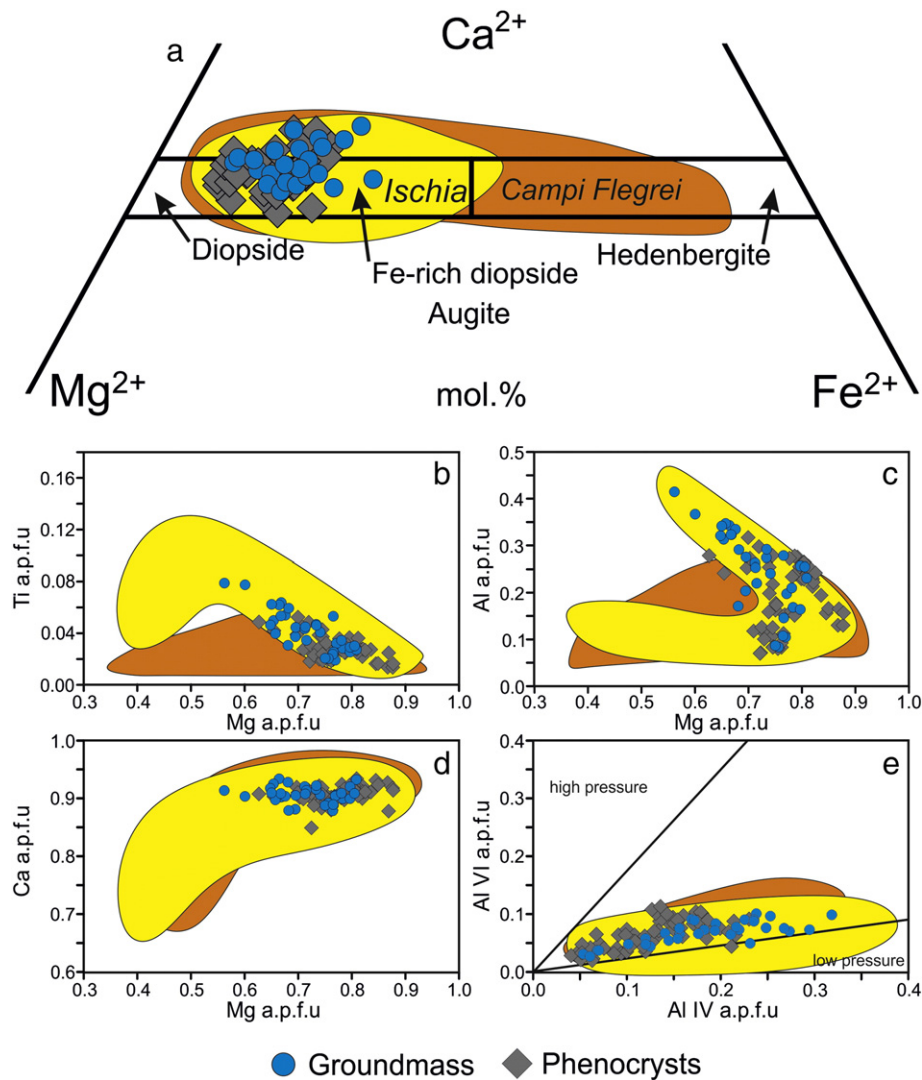


Fig. 4. Classification (a) and variation of chemical composition diagrams (b-e) of clinopyroxene found in Arso volcanic rocks. Data for compositional field of minerals are taken from Melluso et al. (2012, 2014 and references therein).

other rocks of Ischia (MnO max measured value ~12; Melluso et al., 2014).

2.3. Major and trace elements composition

Whole rock major and trace element data of the analyzed Arso samples are listed in Table 2. Compositions (Fig. 7) range from latite (whole rocks) to phonolite (interstitial glass). All samples are CIPW nepheline normative (~7.3–9.6 wt.%; calculated assuming $Fe_2O_3/FeO = 0.4$; Middlemost, 1989) and have low Mg# ranging from 51 to 41. CaO/Al_2O_3 (~0.2) and high SiO_2 (~57 wt.%) are coupled with high alkali ($Na_2O + K_2O$: 9.8–12.3 wt.%) and TiO_2 (0.8–1 wt.%) and low MgO (<4 wt.%) and CaO (<6 wt.%) contents. Primitive mantle-normalized incompatible elements patterns (Fig. 8a) show enrichment in some strongly incompatible elements, with positive spikes in Rb, Th, U, K and Pb, and depletion in Nb and Ta. Trace elements compatible in feldspars (Ba, Sr, Eu) are also relatively depleted. Large-Ion Lithophile Elements (LILE) are enriched relative to LREE (Ba/La 9–14) and HFSE (Ba/Nb 9–17). Rare earth elements (REE; Fig. 8b) display strong light REE (LREE) enrichment relative to heavy REE (HREE; $(La/Lu)_n \sim 12$; Lodders et al., 2009). In addition, chondrite-normalized REE patterns show a negative Eu anomaly ($Eu/Eu^* = Eu_n/(Sm_nGd_n)^{1/2} \sim 0.7$). With

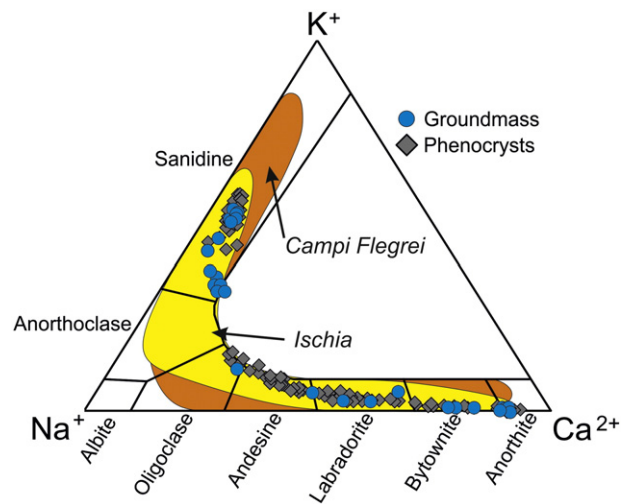


Fig. 5. An-Ab-Or classification for feldspars analyzed in Arso volcanic rocks. Data for compositional field of minerals are taken from Melluso et al. (2012, 2014 and references therein).

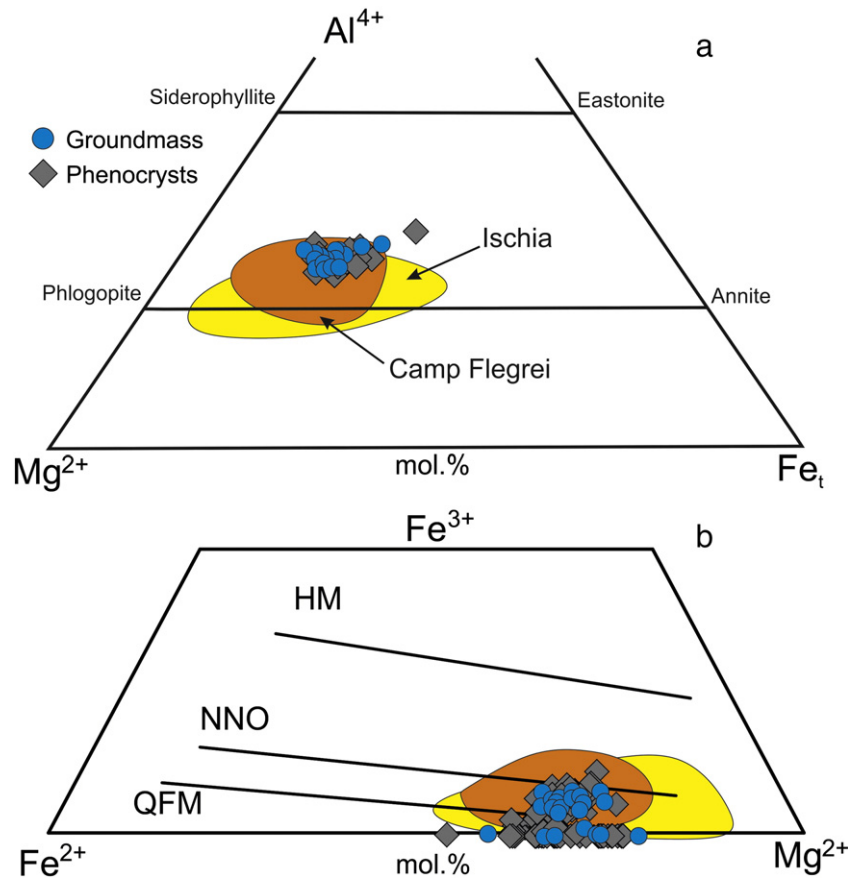


Fig. 6. Classification diagram of brown mica (a) found in Arso products and compositional variation (b) in the Fe^{2+} - Mg^{2+} - Fe^{3+} diagram. The HM (hematite-magnetite), NNO (nickel-nickel oxide) and QFM (quartz-fayalite-magnetite) oxygen buffers indicate the oxidation state of the system (Wones and Eugster, 1965).

these chemical and isotopic characteristics, the Arso products plot fully within the general trend of Ischia volcanic rocks (Fig. 9a–d).

2.4. $^{87}\text{Sr}/^{86}\text{Sr}$ and $\delta^{18}\text{O}$ isotope data

Sr isotope ratios of bulk rock, groundmass, and separated feldspar, pyroxene, and olivine phenocrysts cover a wide compositional range (Table 3 and Fig. 10a). Bulk rock $^{87}\text{Sr}/^{86}\text{Sr}$ value ranges from 0.70640 to 0.70656, while $^{143}\text{Nd}/^{144}\text{Nd}$ is 0.51254. The $^{87}\text{Sr}/^{86}\text{Sr}$ ratio of groundmass ranges from 0.70647 to 0.70667. Feldspar crystals, by contrast, have a rather narrow range (0.70600–0.70608) and show the least radiogenic Sr-isotopic composition in Arso rocks. The values measured on olivine crystals vary from 0.70641 to 0.70680, probably representing values of the crystal-hosted melt inclusions. Pyroxene $^{87}\text{Sr}/^{86}\text{Sr}$ values vary only between 0.70591 and 0.70646. The $^{87}\text{Sr}/^{86}\text{Sr}$ ratios of all analyzed minerals except the groundmass fall into the field of the other latitic products of Ischia, although with a smaller variation (Fig. 10a). $\delta^{18}\text{O}$ values of whole rocks range between $5.01 \pm 0.15\%$ and $6.13 \pm 0.15\%$ (Table 4 and Fig. 10b). The $\delta^{18}\text{O}$ values of feldspar are within the analytical uncertainties at $\sim 6.00\%$, while vary from 5.04 ± 0.15 to $5.27 \pm 0.15\%$ in clinopyroxene and display no systematic variation between the colorless (Mg-rich) and dark (Fe-rich) crystals. Olivine phenocrysts have a wider range from 5.06 ± 0.15 to $5.83 \pm 0.15\%$. Since measured $\delta^{18}\text{O}$ values do not represent initial magmatic values all mineral data were corrected to $\delta^{18}\text{O}_{\text{melt}}$ considering $\Delta(\text{melt-min})$ fractionation between melt and minerals (Table 4). $\delta^{18}\text{O}_{\text{melt}}$ calculated for clinopyroxene and olivine phenocryst separates (Fig. 10b) vary between 5.58 (clinopyroxene phenocryst in Ars 5a) and 6.89% (olivine phenocryst of Ars 5a). The $\delta^{18}\text{O}$ (calculated and corrected) of the Arso

products overlaps and falls partly below the composition measured for the other latitic product of Ischia (D'Antonio et al., 2013).

3. Discussion

3.1. Mineralogical and isotopic disequilibrium

The petrography of Arso rocks with distinct phenocryst populations that are in apparent compositional disequilibrium (highlighted by the occurrence of resorbed phenocrysts, and both normally and reversely zoned feldspar and clinopyroxene) indicates chemical disequilibrium in the magmas. The composition of most olivine and clinopyroxene phenocrysts compared to that of their host lava (Fig. 11a and b) indeed show disequilibrium given the published $^{\text{Fe}/\text{Mg}}\text{Kd}_{\text{ol-liq}}$ distribution coefficients of 0.27–0.33 (Roeder and Emslie, 1970; Matzen et al., 2011) and $^{\text{Fe}/\text{Mg}}\text{Kd}_{\text{cpx-liq}} = 0.27 \pm 0.03$ (Grove and Bryan, 1983; Sisson and Grove, 1993; Putirka et al., 2003; Mollo et al., 2013). In most cases, the plagioclase-host pairs also fall outside the calculated equilibrium field determined by the equilibrium distribution coefficients ($^{\text{plag-melt}}\text{Kd}_{\text{Ab/An}} = \text{Na}_{\text{plag}} * \text{XAl}_{\text{liq}} * \text{XC}_{\text{liq}}/\text{XC}_{\text{plag}} * \text{XNa}_{\text{liq}} * \text{XSi}_{\text{liq}} = 0.1 \pm 0.05$; Putirka, 2008). Only the labradoritic plagioclase seems to be in equilibrium with the host lava (Fig. 11c). Furthermore, we have examined the Or-Ab equilibrium between K-feldspar and liquid according to the Mollo et al. (2015) approach. As shown in Fig. 11d, all sanidine crystals, seem to be in chemical equilibrium with the Arso host lava.

Sr-isotopic analyses also show that different phenocryst phases are in isotopic disequilibrium among themselves and with the groundmass. Single crystals and mineral fractions sized between 0.3 and 1 mm highlight differences in Sr-isotopic composition for the same mineral phase.

Chapter 2: Source and magmatic evolution inferred from geochemical and Sr-O-isotope data on hybrid lavas of Arso, the last eruption at Ischia island (Italy; 1302 AD)

Table 2
Chemical composition of Arso volcanic rocks.

Samples	ARS1a	ARS4b	ARS5a	Piochi et al. (1999)	Piochi et al. (1999)	Piochi et al. (1999)	Piochi et al. (1999)	Vezzoli (1988)	Vezzoli (1988)	Vezzoli (1988)	Vezzoli (1988)	Melluso et al. (2014)	Melluso et al. (2014)
SiO ₂	57.79	55.53	56.85	56.38	56.46	56.44	58.08	58.02	55.17	55.11	55.04	58.03	60.66
TiO ₂	0.83	1.01	0.90	0.99	0.99	0.99	0.86	0.82	1.04	1.06	1.03	0.82	0.75
Al ₂ O ₃	18.41	18.01	18.03	18.94	18.84	18.94	18.77	18.28	17.41	17.32	17.88	18.26	18.29
Fe ₂ O _{3t}	4.82	6.17	5.35	4.95	4.91	4.91	4.21	4.98	6.74	6.76	6.53	4.98	4.14
MnO	0.14	0.14	0.14	0.13	0.14	0.13	0.13	0.12	0.13	0.12	0.14	0.12	0.14
MgO	1.75	3.22	2.45	2.34	2.24	2.53	1.95	1.99	3.44	3.41	3.05	1.99	1.01
CaO	3.73	5.74	4.70	5.31	5.00	5.24	4.15	4.29	5.89	6.55	6.28	4.29	2.77
Na ₂ O	5.66	5.03	5.19	5.24	5.08	6.06	5.34	5.03	4.69	4.26	4.39	5.03	5.34
K ₂ O	6.59	4.74	6.06	5.28	5.92	4.29	6.20	6.20	5.18	5.08	5.17	6.20	6.68
P ₂ O ₅	0.28	0.42	0.33	0.44	0.42	0.42	0.30	0.27	0.30	0.33	0.49	0.27	0.23
Sum	100.00	100.00	100.00	100.00	100.00	100.00	100.00	100.00	100.00	100.00	100.00	100.00	100.00
LOI	1.19	0.93	1.29	0.82	1.11	0.86	0.48	0.09	0.55	0.00	0.42	0.09	0.69
Alk	12.25	9.77	11.26	10.52	11	10.36	11.54	11.22	9.87	9.34	9.56	11.23	12.01
K ₂ O/Na ₂ O	1.16	0.94	1.17	1.01	1.17	0.71	1.16	1.23	1.10	1.19	1.18	1.23	1.25
CaO/Al ₂ O ₃	0.2	0.32	0.26	0.28	0.27	0.28	0.22	0.23	0.34	0.38	0.35	0.24	0.15
FeO(t)	4.34	5.55	4.81	4.46	4.42	4.45	3.79	4.48	6.07	6.08	5.88	4.48	3.72
Mg#	41.84	50.82	47.55	48.39	47.48	50.35	47.82	44.16	50.29	49.96	48.02	44.16	32.58
PI	0.89	0.74	0.84	0.76	0.78	0.77	0.83	0.82	0.77	0.72	0.72	0.82	0.88
Sc	9	16	13					7	17	17	13	7	5
V				149	141	142	104	93	104	110	166	93	71
Cr				19	19	26	21	27	48	49	40	27	
Co	8	16	12	13	12	13	9		18	19	17		5
Ni	11	24	16								30		
Cu	12	18	17	28	73	31	22				40		
Zn	65	62	64								70		70
Rb	273	169	238	236	255	168	252	254	201	184	240	254	306
Sr	317	497	400	502	453	471	342	330	486	554	513	330	232
Y	40	36	37	36	38	35	37	386	49	46	29	39	37
Zr	335	301	332.3	286	307	288	315	343	242	216	274	343	389
Nb	61	48	54	43	48	45	50	53	41	35	50	53	75
Ba	567	806	679	841	768	819	575	618	893	1168	873	618	471
La	65.4	56.4	59.8	62.8	64.5	61.1	63.7	55.8	50.1	48.1	62.9	55.8	81.8
Ce	124.9	110.6	115.9	125.1	130.1	122.1	127.1	108.1	115.1	103.1	121.1	108.1	152.1
Pr	15.1	13.4	13.9								14.2		17.1
Nd	53.5	50.3	51.0	53.1	53.2	49.9	50.8	48.4	51.1	46.1	47.4	48.4	53.8
Sm	9.8	9.4	9.3	10.0	10.2	9.5	9.8	9.1	8.9	8.6	9.3	9.1	9.9
Eu	1.9	2.1	1.9	2.3	2.1	2.1	1.9	1.8	2.1	2.2	2.1	1.8	1.7
Gd	8.4	8.2	8.0	8.5	8.7	8.4	7.9	6.9			7.1	6.9	7.5
Tb	1.2	1.1	1.1						0.8	0.9	1.1		1.2
Dy	7.2	6.6	6.8	6.6	6.8	6.4	6.6	6.1			6.1	6.1	6.8
Ho	1.4	1.3	1.3								1.2		1.3
Er	4.1	3.6	3.8	3.3	3.4	3.2	3.4	3.1			3.2	3.1	3.9
Tm	0.6	0.5	0.5								0.5		0.6
Yb	4.0	3.4	3.6	3.7	3.4	3.5	3.7	3.3	2.9	2.6	3.1	3.3	4.1
Lu	0.6	0.5	0.5	0.5	0.6	0.5	0.5	0.5	0.5	0.4	0.5	0.5	0.6
Hf	7.5	6.8	7.5	6.9	7.1	6.9	7.5		6.1	5.3	6.7		9.3
Ta	3.1	2.3	2.7						2.9	2.4	2.7		4.1
Pb	27.1	14.0	25.4								29.1		39.1
Th	28.1	21.5	24.2	22.6	24.8	23.2	26.1		20.1	16.8	20.5		30.6
U	8.2	6.4	7.2	6.7	7.5	6.3	7.5		5.9	4.8	7.1		10.4
Zr/Hf	45	44	44	41	43	42	42		40	41	41		42
Nb/Yb	15	14	15	12	14	13	14	16	14	13	16	16	19
Th/Yb	7	6	7	6	7	7	7	0	7	6	7	0	8
Ba/La	9	14	11	13	12	13	9	11	18	24	14	11	6
(La/Lu) _n	11.8	12.1	11.9	13.1	11.2	12.7	13.2	10.7	11.2	11.9	13.1	11.6	14.1
Eu/Eu*	0.64	0.74	0.68	0.76	0.68	0.68	0.66	0.69			0.76	0.71	0.61

Major elements. Sum of alkalis (Alk), FeO, and LOI (loss on ignition) are reported as oxides wt.%. Trace elements are reported as ppm. Mg# are calculated as $100 * (Mg/Mg + Fe_t)_{mol}$. PI is the peralkaline index and is calculated as $(Na + K/Al)_{mol}$. (La/Lu)_n and Eu/Eu* ratios are calculated after normalization to primordial mantle values (Lyubetskaya and Korenaga, 2007).

The overall range in $^{87}Sr/^{86}Sr$ of minerals (0.70591–0.70680) is much larger than that of the groundmass (0.70647–0.70667). Moreover, $^{87}Sr/^{86}Sr$ values (0.70641–0.70680) detected in olivine are, on average, higher than those of clinopyroxene (0.70591–0.70646; Table 3 and Fig. 10a), but similar to those of olivine found in other mafic rocks of Ischia (Vateliere, Cava Nocelle, and Molaro; D'Antonio et al., 2013).

3.2. Fractional crystallization

Fractional crystallization (FC) has been proposed to be the main process for the evolution of Ischia magmas from latite (whole rocks) to

phonolite (interstitial glass) (e.g., Brown et al., 2014; Melluso et al., 2014). Arso eruption extruded a magma varying in composition. To test this hypothesis, least-squares mass balance calculations (XLFRAC; Stormer and Nicholls, 1978) have been performed. Parameters and results are listed in the Supplementary Electronic Material. The results of a first calculation indicate that removal of about 38% of a monzo-gabbro mineral assemblage made up of andesine (16%), Fe-rich diopside (9%), alkali-feldspar (7%), Fe-olivine (3%), brown mica (2%) and Ti-magnetite (1%) matches ($\sum R^2 = 0.09$) the compositional variation between a latite (SiO₂ = 55.5 wt.%, MgO = 3.22 wt.%) and a trachyphonolite (SiO₂ = 58.7 wt.%, MgO = 1.75 wt.%). A second

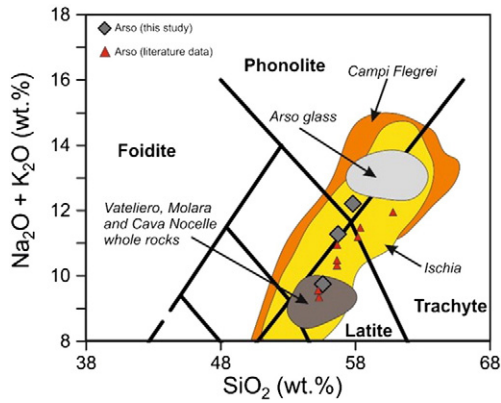


Fig. 7. Total alkalis ($\text{Na}_2\text{O} + \text{K}_2\text{O}$ wt.%) vs silica (SiO_2 wt.%) diagram (after Le Bas et al., 1986) classification for Arso products (recalculated to 100% on anhydrous basis). Literature data on Arso whole rocks are from Vezzoli (1988), Piochi et al. (1999) and Melluso et al. (2014). Literature composition for Arso glass is from Piochi et al. (1999). Reference data for Ischia and Campi Flegrei (whole rock and glass) are from Lustrino et al. (2011 and references therein), Brown et al. (2014), D'Antonio et al. (2013), Insinga et al. (2014), Melluso et al. (2012, 2014), Tomlinson et al. (2012, 2014), and Petrosino et al. (2014, 2015).

calculation, based on the fractionation of a syenitic assemblage including alkali-feldspar (31%), bytownitic plagioclase (9%), diopsidic clinopyroxene (8%), Mg-olivine (3%) and Ti-magnetite (4%), has accounted for the same chemical evolution with a good approximation

($\sum R^2 = 0.2$). This underlines that simple mass balance calculations do not produce unique results. FC modeling has been carried out using the concentrations and partition coefficients of trace elements and the Rayleigh fractionation equation using the monzo-gabbro assemblage. Trace element modeling also gives excellent agreement between the calculated liquid and the composition chosen as the evolved magma (model parameters and figures in Supplementary Electronic Material). A second step, from a trachyphonolitic to a phonolitic melt, indicates removal of about 73% of a syenitic solid, made up of alkali-feldspar (52%), andesine plagioclase (7%), salitic clinopyroxene (6%), brown mica (6%) and Ti-magnetite (3%), with a perfect match ($\sum R^2 = 0.1$). These results indicate that fractional crystallization in principle could be a major mechanism in generating the compositional range of the Arso magma. However, the disequilibrium mineral assemblages documented here clearly exclude a simple crystal fractionation process.

3.3. Mixing processes

The volcanic rocks of Ischia have long been known for bearing strong witness to open system magma evolution processes (Poli et al., 1987; Crisci et al., 1989; Civetta et al., 1991; Turi et al., 1991; Di Girolamo et al., 1995; Piochi et al., 1999; Tonarini et al., 2004; D'Antonio et al., 2007, 2013; Brown et al., 2014). Mineral composition of Arso lavas and isotopic data require that magma mixing processes must have occurred between compositionally and isotopically distinct magma batches. The different phenocryst populations are likely derived from mafic (Mg-rich olivine, diopside and Ca-rich plagioclase) and evolved

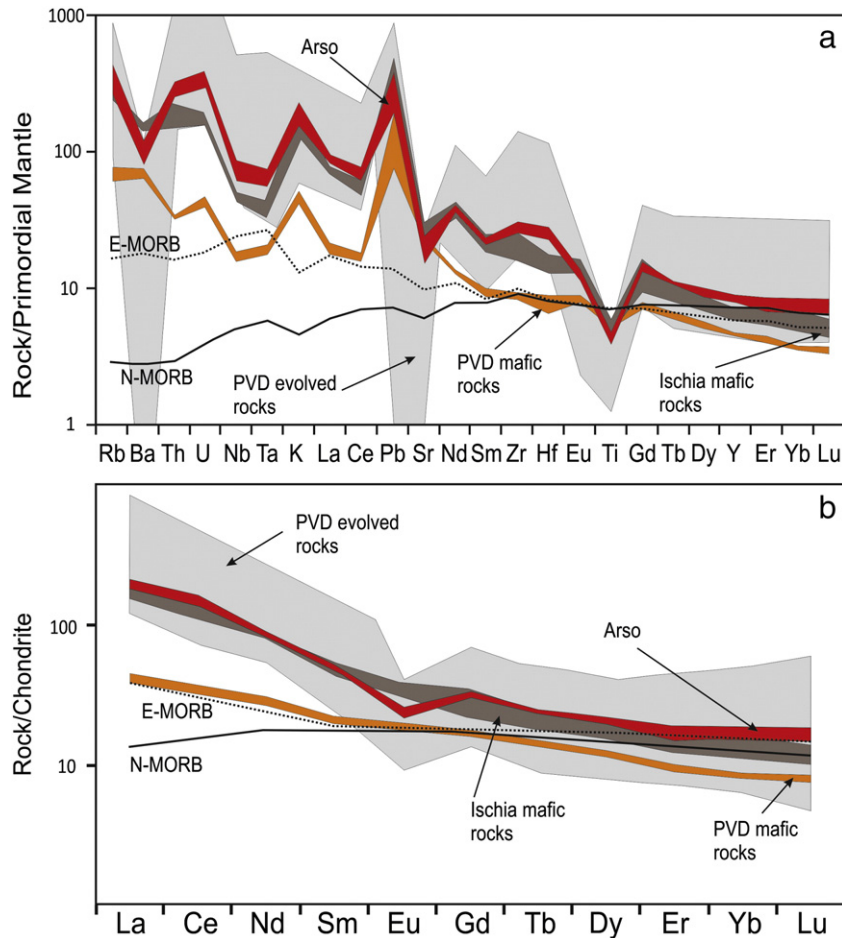


Fig. 8. a) Primordial mantle normalized multi-element variation diagram for Arso products reported as a field. b) Chondrite-normalized Rare Earth Element patterns for Procida K-basalts reported as a field for comparison. The Arso pattern is compared to those of average normal and enriched mid-ocean ridge basalts (N-MORB, E-MORB; Gale et al., 2013) and Phlegrean volcanic district (PVD) mafic ($\text{MgO} > 6$ wt.%) and evolved rocks (source of reference data as in Fig. 7). (a) Normalization values are taken from Lyubetskaya and Korenaga (2007). (b) The chondrite values used for normalization are taken from Lodders et al. (2009).

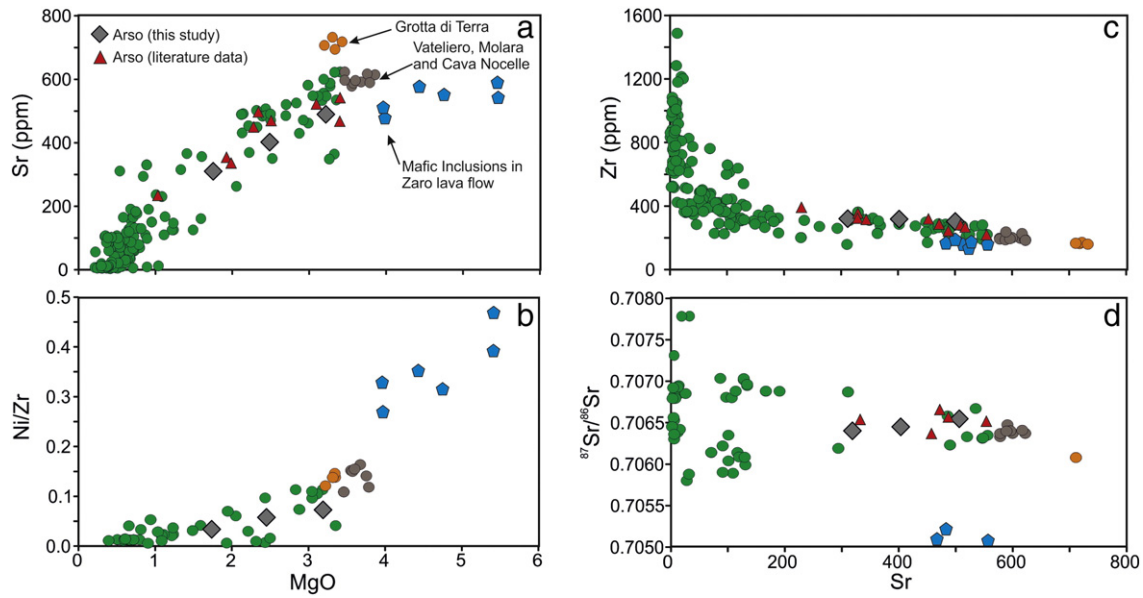


Fig. 9. Binary diagrams MgO vs Sr (a), MgO vs Ni/Zr (b), Sr vs Zr (c) and Sr vs $^{87}\text{Sr}/^{86}\text{Sr}$ (d). Reference data as in Fig. 7.

(Fe-rich olivine, Fe-rich diopside and Na-rich plagioclase) magma batches: (a) a mafic magma with $^{87}\text{Sr}/^{86}\text{Sr}$ of ~ 0.7068 , value represented by Mg-rich olivine in the Arso products but recognized in pyroxenes of other latitic rocks (D'Antonio et al., 2013) and (b) an evolved trachytic melt with $^{87}\text{Sr}/^{86}\text{Sr}$ of ~ 0.7059 , value represented by Fe-rich diopside in the Arso products but recognized in feldspars of other latitic rocks (D'Antonio et al., 2013). Labradoritic plagioclase and all sanidine crystals, minerals of intermediate Sr-isotope composition, appear to be in equilibrium with the intermediate hybrid melt and represent phenocrysts that mostly crystallized from the hybrid magma mixing. An origin as xenocrysts from earlier crystallization of isotopically intermediate magmas, picked up from the plumbing system is also possible but less likely because it would call for fortuitously matching isotope compositions. Our preferred scenario implies mixing between mafic and highly enriched in radiogenic Sr magmas, and more evolved and less enriched in radiogenic Sr ones. Interestingly, such unusual isotopic features are displayed also by other 3 ka old latitic rocks of Ischia (Vateliero, Molara and Cava Nocelle, Fig. 1c; D'Antonio et al., 2013), suggesting that mixing has been the general process in its magmatic plumbing system. Endmember compositions may be related by fractional crystallization, as shown above. However, isotopic differences suggest in addition variable mantle sources or crustal assimilation, as discussed below.

3.4. Source enrichment and crustal contamination

The Arso mineral phases display a range of $\delta^{18}\text{O}$ -melt values that are much larger than analytical uncertainty (Fig. 10b). Higher values of this range are clearly outside the "normal" mantle values (Mattey et al., 1994; Eiler, 2001). These isotopic features are also shown by the Ischia magmas erupted over the past 3 kyr (D'Antonio et al., 2013). Sr-O isotope relationships in igneous rocks are a powerful tool to distinguish variable magma sources from assimilation processes as a cause for enriched or crustal signatures in the magmas. Downward- and upward-convex curves in the O-Sr isotope space (inset in Fig. 12) discriminate between mantle source enrichment and crustal assimilation processes, respectively (e.g., James, 1981; Van Soest et al., 2002; Bindeman et al., 2004; Handley et al., 2010). The Sr-O isotope data here presented for the Arso products have been plotted along with previously published data for Ischia and other Italian volcanoes (Fig. 12). Compared to the other Ischia volcanic rocks, a large number of minerals shows $\delta^{18}\text{O}$ values lower than the literature data while only three minerals fall within or close, the Ischia isotopic compositional field previously obtained from minerals (Fig. 12). The heavier O-isotope signature in phenocrysts is obscured in whole rock data that are dominated by the matrix in their mass balance. Overall, both literature and

Table 3
 $^{87}\text{Sr}/^{86}\text{Sr}$ isotopic ratios measured on the Arso igneous rocks.

Analyzed material	$^{87}\text{Sr}/^{86}\text{Sr}$		$^{87}\text{Sr}/^{86}\text{Sr}$		$^{87}\text{Sr}/^{86}\text{Sr}$		$^{143}\text{Nd}/^{144}\text{Nd}$	
	Ars1a	2s	Ars4b	2s	Ars5a	2s	Ars5a	2s
Whole rock	0.706400	±3	0.706557	±6	0.706470	±3	0.512544	±3
Ground mass (1.5–3 mm)	0.706470	±6	0.706674	±5	0.706540	±6		
Olivine (s.c. 1 mm)	0.706690	±10	0.706426	±6	0.706530	±6		
Pyroxene (s.c. 1 mm)	0.706190	±5	0.705909	±6	0.706360	±6		
Feldspar (s.c. 1 mm)	0.706080	±6	0.706069	±6	0.706000	±6		
Olivine (0.5–3 mm)	0.706490	±6	0.706800	±7	0.706510	±7		
Pyroxene (0.5–3 mm)	0.706260	±5	0.706449	±6	0.706300	±6		
Feldspar (0.5–3 mm)	0.706070	±6	0.706061	±6	0.706030	±6		
Olivine (0.5–3 mm)	0.706570	±6	0.706582	±6	0.706410	±6		
Pyroxene (0.5–3 mm)	0.706300	±6	0.706462	±6	0.706330	±6		
Feldspar (0.5–3 mm)	0.706080	±5	0.706061	±6	0.706070	±6		

Abbreviation: s.c. = single crystal; 2s is the standard deviation and refers to the last digit.

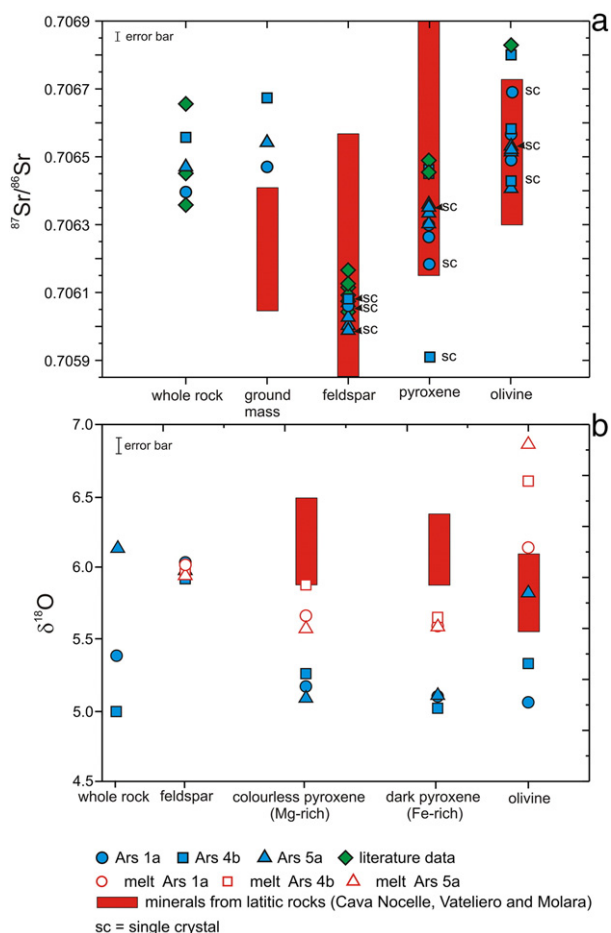


Fig. 10. a) $^{87}\text{Sr}/^{86}\text{Sr}$ isotopic data of groundmass and minerals from this work (Ars1a, Ars4b, Ars5a), together with isotopic data of four samples (OIS 103A, OIS 103E, OIS 104A, OIS 104B) analyzed by Piochi et al. (1999). All data were corrected using the recommended value of NIST SRM 987 $^{87}\text{Sr}/^{86}\text{Sr}$ ratio. The errors on the measured ratios are within the symbol; b) O-isotope compositions of whole-rocks, minerals and calculated melt composition of Arso igneous rocks. $\delta^{18}\text{O}_{\text{melt}}$ is calculated using the Bindeman et al. (2004) approach. The error of each measurement is calculated as standard deviation of the S. Carlos olivine standard and is $\sim 0.15\%$. Errors for calculated melt values are those measurement errors, calibration errors in the recalculation scheme (Bindeman et al., 2004) are not considered. Literature data for latitic rocks of Ischia are from D'Antonio et al. (2013).

Table 4
O-isotope compositions of whole-rocks, minerals and calculated melt composition of Arso igneous rocks.

Sample	Analyzed material	$\delta^{18}\text{O}$ (‰)	$\pm 1\sigma$	SiO_2 (wt. %)	$\delta^{18}\text{O}_{\text{melt}}$ (‰)*
Ars 1a	whole rock	5.39	0.15	57.79	
	feldspar	6.07	0.15		6.05
	colorless pyroxene	5.16	0.15		5.67
	dark pyroxene	5.14 ⁺	0.15		5.65
	olivine	5.06	0.15		6.15
Ars 4b	whole rock	5.01	0.15	55.53	
	feldspar	5.96	0.15		5.99
	colorless pyroxene	5.27	0.15		5.90
	dark pyroxene	5.04	0.15		5.67
	olivine	5.36	0.15		6.64
Ars 5a	whole rock	6.13	0.15	56.85	
	feldspar	6.00	0.15		5.97
	colorless pyroxene	5.09	0.15		5.58
	dark pyroxene	5.11 ⁺	0.15		5.60
	olivine	5.83	0.15		6.89

The error on each measurement is calculated as standard deviation of the San Carlos olivine standard and is $\sim 0.15\%$. Errors for melt values were obtained by measurements errors.

* $\delta^{18}\text{O}_{\text{melt}}$ is calculated using the formula $\Delta(\text{melt-min}) = a[\text{SiO}_2 \text{ wt. \%}] + b$ after Bindeman et al. (2004).

⁺ average of two measurements.

new data show large variability in $\delta^{18}\text{O}$ and Sr-isotope values, similar to the neighboring Cfc and Somma-Vesuvius.

Projecting the Arso data field down onto a mantle-sediment mixing line suggests that the Ischia mantle source was modified likely by addition of subduction-derived sedimentary components (pelagic clays), as was also suggested for all Neapolitan volcanoes (e.g., Mazzeo et al., 2014, and references therein). Taking only our new single mineral data for Sr and O-isotopes from individual eruptions from Ischia and Cfc even form more coherent steep trends that start from a modified mantle source towards increasing crustal assimilation of magmas. $\sim 1\%$ source contamination along a concave mixing curve explains well the position of the least contaminated Ischia magmas, as well as those of Ernici and Somma-Vesuvius (Fig. 12).

In order to quantify the relative role of further assimilation in the Arso magmas, we have modeled the effects of crustal addition through the energy-constrained assimilation + fractional crystallization modeling (EC-AFC; Spera and Bohron, 2001). A possible assimilant for Ischia magmas may be the Hercynian granodiorite crust that likely constitutes the local deep basement (Pappalardo et al., 2002; Di Renzo et al., 2007, 2011; D'Antonio et al., 2013; Gebauer et al., 2014; Mazzeo et al., 2014). The modeling parameters are listed in Table 5 and results shown in the diagram of Fig. 12. In order to explore different assimilation models in the $^{87}\text{Sr}/^{86}\text{Sr}$ vs $\delta^{18}\text{O}$ diagram, differently modified mantle sources and assimilants with different isotopic compositions have been used (curves 1 and 2 in Fig. 12). Our modeling explains the Sr-O isotope features of Arso products by a maximum of $\sim 7\%$ assimilation of continental crust into a mafic magma which already had inherited an enriched crustal isotopic signature in the mantle source by variable additions of <0.5 to 1% of subducted sediment. Previous modeling of AFC processes provided a similar estimate (7% ; curve 3 in Fig. 12) for the maximum amount of crustal assimilation needed to explain the other 3 ka old latitic products of Ischia (D'Antonio et al., 2013). Only the model curve 2 produces a vertical trend that parallels the data fields of Arso and the similar trend of Vesuvius and Campi-Flegrei magmas. This model assumes an incompatible behavior for Sr in the magma ($D_0 = 0.5$; Table 5), followed by compatible behavior at decreasing MgO (Fig. 6a) and a low concentration of 50 ppm Sr in the contaminant. Such a crustal endmember could be realized by low-P melting of silicic metamorphic rocks. Altogether, literature and new data suggest that the mantle sector that fed the past <3 ka volcanic activity at Ischia was heterogeneous in terms of Sr isotopes ranging between 0.7053 (lower Sr-endmember in our modeling) and 0.7063 (higher Sr-endmember; in D'Antonio et al., 2013). This heterogeneity is likely the result of either variable amount or nature of the subducted ^{87}Sr -rich sedimentary components added to the mantle source. Magmas formed by partial melting of this heterogeneous mantle source subsequently underwent up to 7% of continental crustal assimilation during their rise and storage in the shallow plumbing system below Ischia.

3.5. Implications for the shallow magmatic plumbing system below Ischia

Regardless of their disequilibrium relations with the host rock, the mineral phases in the Arso lavas allow us to make some conclusions about the Ischia magmatic system. In most clinopyroxene crystals, Ti and Al contents increase, while Si, Mg and Na decrease from the core to the rim. According to Wass (1979), these features are typical of low-pressure crystallization and indeed, taking into account the distribution between Al^{IV} and Al^{VI} (Fig. 4e), none of the analyzed Cpx seems to have formed at high pressure, a common feature at Ischia and Cfc (Melluso et al., 2012, 2014). The calculated equilibration pressure of clinopyroxene in equilibrium (Putirka, 2008) provides a pressure range of 0.2–0.9 kbar, which implies depths to only three km. Furthermore, the increasing of Ti and Al at decreasing Mg# values (Fig. 4b and c), and the absence of a correlation between Ca and Mg (Fig. 4d) in Arso lava cpx can be explained by the absence of a significant co-precipitation of Ti-magnetite and plagioclase. The Fe^{3+} - Fe^{2+} -Mg variations in phlogopite indicate a low oxidized fugacity close to the

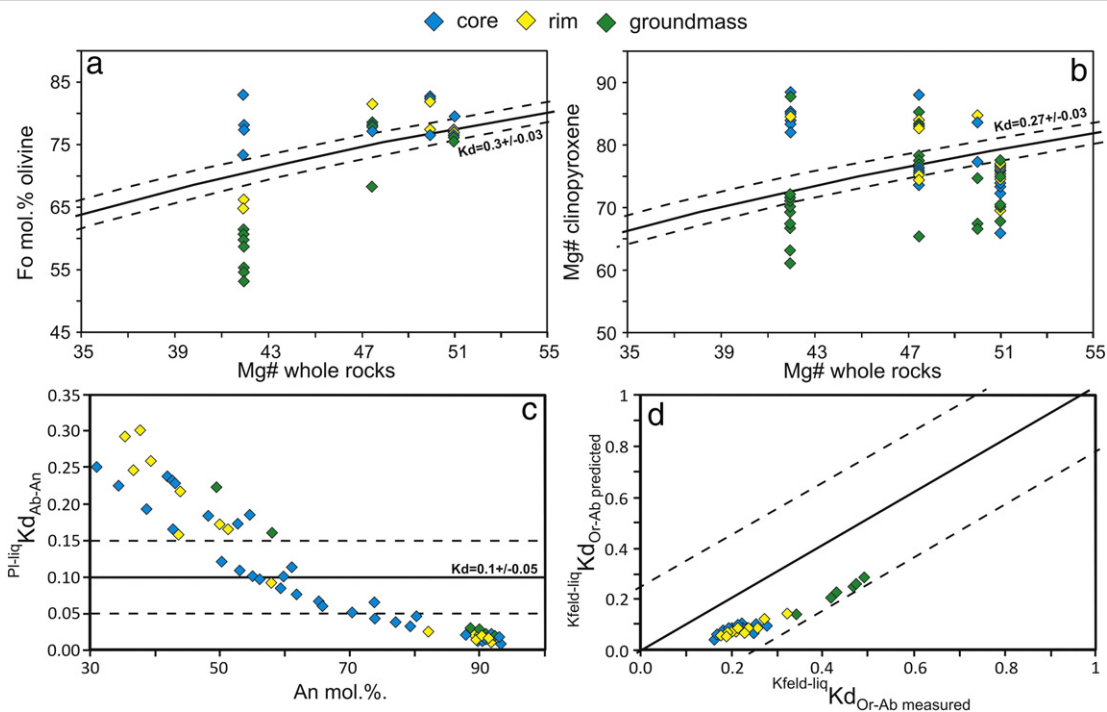


Fig. 11. a) Fe-Mg partitioning between olivine and host rock ($^{Fe/Mg}Kd^{Ol-liq} = 0.27-0.33$; Roeder and Emslie, 1970; Matzen et al., 2011); b) Fe-Mg partitioning between clinopyroxene and host rock ($^{Fe/Mg}Kd^{Cpx-liq} = 0.27 \pm 0.03$; Grove and Bryan, 1983; Sisson and Grove, 1993; Putirka et al., 2003; Mollo et al., 2013); c) variation diagram of An (mol%) vs calculated $^{Pl-liq}Kd_{Ab-An}$. The plagioclase-melt stability field was drawn using a value for $^{Pl-melt}Kd_{Ab-An}$ of 0.1 ± 0.05 (Putirka, 2008); d) $^{Kfeld-liq}Kd_{Or-Ab}$ test for equilibrium based on Or-Ab exchange between K-feldspar and liquid (Mollo et al., 2015).

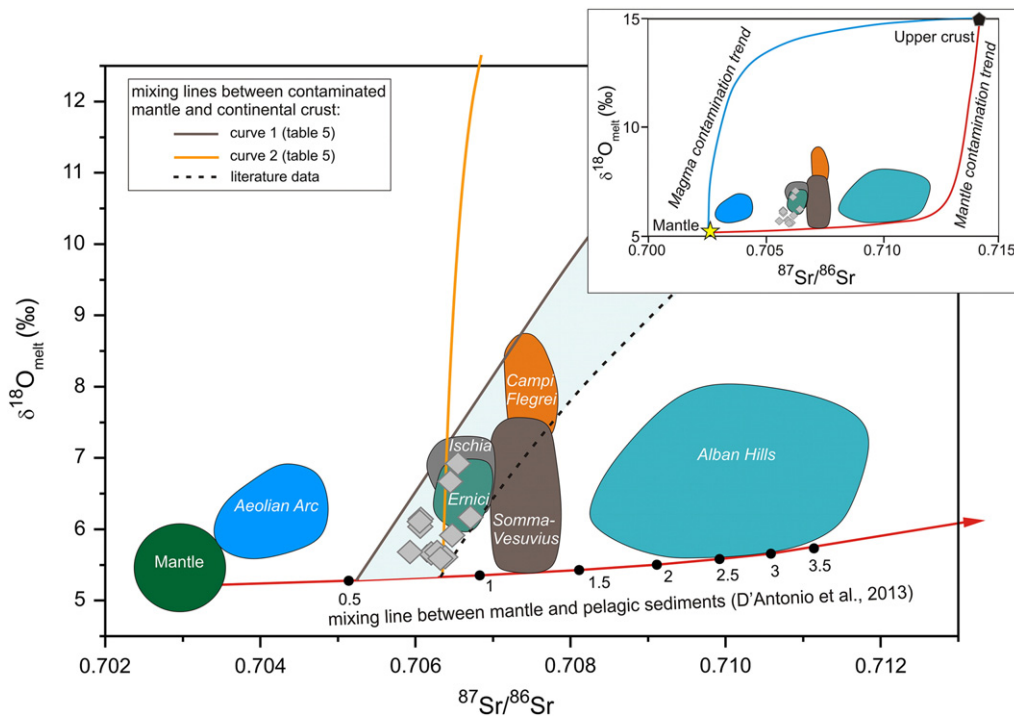


Fig. 12. $\delta^{18}O$ versus $^{87}Sr/^{86}Sr$ binary diagram for the Arso volcanic rocks compared with data from other volcanic centers from the Italian peninsula after correction of $\delta^{18}O$ data. The red curve represents a source enrichment process involving MORB mantle to which fluids/melts from pelagic sediments have been added in different percentages while the blue curve represents a magma contamination involving continental crust (see D'Antonio et al., 2013 for numerical parameters used in the modeling). The orange and gray curves represent modeled AFC processes involving a primitive magma segregated by the subduction-modified mantle sector below Ischia, that crystallizes and assimilates continental crust (see table 5 for numerical parameters used in the modeling). The dash black curve represents the results of a literature EC-AFC processes proposed for Ischia volcanic rocks (D'Antonio et al., 2013). See text for further details (Campi Flegrei are own unpublished data; Ischia data are from D'Antonio et al. (2013); Somma-Vesuvius are from Santacroce et al. (1993), Cioni et al. (1995), Piochi et al. (2006), and Dallai et al. (2011), Alban Hills are from Dallai et al. (2004), Gaeta et al. (2006), and Di Rocco et al. (2012); Ernici are from Frezzotti et al. (2007); Aeolian Arc are from Peccerillo et al. (2004) and Santo and Peccerillo (2008); mantle data are from Matthey et al. (1994) and Eiler (2001).

Table 5
Parameters and results of the isotopic modeling of EC-AFC processes of the Arso product.

Curve 1			Curve 2		
Teq	1000	°C	Teq	1000	°C
Tlm	1400	°C	Tlm	1400	°C
Tm0	1350	°C	Tm0	1350	°C
Tla	980	°C	Tla	980	°C
Ta0	400	°C	Ta0	400	°C
Ts	750	°C	Ts	750	°C
Cpm	1484	J/kg K	Cpm	1484	J/kg K
Cpa	1388	J/kg K	Cpa	1388	J/kg K
hcry	396000	J/kg	hcry	396000	J/kg
hfus	354000	J/kg	hfus	354000	J/kg
Magma	Sr (ppm)	⁸⁷ Sr/ ⁸⁶ Sr	Magma	Sr (ppm)	⁸⁷ Sr/ ⁸⁶ Sr
	500	0.7053		600	0.7063
	D ₀	δ ¹⁸ O		D ₀	δ ¹⁸ O
	1.1	5.4		0.5	5.4
	Assimilant	⁸⁷ Sr/ ⁸⁶ Sr		Assimilant	⁸⁷ Sr/ ⁸⁶ Sr
280	0.713	50	0.713		
D ₀	δ ¹⁸ O	D ₀	δ ¹⁸ O		
0.7	15	2	15		

Abbreviations: Teq = Equilibration temperature; Tlm = Magma liquidus temperature; Tm0 = Initial magma temperature; Tla = Wall-rock liquidus temperature; Ta0 = Initial Wall-rock temperature; Ts = Solidus, required to be the same for magma and assimilant; Cpm = Magma specific heat capacity; Cpa = Assimilant specific heat capacity; hcry = Crystallization enthalpy; hfus = Fusion enthalpy.

QFM and Ni-NiO buffer (Fig. 6b). This feature is also shown by other Ischia (and CFC) phlogopites, in agreement with oxygen fugacity values (based on spinel composition) just above the Ni-NiO buffer for mafic rocks and near the QFM buffer for more evolved rocks (Melluso et al., 2014). These latter authors did not find any difference in the oxidation state of magma of the PVD feeding system with respect to those of the other Italian peninsular magmatic provinces (see also Moretti et al., 2013). All these features suggest that the final crystallization of Arso magmas occurred at shallow (<3 km) depth in the magmatic plumbing system of Ischia. Distinct magma components resided in separate reservoirs filled with melts of variable chemical and isotopic composition and variable degrees of magmatic evolution in closed-to-open system under different crystallization conditions.

4. Conclusions

The overall geochemical, mineralogical and Sr-O isotopic characteristics of the rocks formed during the Arso eruption, along with those of the other known latitic products (Vateliero, Molarà and Cava Nocelle) emplaced at Ischia island over the past 3 ka, suggest a common history and a common set of magmatic processes. The most mafic magmas of this period are generated in a mantle source region modified by addition of ~1% of subducted sediments and later modified by crustal assimilation of Hercynian metaplutonic rocks from the overlying continental crust (up to 7%). The strong isotopic variability of the intermediate latitic magmas suggests that the activity of Ischia in the past three thousand years has been derived from distinctly different, small sized magma batches. For example, the hybrid latitic eruptions in the younger history of Ischia produced only small volumes of geochemically distinct rocks (<1 km³; de Vita et al., 2010). Thus, it is very likely that small batches of magmas of deep origin mixed during their ascent towards the surface, and in the process intercepted minerals accumulated from previous magmas. Such mixing processes are well recognizable through the Sr-isotopic signature of the end-members. The presented data leave open the possibility that, even during the present quiescence of the volcano, a small batch of magma coming from the source could reach the shallow plumbing system.

Acknowledgements

We are grateful to Malcolm Rutherford and Meritxell Aulinas for their reviews, which contributed to the improvement of this paper.

We thank R. Przybilla and N. Albrecht for O-isotope analyses and A. Pack and A. Kronz for making analytical facilities available to us. We are grateful to S. Rout for improving the quality of the English style. This work has been financially supported by the Italian Ministero dell'Università, Istruzione e Ricerca PRIN-COFIN 2008 grant (LC) and the Italian Dipartimento per la Protezione Civile (DPC) - Istituto Nazionale di Geofisica e Vulcanologia Project V3_3/03 "V3_3_Ischia" 2004–2006 grants (MD and GO), and DFG-project Wo 362/42-1 funded to G.W. This paper does not necessarily represent DPC official opinions and policies.

Appendix A. Supplementary data

Supplementary data to this article can be found online at <http://dx.doi.org/10.1016/j.jvolgeores.2016.08.008>.

References

- Acocella, V., Funicello, R., 2006. Transverse systems along the extensional Tyrrhenian margin of central Italy and their influence on volcanism. *Tectonics* 25, TC2003. <http://dx.doi.org/10.1029/2005TC001845>.
- Arienzo, I., Carandente, A., Di Renzo, V., Belviso, P., Civetta, L., D'Antonio, M., Orsi, G., 2013. Sr and Nd isotope analysis at the Radiogenic Isotope Laboratory of the Istituto Nazionale di Geofisica e Vulcanologia, Sezione di Napoli - Osservatorio Vesuviano. *Rapporti Tecnici INGV 260*, pp. 1–18 (available online at <http://istituto.ingv.it/lingv/produzionescientifica/rapporti-tecnici-ingv/archivio/rapporti-tecnici-2013/>).
- Bindeman, I.N., Ponomareva, V.V., Bailey, J.C., Valley, J.W., 2004. Volcanic arc of Kamchatka: a province with high-δ¹⁸O magma sources and large-scale ¹⁸O/¹⁶O depletion of the upper crust. *Geochim. Cosmochim. Acta* 68, 841–865.
- Bindeman, I., Gurenko, A., Sigmarsson, O., Chaussidon, M., 2008. Oxygen isotope heterogeneity and disequilibria of olivine crystals in large volume Holocene basalts from Iceland: evidence for magmatic digestion and erosion of Pleistocene hyaloclastites. *Geochim. Cosmochim. Acta* 72, 4397–4420.
- Brown, R.J., Orsi, G., de Vita, S., 2008. New insights into Late Pleistocene explosive volcanic activity and caldera formation on Ischia (southern Italy). *Bull. Volcanol.* 70, 583–603.
- Brown, R.J., Civetta, L., Arienzo, I., D'Antonio, M., Moretti, R., Orsi, G., Tomlinson, E.L., Albert, P.G., Menzies, M.A., 2014. Geochemical and isotopic insights into the assembly, evolution and disruption of a magmatic plumbing system before and after a cataclysmic caldera-collapse eruption at Ischia volcano (Italy). *Contrib. Mineral. Petrol.* 168, 1–23.
- Buchner, G., 1986. *Eruzioni vulcaniche e fenomeni vulcano-tettonici di età preistorica e storica nell'Isola d'Ischia*. In: AA., VV. (Eds.), *Eruptions volcaniques, tremblements de terre et vie des hommes dans la Campanie antique* Publ. 7. Centre Jean Bérard, a cultural organization in Naples, Italy, Napoli.
- Capuano, P., De Matteis, R., Russo, G., 2015. The structural setting of the Ischia Island Caldera (Italy): first evidence from seismic and gravity data. *Bull. Volcanol.* 77, 97.
- Chalokwu, C.I., Ripley, E.M., Park, Y.R., 1999. Oxygen isotopic systematics of an open-system magma chamber: an example from the Freetown Layered Complex of Sierra Leone. *Geochim. Cosmochim. Acta* 63, 675–685.
- Chiesa, S., Poli, S., Vezzoli, L., 1986. Studio dell'ultima eruzione storica dell'isola di Ischia. *Boll. GNV* 1, 153–166.
- Cioni, R., Civetta, L., Marianelli, P., Métrich, N., Santacroce, R., Sbrana, A., 1995. Compositional layering and syn-eruptive mixing of a periodically refilled shallow magma chamber: the AD 79 Plinian eruption of Vesuvius. *J. Petrol.* 36, 739–776.
- Civetta, L., Gallo, G., Orsi, G., 1991. Sr- and Nd-isotope and trace-element constraints on the chemical evolution of the magmatic system of Ischia (Italy) in the last 55 ka. *J. Volcanol. Geotherm. Res.* 46, 213–230.
- Crisci, G.M., De Francesco, A.M., Mazzuoli, R., Poli, G., Stanzione, D., 1989. Geochemistry of recent volcanics of Ischia Island, Italy: evidences for fractional crystallization and magma mixing. *Chem. Geol.* 78, 15–33.
- D'Antonio, M., Taroni, S., Arienzo, I., Civetta, L., Di Renzo, V., 2007. Components and processes in the magma genesis of the Phlegrean Volcanic District, southern Italy. In: Beccalusa, L., Bianchini, G., Wilson, M. (Eds.), *Cenozoic Volcanism in the Mediterranean Area*: Boulder, CO. Geological Society of America Special Papers 418, pp. 203–220.
- D'Antonio, M., Taroni, S., Arienzo, I., Civetta, L., Dallai, L., Moretti, R., Orsi, G., Andria, M., Trecalli, A., 2013. Mantle and crustal processes in the magmatism of the Campania region: inferences from mineralogy, geochemistry, and Sr-Nd-O isotopes of young hybrid volcanics of the Ischia island (South Italy). *Contrib. Mineral. Petrol.* 165, 1173–1194.
- Dallai, L., Ghezzi, C., Sharp, Z.D., 2003. Oxygen isotope evidence for crustal assimilation and magma mixing in the Granite Harbour Intrusives, Northern Victoria Land, Antarctica. *Lithos* 67, 135–151.
- Dallai, L., Freda, C., Gaeta, M., 2004. Oxygen isotope geochemistry of pyroclastic clinopyroxene monitors carbonate contributions to Roman-type ultrapotassic magmas. *Contrib. Mineral. Petrol.* 148, 247–263.
- Dallai, L., Cioni, R., Boschi, C., D'Orlando, C., 2011. Carbonate-derived CO₂ purging magma at depth: influence on the eruptive activity of Somma-Vesuvius, Italy. *Earth Planet. Sci. Lett.* 310, 84–95.
- de Vita, S., Sansivero, F., Orsi, G., Marotta, E., 2006. Cyclical slope instability and volcanism related to volcano-tectonism in resurgent calderas: the Ischia Island (Italy) case study. *Eng. Geol.* 86, 148–165.

Chapter 2: Source and magmatic evolution inferred from geochemical and Sr-O-isotope data on hybrid lavas of Arso, the last eruption at Ischia island (Italy; 1302 AD)

- de Vita, S., Sansivero, F., Orsi, G., Marotta, E., Piochi, M., 2010. Volcanological and structural evolution of the Ischia resurgent caldera (Italy) over the past 10 ky. In: Groppelli, G., Viereck-Goette, L. (Eds.), *Stratigraphy and Geology of Volcanic Areas*: Boulder, CO. Geological Society of America Special Papers 464, pp. 193–241.
- Della Seta, M., Marotta, E., Orsi, G., De Vita, S., Sansivero, F., Fredi, P., 2012. Slope instability induced by volcano-tectonics as an additional source of hazard in active volcanic areas: the case of Ischia island (Italy). *Bull. Volcanol.* 74, 79–106.
- Di Girolamo, P., Melluso, L., Morra, V., Secchi, F.A.G., 1995. Evidence of interaction between mafic and differentiated magmas in the youngest phase of activity at Ischia island (Italy). *Period. Mineral.* 64, 393–411.
- Di Napoli, R., Federico, C., Aiuppa, A., D'Antonio, M., Valenza, M., 2013. Quantitative models of hydrothermal fluid-mineral reaction: the Ischia case. *Geochim. Cosmochim. Acta* 105, 108–129.
- Di Renzo, V., Di Vito, M.A., Arienzo, I., Carandente, A., Civetta, L., D'Antonio, M., Giordano, F., Orsi, G., Tonarini, S., 2007. Magmatic history of Somma-Vesuvius on the basis of new geochemical and isotopic data from a deep borehole (Camaldoli della Torre). *J. Petrol.* 48, 753–784.
- Di Renzo, V., Arienzo, I., Civetta, L., D'Antonio, M., Tonarini, S., Di Vito, M.A., Orsi, G., 2011. The magmatic feeding system of the Campi Flegrei caldera: architecture and temporal evolution. *Chem. Geol.* 281, 227–241.
- Di Rocco, T., Freda, C., Gaeta, M., Mollo, S., Dallai, L., 2012. Magma chambers emplaced in carbonate substrate: petrogenesis of skarn and cumulate rocks and implications for CO₂ degassing in volcanic areas. *J. Petrol.* 1–26.
- Di Stefano, R., Bianchi, I., Ciaccio, M.G., Carrara, G., Kissling, E., 2011. Three-dimensional Moho topography in Italy: new constraints from receiver functions and controlled source seismology. *Geochem. Geophys. Geosyst.* 12. <http://dx.doi.org/10.1029/2011GC003649>.
- Eiler, J.M., 2001. Oxygen isotope variations of basaltic lavas and upper mantle rocks. In: Valley, J.W., Cole, D.R. (Eds.), *Stable Isotope Geochemistry*. Mineralogical Society of America and Reviews in Mineralogy and Geochemistry 43, pp. 319–364.
- Ellam, R.M., Harmon, R.S., 1990. Oxygen isotope constraints on the crustal contribution to the subduction-related magmatism of the Aeolian Islands, southern Italy. *J. Volcanol. Geotherm. Res.* 44, 105–122.
- Forcella, E., Gnaccolini, M., Vezzoli, L., 1981. Stratigrafia e sedimentologia dei depositi piroclastici affioranti nel settore sudoccidentale dell'isola d'Ischia. *Riv. Ital. Paleontol. Stratigr.* 87, 329–366.
- Forcella, E., Gnaccolini, M., Vezzoli, L., 1983. I depositi piroclastici del settore sudorientale dell'isola d'Ischia (Italia). *Riv. Ital. Paleontol. Stratigr.* 89, 1–35.
- Frezzotti, M.L., De Astis, G., Dallai, L., Ghezzi, C., 2007. Coexisting calcalkaline and ultrapotassic magmatism at Monti Ernici, Mid Latina Valley (Latium, central Italy). *Eur. J. Mineral.* 19, 479–497.
- Gaeta, M., Freda, C., Christensen, J.N., Dallai, L., Marra, F., Karner, D.B., Scarlato, P., 2006. Time-dependent geochemistry of clinopyroxene from the Alban Hills (Central Italy): clues to the source and evolution of ultrapotassic magmas. *Lithos* 86, 330–346.
- Gale, A., Dalton, C.A., Langmuir, C.H., Su, Y., Schilling, J.G., 2013. The mean composition of ocean ridge basalts. *Geochem. Geophys. Geosyst.* 14, 489–518.
- Gebauer, S.K., Schmitt, A.K., Pappalardo, L., Stockli, D.F., Lovera, O.M., 2014. Crystallization and eruption ages of Breccia Museo (Campi Flegrei caldera, Italy) plutonic clasts and their relation to the Campanian ignimbrite. *Contrib. Mineral. Petrol.* 167, 1–18.
- Goldstein, S.L., Deines, P., Oelkers, E.H., Rudnick, R.L., Walter, L.M., 2003. Standards for publication of isotope ratio and chemical data in *Chemical Geology*. *Chem. Geol.* 202, 1–4.
- Grove, T.L., Bryan, W.B., 1983. Fractionation of pyroxene-phyric MORB at low pressure: an experimental study. *Contrib. Mineral. Petrol.* 84, 293–309.
- Handley, H.K., Macpherson, C.G., Davidson, J.P., 2010. Geochemical and Sr-O isotopic constraints on magmatic differentiation at Gede Volcanic Complex, West Java, Indonesia. *Contrib. Mineral. Petrol.* 159, 885–908.
- Ininga, D.D., Tamburrino, S., Lirer, F., Vezzoli, L., Barra, M., De Lange, G.J., Tiepolo, M., Vallefucio, M., Mazzola, S., Sprovieri, M., 2014. Tephrochronology of the astronomically tuned KC01B deep-sea core, Ionian Sea: insights into the explosive activity of the Central Mediterranean area during the last 200 ka. *Quat. Sci. Rev.* 85, 63–84.
- James, D.E., 1981. The combined use of oxygen and radiogenic isotopes as indicators of crustal contamination. *Annu. Rev. Earth Planet. Sci.* 9, 311–344.
- Lackey, J.S., Valley, J.W., Chen, J.H., Stockli, D.F., 2008. Dynamic magma systems, crustal recycling, and alteration in the central Sierra Nevada batholith: the oxygen isotope record. *J. Petrol.* 49, 1397–1426.
- Le Bas, M.J., Le Maitre, R.W., Streckeisen, A., Zanettin, B., 1986. A chemical classification of volcanic rocks based on the total alkali-silica diagram. *J. Petrol.* 27, 745–750.
- Lodders, K., Palme, H., Gail, H.P., 2009. *Abundances of the elements in the Solar System*. Solar System. Springer, Berlin Heidelberg, pp. 712–770.
- Lustrino, M., Duggen, S., Rosenberg, C.L., 2011. The Central-Western Mediterranean: anomalous igneous activity in an anomalous collisional tectonic setting. *Earth Sci. Rev.* 104, 1–40.
- Lyubetskaya, T., Korenaga, J., 2007. Chemical composition of Earth's primitive mantle and its variance: 1. Method and results. *J. Geophys. Res. Solid Earth* 112 (B3).
- Mattey, D., Lowry, D., Macpherson, C., 1994. Oxygen isotope composition of mantle peridotite. *Earth Planet. Sci. Lett.* 128, 231–241.
- Matzen, A.K., Baker, M.B., Beckett, J.R., Stolper, E.M., 2011. Fe–Mg partitioning between olivine and high-magnesian melts and the nature of Hawaiian parental liquids. *J. Petrol.* 52, 1243–1263.
- Mazzeo, F.C., D'Antonio, M., Arienzo, I., Aulinas, M., Di Renzo, V., Gimeno, D., 2014. Subduction-related enrichment of the Neapolitan volcanoes (Southern Italy) mantle source: new constraints on the characteristics of the slab-derived components. *Chem. Geol.* 386, 165–183.
- McKinney, C.R., McCrea, J.M., Epstein, S., Allen, H.A., Urey, H.C., 1950. Improvements in mass spectrometers for the measurement of small differences in isotope abundance ratios. *Rev. Sci. Instrum.* 21, 724–730.
- Melluso, L., De Gennaro, R., Fedele, L., Franciosi, L., Morra, V., 2012. Evidence of crystallization in residual, Cl-F-rich, apatitic, trachyphonolitic magmas and primitive Mg-rich basalt-trachyphonolite interaction in the lava domes of the Phlegraean Fields (Italy). *Geol. Mag.* 149, 532–550.
- Melluso, L., Morra, V., Guarino, V., De Gennaro, R., Franciosi, L., Grifa, C., 2014. The crystallization of shoshonitic to peralkaline trachyphonolitic magmas in a H₂O–Cl–F-rich environment at Ischia (Italy), with implications for the feeder system of the Campania Plain volcanoes. *Lithos* 210, 242–259.
- Middlemost, E.A.K., 1989. Iron oxidation ratios, norms and the classification of volcanic rocks. *Chem. Geol.* 77, 19–26.
- Mollo, S., Putirka, K., Misiti, V., Soligo, M., Scarlato, P., 2013. A new test for equilibrium based on clinopyroxene–melt pairs: clues on the solidification temperatures of eutectic alkaline melts at post-eruptive conditions. *Chem. Geol.* 352, 92–100.
- Mollo, S., Masotta, M., Forni, F., Bachmann, O., De Astis, G., Moore, G., Scarlato, P., 2015. A K-feldspar-liquid hygrometer specific to alkaline differentiated magmas. *Chem. Geol.* 392, 1–8.
- Moretti, R., Arienzo, I., Orsi, G., Civetta, L., D'Antonio, M., 2013. The deep plumbing system of Ischia: a physico-chemical window on the fluid-saturated and CO₂-sustained Neapolitan volcanism (southern Italy). *J. Petrol.* 54, 951–984.
- Orsi, G., Gallo, G., Zanchi, A., 1991. Simple-shearing block resurgence in caldera depressions. A model from Pantelleria and Ischia. *J. Volcanol. Geotherm. Res.* 47, 1–11.
- Orsi, G., Piochi, M., Campajola, L., D'Onofrio, A., Gialanella, L., Terrasi, F., 1996. ¹⁴C geochronological constraints for the volcanic history of the island of Ischia (Italy) over the last 5000 years. *J. Volcanol. Geotherm. Res.* 71, 249–257.
- Orsi, G., de Vita, S., Di Vito, M.A., Isaia, R., Nave, R., Heiken, G., 2003. Facing volcanic and related hazards in the Neapolitan area. In: Heiken, G., Fakundiny, R., Sutter, J. (Eds.), *Earth Sciences in the Cities: A Reader*. American Geophysical Union Special Publication Series 56, pp. 121–170.
- Pack, A., Tanaka, R., Hering, M., Sengupta, S., Peters, S., Nakamura, E., 2016. The oxygen isotope composition of San Carlos olivine on the VSMOW2-SLAP2 scale. *Rapid Communications Mass Spectrometry* 30, 1495–1504. <http://dx.doi.org/10.1002/rcm.7582>.
- Paoletti, V., D'Antonio, M., Rapolla, A., 2013. The structural setting of the Ischia Island (Phlegraean Volcanic District, Southern Italy): inferences from geophysics and geochemistry. *J. Volcanol. Geotherm. Res.* 249, 155–173.
- Pappalardo, L., Piochi, M., D'Antonio, M., Civetta, L., Petrini, R., 2002. Evidence for multi-stage magmatic evolution during the past 60 kyr at Campi Flegrei (Italy) deduced from Sr, Nd and Pb isotope data. *J. Petrol.* 43, 1415–1434.
- Peccerillo, A., Dallai, L., Frezzotti, M.L., Kempton, P.D., 2004. Sr–Nd–Pb–O isotopic evidence for decreasing crustal contamination with ongoing magma evolution at Alicudi volcano (Aeolian arc, Italy): implications for style of magma-crust interaction and for mantle source compositions. *Lithos* 78, 217–233.
- Petrosino, P., Jicha, B.R., Mazzeo, F.C., Ermolli, E.R., 2014. A high resolution tephrochronological record of MIS 14–12 in the Southern Apennines (Acerno Basin, Italy). *J. Volcanol. Geotherm. Res.* 274, 34–50.
- Petrosino, P., Jicha, B.R., Mazzeo, F.C., Ciaranfi, N., Girono, A., Maiorano, P., Marino, M., 2015. The Montalbano Jonico marine succession: an archive for distal tephra layers at the Early–Middle Pleistocene boundary in southern Italy. *Quat. Int.* 383, 89–103.
- Piochi, M., Civetta, L., Orsi, G., 1999. Mingling in the magmatic system of Ischia (Italy) in the past 5 ka. *Mineral. Petrol.* 66, 227–258.
- Piochi, M., Ayuso, R.A., De Vivo, B., Somma, R., 2006. Crustal contamination and crystal entrapment during polybaric magma evolution at Mt. Somma-Vesuvius volcano, Italy: geochemical and Sr isotope evidence. *Lithos* 86, 303–329.
- Piochi, M., Kilburn, C.R.J., Di Vito, M.A., Mormone, A., Tramelli, A., Troise, C., De Natale, G., 2014. The volcanic and geothermally active Campi Flegrei caldera: an integrated multidisciplinary image of its buried structure. *Int. J. Earth Sci.* 103, 401–421.
- Poli, S., Chiesa, S., Gillot, P.Y., Gregnanin, A., Guichard, F., 1987. Chemistry versus time in the volcanic complex of Ischia (Gulf of Naples, Italy): evidence of successive magmatic cycles. *Contrib. Mineral. Petrol.* 95, 322–335.
- Poli, S., Chiesa, S., Gillot, P.Y., Guichard, F., Vezzoli, L., 1989. Time dimension in the geochemical approach and hazard estimates of a volcanic area: the isle of Ischia case (Italy). *J. Volcanol. Geotherm. Res.* 36, 327–335.
- Putirka, K.D., 2008. Thermometers and barometers for volcanic systems. *Rev. Mineral. Geochem.* 69, 61–120.
- Putirka, K., Ryerson, F.J., Mikaelian, H., 2003. New igneous thermobarometers for mafic and evolved lava compositions, based on clinopyroxene + liquid equilibria. *Am. Mineral.* 88, 1542–1554.
- Rittman, A., Gottini, V., 1980. L'isola d'Ischia. *Geologia Bollettino. Serv. Geol. Ital.* 101, 131–274.
- Roeder, P.L., Emslie, R., 1970. Olivine-liquid equilibrium. *Contrib. Mineral. Petrol.* 29, 275–289.
- Rosi, M., Sbrana, A., Vezzoli, L., 1988. Correlazioni tefrostratigrafiche di alcuni livelli di Ischia, Procida e Campi Flegrei. *Mem. Soc. Geol. Ital.* 41, 1015–1027.
- Santacroce, R., Bertagnini, A., Civetta, L., Landi, P., Sbrana, A., 1993. Eruptive dynamics and petrogenetic processes in a very shallow magma reservoir: the 1906 eruption of Vesuvius. *J. Petrol.* 34, 383–425.
- Santo, A.P., Peccerillo, A., 2008. Oxygen isotopic variation in the clinopyroxene from the Filicudi volcanic rocks (Aeolian Islands, Italy): implications for open-system magma evolution. *Open Mineral. J.* 2, 22–33.
- Sbrana, A., Fulignati, P., Marianelli, P., Boyce, A.J., Cecchetti, A., 2009. Exhumation of an active magmatic-hydrothermal system in a resurgent caldera environment: the example of Ischia (Italy). *J. Geol. Soc.* 166, 1061–1073.
- Sisson, T.W., Grove, T.L., 1993. Experimental investigations of the role of water in calcalkaline differentiation and subduction zone magmatism. *Contrib. Mineral. Petrol.* 113, 143–166.

Chapter 2: Source and magmatic evolution inferred from geochemical and Sr-O-isotope data on hybrid lavas of Arso, the last eruption at Ischia island (Italy; 1302 AD)

- Spera, F.J., Bohron, W.A., 2001. Energy-constrained open-system magmatic processes I: general model and energy-constrained assimilation and fractional crystallization (EC-AFC) formulation. *J. Petrol.* 42, 999–1018.
- Stormer, J.C., Nicholls, J., 1978. XLFAC: a program for the interactive testing of magmatic differentiation models. *Comput. Geosci.* 4, 143–159.
- Taylor, H.P., Sheppard, S.M.F., 1986. Igneous rocks; I, processes of isotopic fractionation and isotope systematics. *Rev. Mineral. Geochem.* 16, 227–271.
- Tomlinson, E.L., Arienzo, I., Civetta, L., Wulf, S., Smith, V.C., Hardiman, M., Lane, S.S., Carandente, A., Orsi, G., Rosi, M., Muller, W., Menzies, M.A., 2012. Geochemistry of the Phlegraean Fields (Italy) proximal sources for major Mediterranean tephra: implications for the dispersal of Plinian and co-ignimbritic components of explosive eruptions. *Geochim. Cosmochim. Acta* 93, 102–128.
- Tomlinson, E.L., Albert, P.G., Wulf, S., Brown, R.J., Smith, V.C., Keller, J., Orsi, G., Bourne, A.J., Menzies, M.A., 2014. Age and geochemistry of tephra layers from Ischia, Italy: constraints from proximal-distal correlations with Lago Grande di Monticchio. *J. Volcanol. Geotherm. Res.* 287, 22–39.
- Tonarini, S., Leeman, W.P., Civetta, L., D'Antonio, M., Ferrara, G., Necco, A., 2004. B/Nb and $\delta^{11}\text{B}$ systematics in the Phlegraean Volcanic District, Italy. *J. Volcanol. Geotherm. Res.* 133, 123–139.
- Turi, B., Taylor Jr., H.P., Ferrara, G., 1991. Comparisons of $^{18}\text{O}/^{16}\text{O}$ and $^{87}\text{Sr}/^{86}\text{Sr}$ in volcanic rocks from the Pontine Islands, M. Ernici, and Campania with other areas in Italy. In: Taylor, H.P., O'Neil, J.R., Kaplan, I.R. (Eds.), *Stable Isotope Geochemistry: A Tribute to Samuel Epstein*. Geochemical Society Special Publications 3, pp. 325–337.
- Van Soest, M.C., Hilton, D.R., Macpherson, C.G., Matthey, D.P., 2002. Resolving sediment subduction and crustal contamination in the Lesser Antilles Island Arc: a combined He-O-Sr isotope approach. *J. Petrol.* 43, 143–170.
- Vezzoli, L., 1988. Island of Ischia. Quaderni de "La Ricerca Scientifica". Consiglio Naz. Ricerche 114 (10) (122 pp.).
- Vezzoli, L., Principe, C., Malfatti, J., Arrighi, S., Tanguy, J.-C., Le Goff, M., 2009. Modes and times of caldera resurgence: the <10 ka evolution of Ischia Caldera, Italy, from high-precision archaeomagnetic dating. *J. Volcanol. Geotherm. Res.* 186, 305–319.
- Wass, S.Y., 1979. Multiple origin of clinopyroxenes in alkali basaltic rocks. *Lithos* 12, 115–132.
- Wolff, J.A., Grandy, J.S., Larson, P.B., 2000. Interaction of mantle-derived magma with island crust? Trace element and oxygen isotope data from the Diego Hernandez Formation, Las Canadas, Tenerife. *J. Volcanol. Geotherm. Res.* 103, 343–366.
- Wones, D.R., Eugster, H.P., 1965. Stability of biotite: experiment, theory, and application. *Am. Mineral.* 50, 1228–1272.
- Wörner, G., Staudigel, H., Zindler, A., 1985. Isotopic constraints on open system evolution of the Laacher See magma chamber (Eifel, West Germany). *Earth Planet. Sci. Lett.* 75, 37–49.
- Zaniboni, F., Pagnoni, G., Tinti, S., Della Seta, M., Fredi, P., Marotta, E., Orsi, G., 2013. The potential failure of Monte Nuovo at Ischia Island (Southern Italy): numerical assessment of a likely induced tsunami and its effects on a densely inhabited area. *Bull. Volcanol.* 75, 763.

Chapter 3: Coupled $\delta^{18}\text{O}$ - $\delta^{17}\text{O}$ and $^{87}\text{Sr}/^{86}\text{Sr}$ isotope compositions suggest a radiogenic and ^{18}O -enriched magma source for Neapolitan volcanoes (Southern Italy)

Raffaella Silvia Iovine^(1,*), Fabio Carmine Mazzeo⁽²⁾, Gerhard Wörner⁽¹⁾, Carlo Pelullo⁽²⁾, Gianluca Cirillo⁽³⁾, Ilenia Arienzo⁽⁴⁾, Andreas Pack⁽¹⁾, Massimo D'Antonio^(2,4)

(1) Geowissenschaftliches Zentrum, Georg-August-Universität, Göttingen, Germany

(2) Dipartimento di Scienze della Terra, dell'Ambiente e delle Risorse, University Federico II of Naples, Italy

(3) Istituto comprensivo Luigi Credaro Livigno Plazal dali Sckòla, 77 - 23030 Livigno, Italy

(4) Istituto Nazionale di Geofisica e Vulcanologia - sezione di Napoli Osservatorio Vesuviano, Naples, Italy

* corresponding author: raffaella-silvia.iovine@geo.uni-goettingen.de

Abstract

The role and the relative importance of sediment subduction versus crustal assimilation in magmatism of the Campanian volcanic district, including Vesuvius and Campi Flegrei, has always been contentious. Here we use isotopic ($^{87}\text{Sr}/^{86}\text{Sr}$ and $^{18}\text{O}/^{16}\text{O} - ^{17}\text{O}/^{16}\text{O}$) data on separated minerals (feldspar, Fe-cpx, Mg-cpx, olivine phenocrysts) from pyroclastic and lava products of the Neapolitan volcanic area (Phlegrean Volcanic District and Mt. Somma Vesuvius complex, Southern Italy) and constrain that the mantle source was enriched by no more than 1.5% and 40% of subducted sediments and fluids, respectively. Sr-O-isotope values of Campi Flegrei and Mt. Somma Vesuvius magmas together form one vertical trend in Sr-O isotope space that deviates profoundly from all other worldwide subduction-related magmas. Magmatic oxygen isotope ratios recalculated from olivine and clinopyroxene phenocrysts that were in equilibrium with mantle-derived magmas have $\delta^{18}\text{O}$ up to almost 9‰ relative to SMOW, compositions that are very different from those of typical mantle sources. These results suggest that magmas from the Neapolitan volcanoes were derived from 1) a mantle source contaminated by no more than 10% of pelagic sediments and limestone that caused high $\delta^{18}\text{O}$ values but did not significantly affect the Sr-isotope composition, and 2) assimilation of Hercynian crust. In detail our modelings explain

the Sr-O isotope features of Campi Flegrei and Somma Vesuvius products by a maximum of ~12% and ~21% assimilation, respectively, of Hercynian crust into a mafic magma. Crustal assimilation by either carbonates, or altered pre-existing pyroclastic rocks can be excluded by the lack of a link between isotope data and major and trace element signatures. Assimilation by silicic rocks at deeper crustal levels remains a possibility but is difficult to reconcile with the mafic (Mg#=70) nature of host magmas of minerals analyzed. Triple oxygen isotope variations ($\Delta^{17}\text{O}$), including both $^{18}\text{O}/^{16}\text{O}$ and $^{17}\text{O}/^{16}\text{O}$ ratios in magmatic systems, are in agreement with these conclusions.

Keywords

Neapolitan Volcanoes; Radiogenic and stable isotopes; $\Delta^{17}\text{O}$ variations; Mantle enrichment; Crustal assimilation

1. Introduction

The isotopic composition of igneous rocks provide information about the processes and sources involved in their formation. In particular, combined radiogenic Sr- and stable O-isotopes are a powerful tool to distinguish between (a) enrichment of mantle magma sources by fluids and subducted lithosphere (altered oceanic crust and its sedimentary cover) and (b) crustal assimilation during magma ascent through the crust (e.g., Iovine et al. 2017 and references therein). In contrast to trace elements abundance ratios, which can be affected by melting and crystallization processes, Sr isotopes are insensitive to melting and crystallization processes and therefore directly record (mixtures of) the mantle and crust components of igneous rocks. $^{18}\text{O}/^{16}\text{O}$ ratios of natural materials are also widely used as proxies for geologic, biologic and hydrologic processes. ^{17}O is another, less utilized, stable isotope of oxygen whose abundance relative to ^{18}O and ^{16}O is often described as a departure from a reference line with a slope close to 0.5 on a triple oxygen isotope plot (Clayton et al. 1973; Clayton and Mayeda, 1983). Understanding the sources and the nature of open-system processes (e.g., crustal assimilation, magma chamber recharge, volatile exsolution, and magma mingling/mixing) in a magmatic feeding system of active volcanoes remains an important goal in igneous geochemistry.

We study whole rock and mineral Sr- and O isotope compositions ($^{87}\text{Sr}/^{86}\text{Sr}$ and $\delta^{18}\text{O}$ - $\delta^{17}\text{O}$) of volcanic deposits from the Campanian Volcanic Zone, including the Phlegrean Volcanic District (PVD) covering the Campi Flegrei (CF) caldera, the nearby volcanic islands of Ischia and Procida, as well as the Mt. Somma-Vesuvius (SV) complex in South Italy to constrain their magma sources and potential assimilation processes in the crust. $\Delta^{17}\text{O}$ ratios have been analyzed for the first time

on a large set of igneous samples and potential contaminant crustal minerals and rocks. This approach using triple oxygen isotope studies ($\Delta^{17}\text{O}$), which include the use of both $^{18}\text{O}/^{16}\text{O}$ and $^{17}\text{O}/^{16}\text{O}$ ratios, is tested to address the long-existing questions related to the sources of magmatism in the Neapolitan area, in particular relating to the nature of the contaminants (e.g., limestone). We thus address the important question whether or not limestone assimilation, leading to the generation of CO_2 -rich fluid phases, could increase the gas content of the magmas and enhance their potential for explosive eruptions. In addition, our new mineral data are compared with published $\delta^{18}\text{O}$ -isotope data from subduction zones worldwide in order to characterize and systemize their sources in Sr-O isotope space. Based on our observations, we propose that a major source for magmatism in this area is a mixture between subducted crustal material and limestone added in the mantle source and assimilation of Hercynian crust.

2. Geological setting and volcanic history

The Neapolitan volcanic area, located near the margin of the Campania Plain in Southern Italy, includes the PVD and the SV volcanic complexes (Fig. 1). This area has been the site of intense Plio-Quaternary magmatic activity related to subduction of the Ionian oceanic plate (Mazzeo et al. 2014 and references therein). Parent magmas in the Campanian Province (PVD and SV) are potassic (PVD) to ultrapotassic (SV) and derived from a phlogopite-bearing metasomatized (lithospheric?) mantle with MORB affinity that was enriched by subduction-related fluids and melts (e.g., Schiano et al. 2004; Mazzeo et al. 2014). Due to the explosive character and high frequency of volcanic events and the large population (>2.5 million) living in the Neapolitan area the risk and vulnerability from volcanic eruptions is among the highest on Earth.

The volcanic history of *Procida* island was revisited by De Astis et al. (2004) and Perrotta et al. (2010). They recognized five monogenetic volcanic edifices (Vivara, Terra Murata, Pozzo Vecchio, Fiumicello and Solchiaro; from the oldest to the youngest), covered by the products of later eruptions from nearby CF and Ischia (e.g. Rosi et al. 1988). Field evidence and available absolute ages constrain its volcanic activity between ~75 and ~22 ka for Solchiaro, the last recorded eruption (Morabito et al. 2014). Xenoliths of high-K basaltic composition in the Solchiaro tuff represent the least-evolved rocks of the whole PVD; other eruptive products on the island range from poorly evolved to intermediate trachy-basalt and latite; trachytes are rare (D'Antonio et al. 1999a; De Astis et al. 2004). The Sr-Nd isotopic composition of Procida products is variable; however, the scarcity of geochronological data does not allow identification of clear compositional trends through time.

Ischia is a volcanic island located at the NW corner of the Gulf of Naples (Fig. 1). The oldest dated rocks (150 ka) are poorly exposed along the southern coast. Volcanic products range in composition from shoshonite through latite to abundant trachyte and phonolite. After a long quiescence, the Mt. Epomeo Green Tuff eruption (55 ka) generated the most voluminous pyroclastic deposit on the island and the related caldera collapse caused subsidence of the central portion of the island below sea level (e.g., Orsi et al. 1991). The last 55 ka of activity on Ischia have been divided into three magmatic cycles based on stratigraphic, geochronological, geochemical, and Sr isotopic data (Brown et al. 2014, and references therein). Deformation, shape, and uplift of the Mt. Epomeo resurgent block have affected the distribution of the youngest volcanic centers of the last cycle (10 ka–1302 A.D.) which all cluster along the eastern margin of the resurgent block (Orsi et al. 1991). Only the Zaro eruption occurred in the NW of the island. This last cycle was characterized by the eruption of latitic to phonolitic magmas with a wide range of isotope compositions. Petrographic, geochemical and isotopic characteristics of the most recent latites erupted over the past 3 ka (Molara, Vateliero, Cava Nocelle and Arso eruptions) have been studied in most detail and suggest mingling and mixing among variably evolved, small magma batches, and the incorporation of crystals inherited from previous eruptions (e.g., Civetta et al. 1991; D'Antonio et al. 2013; Melluso et al. 2014; Iovine et al. 2017). The Arso eruption, the most widespread effusive eruption on the island in recent times (1302 A.D.) and the Casamicciola earthquakes (1883 and 2017 A.D.) were the latest major events on Ischia island.

Campi Flegrei (CF) volcanic activity began prior to 80 ka (Scarpati et al. 2013), fed by magmas ranging from shoshonite to (peralkaline) phonolite in composition. However, trachytes and phonolites are by far the most abundant rocks, accounting for more than 99 vol.% of the products (e.g., D'Antonio et al. 1999b; Melluso et al. 2012). Two large explosive eruptions accompanied by caldera collapse events, the Campanian Ignimbrite (CI, ~39 ka; Fedele et al. 2008 and references therein) and the Neapolitan Yellow Tuff (NYT, ~15 ka; Deino et al. 2004), are the most voluminous volcanic events and important stratigraphic markers, allowing for subdivision of the Campi Flegrei volcanic history into three periods: period I, pre-CI; period II, between CI and NYT; and period III, post-NYT (Orsi et al. 1996). In the past 15 kyr (period III) only, volcanic activity was characterized by at least 72 explosive eruptions of variable magnitude, fed by magma batches of less than 1 km³ of volume (Orsi et al. 2009; Smith et al. 2011). The last and only historic eruption occurred in 1538 A.D. after 3 ka of quiescence and produced the Monte Nuovo tuff cone (Guidoboni and Ciuccarelli, 2011 and references therein). Recent unrest started in the 1950s with subdued seismicity, slow continuous uplift, and changes in the geochemical parameters of

fumaroles and thermal springs (e.g., Chiodini et al. 2015; D’Auria et al. 2015 and references therein).

Petrographic, mineralogical, geochemical, and isotopic data on products spanning the history of the volcano have shown that CF magmatism is fed from compositionally highly variable magma batches. These distinct magmas were activated and accumulated from compositionally distinct smaller reservoirs due to recharge from deeper magma sources, and mixed and mingled prior to eruption of the large volume Campanian and Neapolitan Yellow Tuff Ignimbrite eruptions (e.g., Civetta et al. 1991; D’Antonio et al. 1999b, 2007; Pabst et al. 2008; Arienzo et al. 2016 and references therein; Di Renzo et al. 2011; Melluso et al. 2012).

Somma Vesuvius (SV) is a volcanic complex consisting of the older Mt. Somma volcano, which is deeply dissected by a caldera into which the modern Mt. Vesuvius was built. The oldest evidence for volcanic activity are lavas and tephra dated to > 30 ka (e.g. Sparice et al. 2017 and references therein). However, the present SV volcanic edifice formed just after the emplacement of the CI about 39 ka ago (Di Renzo et al. 2007 and references therein). The older period of activity (39-22

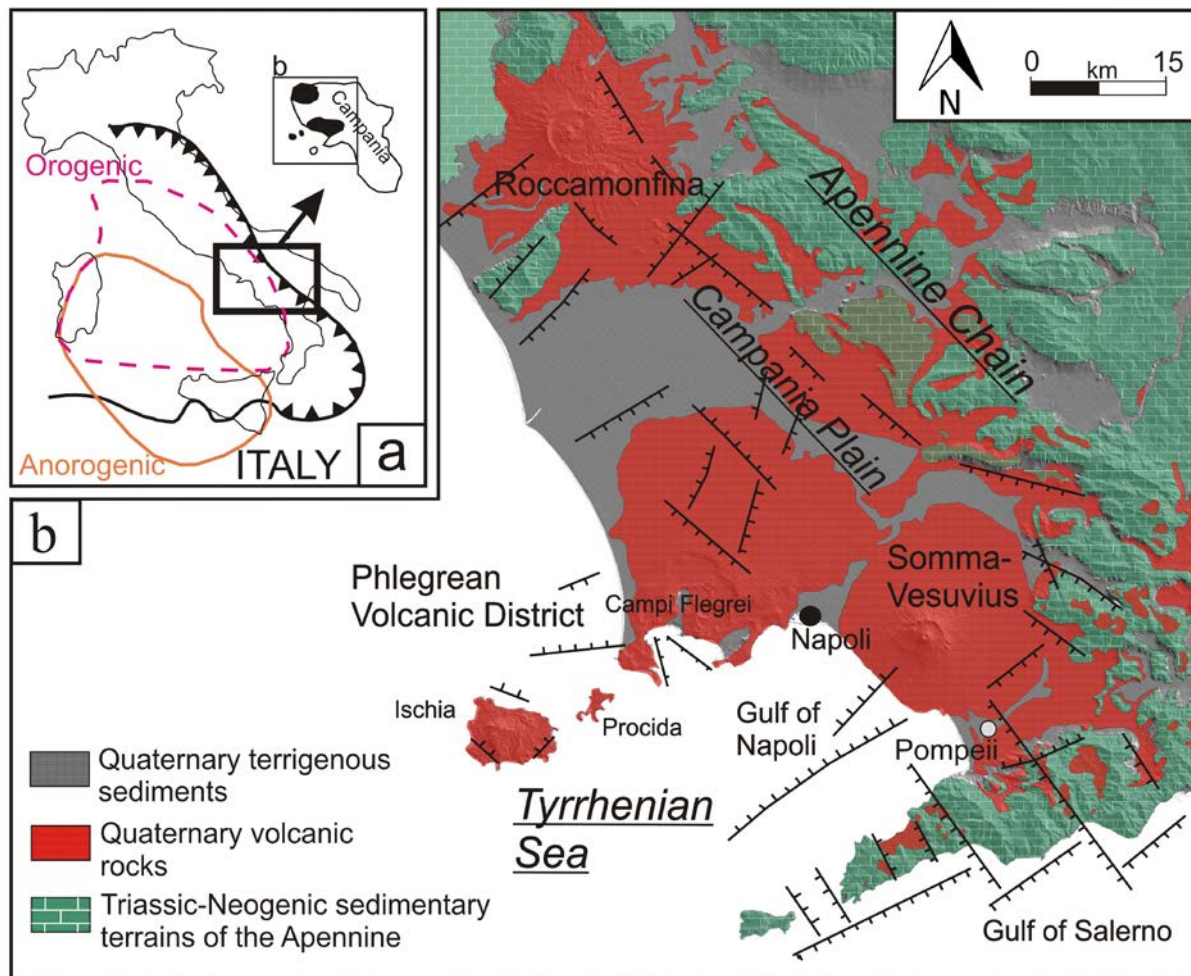


Fig. 1. Schematic geological and structural map of the Tyrrhenian margin of the Campania region (Mazzeo et al. 2014).

ka) built up the Mt. Somma stratovolcano, which is dominated by lava flows with rare low energy explosive events (e.g., Di Renzo et al. 2007; Santacroce et al. 2008; Sparice et al. in press). The collapse of the Mt. Somma volcano and formation of the caldera started with earliest major explosive Plinian eruption (Pomici di Base) at 22 ka (Santacroce et al. 2008) and was completed with the 79 A.D. Pompeii phonolitic eruption. Mt. Vesuvius has grown within this caldera after 79 A.D. eruption mostly by intermediate to mafic lava flows and tephra (leucite and leucite-tephrites) with low-energy open-conduit activity between the 1st and 3rd, 5th and 8th, 10th and 11th centuries. Lava emissions were interrupted by only two sub-Plinian events in 472 A.D. (Rosi and Santacroce, 1983) and 1631 Rolandi et al. 1993; Rosi et al. 1993). Since its last eruption in March 1944 Vesuvius has remained dormant without signs of unrest. Vesuvius rocks are mostly high potassic products, widely variable in terms of their silica undersaturation (e.g., Piochi et al. 2006, Di Renzo et al. 2007 and references therein).

3. Basement underlying the Neapolitan Area

Two NE-SW trending ridges define the Bay of Naples. A main alignment of conjugate NE-SW faults, named “Magnaghi-Sebeto line”, intersects several submarine volcanic banks and separates the bay in two sectors: (1) the NW sector (PVD) without evidence of limestone basement (e.g., Piochi et al. 2014) and (2) a SE sector (SV) where the occurrence of carbonate lithics in pyroclastic rocks is well documented (e.g., Del Moro et al. 2001). This is definitive evidence for a magma reservoir located within Meso-Cenozoic limestones and dolostones that also form the Apennine Mountains in Southern Italy. Although the near-surface Plio-Quaternary seismic stratigraphy of the Bay of Naples is well known, much less is known about the deep morphostructural features of the bay, especially in the CF area. Here, geological and geophysical data collected both at the surface and from boreholes (Capuano et al. 2013; Piochi et al. 2014, and references therein) show that the PVD caldera is filled with pyroclastic deposits interlayered with Quaternary marine and terrestrial sediments down to a depth of 2 km. The upper 500 m consist predominantly of partially consolidated tuffs that are strongly affected by diagenetic alteration. Denser rocks with evidence for a stronger thermo-metamorphic overprint occur between 2 and 4 km depth. A low velocity zone, about 1–2 km-thick was observed at around 8 km depth (Zollo et al. 2008) and interpreted as a zone containing partial melts. This depth agrees with petrologic data of melt inclusions of <15 ka old rocks that indicate volatile saturation at such depths (Mangiaccapra et al. 2008; Arienzo et al. 2010). According to the present model based on geochemical and isotopic evidence (e.g. D'Antonio

et al. 2007; Di Renzo et al. 2011), mafic magmas from the mantle stagnate, differentiate and partially assimilate continental crust at a depth of about 8 km. D'Antonio (2011) proposed that plutonic rocks (likely syenitic in compositions) intrude the crust between 8 to 4 km depth. From there, individual batches of evolved (trachytic) magmas rise to shallower (2-4 km) depth forming multiple reservoirs beneath each center where further evolution and mixing occurs (Arienzo et al. 2010). Single minor eruptions are fed from these reservoirs, whereas increased recharge from depth may result in amalgamation and accumulation of larger volumes of magma that are comprised of distinct compositional components and result in larger caldera-forming eruptions (CI and NYT; e.g. Pabst et al. 2008). For the SV, instead, the presence of metamorphosed carbonate xenoliths (Jolis et al. 2015) and the study of fluid inclusions of ejected nodules (Belkin and De Vivo, 1993) are clear indications of the presence of a shallow magma chamber located between 4 and 10 km b.s.l. within Mesozoic carbonate rocks. Results from deep drilling showed that the shallow structure beneath the volcano comprises 1.5-2 km of inter-bedded lavas and volcanoclastic, marine, and fluvial sedimentary rocks of Pleistocene age, overlying the Mesozoic limestone basement at 2.5-3 km of depth (e.g., Zollo et al. 2002). The Somma Vesuvius area is located on a less dissected and shallower carbonate basement and just outside the zone of intense extensional deformation affecting the PVD. These distinct geological settings can explain the development of different magma supply systems below SV and PVD, which are separated by a distance of only 10 km (Piochi et al., 2005). Whether or not the SV and PVD are fed from a common magmatic feeder zone at depth, is a matter of debate. The results of potential field (e.g., Paoletti et al. 2013) and seismic studies (e.g., Zollo et al. 2008) proposed a single, deep feeding system for the entire Neapolitan Volcanic area at 8–10 km depth. Even though the geochemistry of erupted magmas are largely similar and related to similar mantle sources (e.g., Peccerillo, 2001), geochemical data and the individual eruptive histories do not support this hypothesis. First, isotopic and geochemical features of parent magmas from all the Neapolitan volcanoes are generally similar even over much larger distances (D'Antonio et al. 2007; Di Renzo et al. 2007, 2011). However, in detail there are differences in the melting degrees in the mantle source (Schiano et al. 2004; Mazzeo et al. 2014). Moreover, the individual and distinct magma batches that reside in the middle to upper crust also argue for independent shallow plumbing systems. Finally, the temporal evolution of the different volcanic centers indicate their individual and separate volcanic history that cannot be related to one large common mid-crustal magma reservoir. Based on these observations and arguments, we hold that the relatively poor resolution of geophysical methods may be insufficient to distinguish between separate plumbing systems that are spatially and compositionally distinct but similar in physical properties.

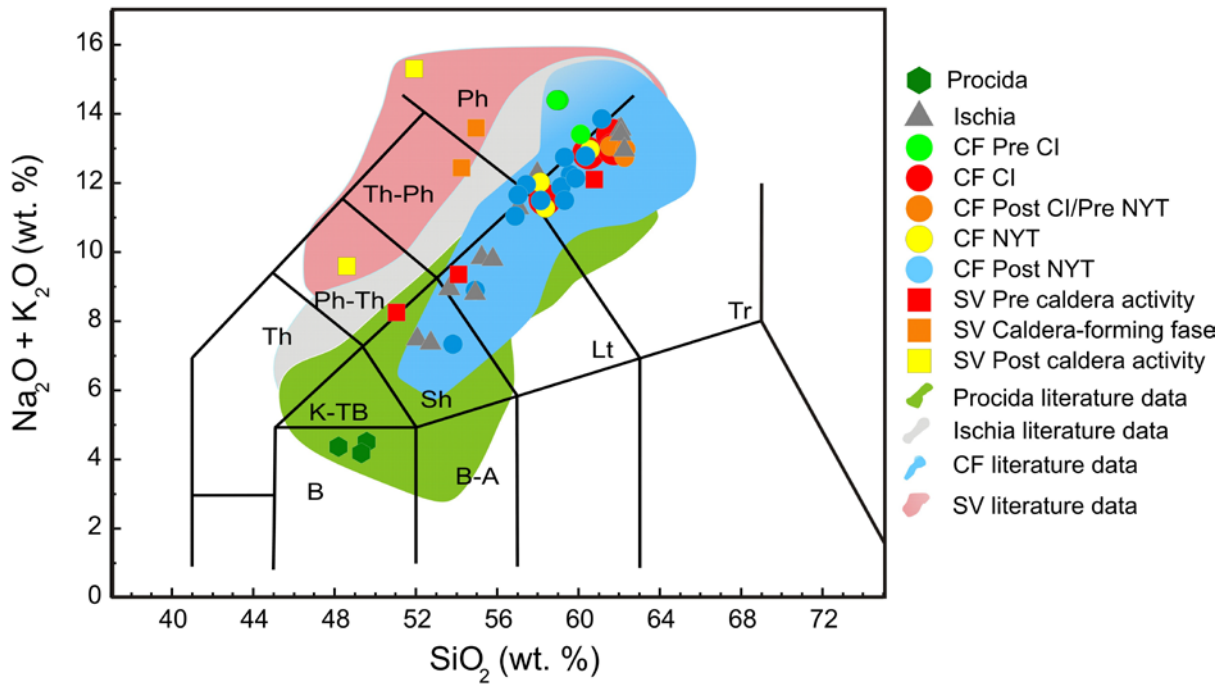


Fig. 2. Total alkalis ($\text{Na}_2\text{O}+\text{K}_2\text{O}$ wt. %) vs silica (SiO_2 wt.%) diagram (after Le Maitre, 2002) classification for Neapolitan products (recalculated to 100% on anhydrous basis).

CF: Campi Flegrei; CI: Campanian Ignimbrite; NYT: Neapolitan Yellow Tuff; SV: Somma-Vesuvius.

Fields are based on literature data. Reference data for Procida and Somma Vesuvius are from Lustrino et al. (2011 and references therein); Ischia and Campi Flegrei are from Iovine et al. (2017 and references therein).

4. Samples

We analyzed Sr-O isotopes of volcanic rocks and their minerals that are representative of the entire compositional range of the Neapolitan volcanoes (Fig. 2). Our samples were chosen within a well-constrained stratigraphic framework in order to cover the main periods of activity of the CF and SV volcanoes. Almost all the samples were previously analyzed for major and trace elements, and partially for isotopes (Table 1, electronic supplement). The chemical composition of additional not previously studied samples was analyzed in this work (Table 2, electronic supplement). Starting from the oldest period, samples from CF have been divided into different age groups as follows: 1. Pre Campanian Ignimbrite samples (Pre CI; >39 ka); 2. Campanian Ignimbrite samples (CI; 39 ka); 3. Post Campanian Ignimbrite/Pre Neapolitan Yellow Tuff samples (Post CI/pre NYT; <39 and >15 ka); Neapolitan Yellow Tuff samples (NYT; 15 ka); Post Neapolitan Yellow Tuff samples (Post NYT; <15 ka). From Procida we selected samples from the Solchiaro eruption, the most mafic magma erupted in the region (D'Antonio et al. 1999a; De Astis et al. 2004). Ischia is represented by eruptive products from the last 10 ka (Vateliero, Cava Nocelle, Arso and Zaro) that were previously characterized geochemically (e.g., Civetta et al. 1991; D'Antonio et al. 2013;

Iovine et al. 2017). For the SV volcanic complex, samples from three main periods were selected: (1) Somma volcano Pre caldera lavas older than 22 ka; (2) Caldera-forming phase spanning from 22 ka to 79 A.D.; (3) Post caldera activity younger than 79 A.D.. Texturally, the samples are mainly pumice or scoria fragments, with subordinate lavas; further petrographic descriptions can be found in the literature mentioned in the electronic supplement. The samples range from high-K basalt through potassic trachybasalt to shoshonite (Procida), from shoshonite through latite and tephriphonolite, to trachyte and phonolite (CF and Ischia; Fig. 2). SV rocks span from shoshonite to trachy-phonolite, partially overlapping the chemical composition of rocks produced at CF, and from trachy-basalt to tephrite and phonolite. The degree of silica undersaturation increases through time, and thus is lowest in the rocks dated between 39 and about 19 ka, and highest in rocks of the last cycle. The products of the last period, i.e. from 79 A.D. to 1944 A.D., range from leucitic tephrite to leucitic phonolite. Chemically, all samples define a variably silica-undersaturated potassic alkaline series (Fig. 2). In addition and to constrain the oxygen isotope composition of potential crustal components that may have contaminated the magmas, we selected one serpentized peridotite from the Mt. Pollino area at the Calabria-Basilicata boundary (Mazzeo et al. 2017 and references therein) and two metapelites from Timpa delle Murge Formation of the North Calabrian Unit, cropping out in the same area. Magma chamber country rocks are represented by two skarn xenoliths from Mt. Somma Vesuvius that are variably metamorphosed and metasomatized and derived by contact metamorphic reaction from Mesozoic limestones (Jolis et al. 2015). Finally, two altered and zeolitized pumices separated from two NYT samples should represent potential contaminants by volcanoclastic materials within the submarine PVD caldera fill.

5. Analytical methods

Whole rock samples were prepared and analyzed for major and trace elements at the Georg August Universität, Göttingen (GZG; Germany). For each sample, about 40 g of rock chips were hand-picked to assure that only the freshest pieces were powdered. The samples were washed again with deionized water (to remove any seawater salt) and dried at 120 °C. Sample powders were produced in a low-blank agate planetary ball mill. For each sample, two pulverization steps were done with 20 g of material each. The volatile content (LOI) was measured using standard thermo-gravimetric methods by igniting rock powders at 1100 °C after drying them overnight at 120°C. Major oxides and some trace elements (Sc, V, Cr, Ni, Rb, Sr, Ba, Y, Zr and Nb) were analyzed on glass-fusion discs using mixtures of lithium tetraborate and lithium metaborate by a PANalytical AXIOS

advanced sequential X-Ray Fluorescence spectrometer (XRF). A full trace element spectrum was analyzed by a FISIONS VG PQ STE Inductively Coupled Plasma Mass Spectrometer (ICP-MS). Analytical precision is better than 1% for most XRF major elements, but varies between 1 and 2% for Na, Mg and P. Precision is 10% for most trace elements, 2-5% for rare earth elements (REE) and Y. For isotopic analyses phenocrysts of feldspar, pyroxene, and olivine were handpicked from selected crushed rocks under a binocular microscope, grains with either glassy matrix attached or other minerals included were discarded. When possible, pyroxene was distinguished by color in dark (Fe-rich) and light (Mg-rich) crystals. Distinction between alkali feldspar and plagioclase phenocrysts was not done. For CF samples only, few Post NYT products (Pomici Principali, Minopoli, Fondo Riccio and Concola, Table 1 in the electronic supplement) contain olivine phenocrysts, while for the Procida, Ischia and SV samples olivine is always present. As possible mantle end-member we handpicked clean pyroxenes from the Mt. Pollino peridotite. Humite, vesuvian, phlogopite and grossular crystals were separated from the calc-silicate matrix of the skarn samples by dissolving the carbonate in oxalic acid. Other crustal materials (metapelites) were analyzed as bulk. After picking, the separated grains phases were washed in an ultrasonic bath with 7% HF and Milli Q[®] H₂O in order to remove any potentially remaining groundmass rinds that could affect the analyses. For $\delta^{18}\text{O}$ - $\delta^{17}\text{O}$ analyses, clean crystals were hand-picked from the grain separates and then washed in beakers with 5% HF in a sand bath at ca. 30°C, then rinsed with Milli Q[®] H₂O, and finally leached with 6N HCl and washed again with Milli Q[®] H₂O. In order to test if the acid treatment may affect the oxygen result some grains were washed with Milli Q[®] H₂O only. No differences in terms of $\delta^{18}\text{O}$ - $\delta^{17}\text{O}$ were found between acid-leached and unleached crystals. Sr isotopic analyses, from the samples not previously analyzed, were performed at the Radiogenic Isotope Laboratories of GZG (Göttingen, Germany) and INGV (Naples, Italy) on separated minerals and whole rocks after dissolution with high-purity HF-HNO₃-HCl mixtures. Sr was separated from the matrix through conventional ion-exchange procedures described in Arienzo et al. (2013) and measured statically by thermal ionization mass-spectrometry on Thermo Finnigan Triton TI instruments. Sr isotope ratios were normalized to the recommended values of the NIST-SRM 987 ($^{87}\text{Sr}/^{86}\text{Sr} = 0.71025$) standard. Sr blanks were on the order of 0.1 ng during the period of sample processing. Measured $^{87}\text{Sr}/^{86}\text{Sr}$ ratios were normalized to $^{86}\text{Sr}/^{88}\text{Sr} = 0.1194$ to correct for isotopic fractionation during measurements. Oxygen isotopic composition of ca. 2 mg of feldspar, clinopyroxene and olivine phenocrysts was measured at GZG by infrared laser fluorination following the procedure described by Pack et al. (2016). Nine San Carlos olivine (standard) and nine unknowns were loaded into an 18-hole Ni metal sample holder. Isotope ratios in the extracted O₂ gas were determined using a Thermo MAT253 gas source isotope ratio mass

spectrometer in dual inlet mode. Variations in triple oxygen isotope ratios ($^{17}\text{O}/^{16}\text{O}$, $^{18}\text{O}/^{16}\text{O}$) are expressed as the δ notation relative to VSMOW (Pack et al. 2016 and references therein). All measurements have been standard-normalized to the recommended $\delta^{18}\text{O}$ and $\Delta^{17}\text{O}$ San Carlos reference value of 5.15‰ and -0.054‰, respectively (Pack et al. 2016). Standards were measured throughout the analyses in order to check daily drifts in mass bias or blank contribution. Based on the standard deviation of the San Carlos standards, normalization was done simply calculating the average of the measured San Carlos olivine standards as a normalization reference value. Small deviation in $^{17}\text{O}/^{16}\text{O}$ from a given reference line are expressed in the form of $\Delta^{17}\text{O}$ that is not a measured quantity but is calculated from the measured $\delta^{18}\text{O}_{\text{VSMOW}}$ - $\delta^{17}\text{O}_{\text{VSMOW}}$ quantities. $\Delta^{17}\text{O}$ data have been calculated using the formula in Pack et al. (2016), where the slope of the reference line, λ_{RL} , is 0.5305. For $\Delta^{17}\text{O}$ data to be comparable among different laboratories and studies two criteria must be met: (1) they must be generated from isotopic measurements of $\delta^{18}\text{O}$ and $\delta^{17}\text{O}$ calibrated to a common reference frame, whether it is a water reference SMOW or a silicate reference, and (2) $\Delta^{17}\text{O}$ must be calculated selecting uniform values for λ_{RL} (or values that can be accurately related to those adopted by another laboratory).

6. Results

6.1 $^{87}\text{Sr}/^{86}\text{Sr}$ and $\delta^{18}\text{O}$ isotope data

Sr isotope ratios of bulk rock, groundmass, and separated minerals cover a wide compositional range from 0.70487 to 0.70848 (Table 3 in electronic supplement, and Fig. 3a). Surprisingly, the least and most radiogenic composition were measured in olivine phenocrysts from a mafic enclave (ZR3C) of the Zaro lava on Ischia and, from a mafic scoria of the Minopoli 2 eruption (Min2; CF, Post NYT), respectively. Within that range, Sr isotopic ratios vary significantly between eruptive periods and for different analyzed mineral and groundmass from a single sample.

The whole range of measured $\delta^{18}\text{O}$ is 4.61 - 8.34‰. Since these measured $\delta^{18}\text{O}$ values do not represent initial magmatic values, all mineral data were corrected to $\delta^{18}\text{O}_{\text{melt}}$ considering $\Delta(\text{melt-min})$ fractionation between melt and minerals (Table 3 in electronic supplement). $\delta^{18}\text{O}_{\text{melt}}$ calculated for phenocrysts (Fig. 3b) vary between 5.19 (dark pyroxene phenocryst in Zaro eruption) and 8.80‰ (olivine phenocryst of Concola eruption, Post NYT period at CF). In case of duplicate analyses we refer to the mean value (e.g., see MIN2 mean olivine in Table 3 of the electronic supplement). Melt calculation based on feldspar crystals does not differ significantly from the $\delta^{18}\text{O}$ measured values, while $\delta^{18}\text{O}_{\text{melt}}$ derived from pyroxene and olivine crystals is higher than the measured mineral values (Fig. 3b). In detail, for samples belonging to Procida and Ischia islands

the ranges are between 5.81 and 6.38‰, and between 5.19 and 6.95‰, respectively. Recalculated $\delta^{18}\text{O}_{\text{melt}}$ values accordingly show a large range for the CF between 6.95 (dark pyroxene from NYT eruption) and 8.80‰ (olivine phenocryst of Concola eruption, Post NYT).

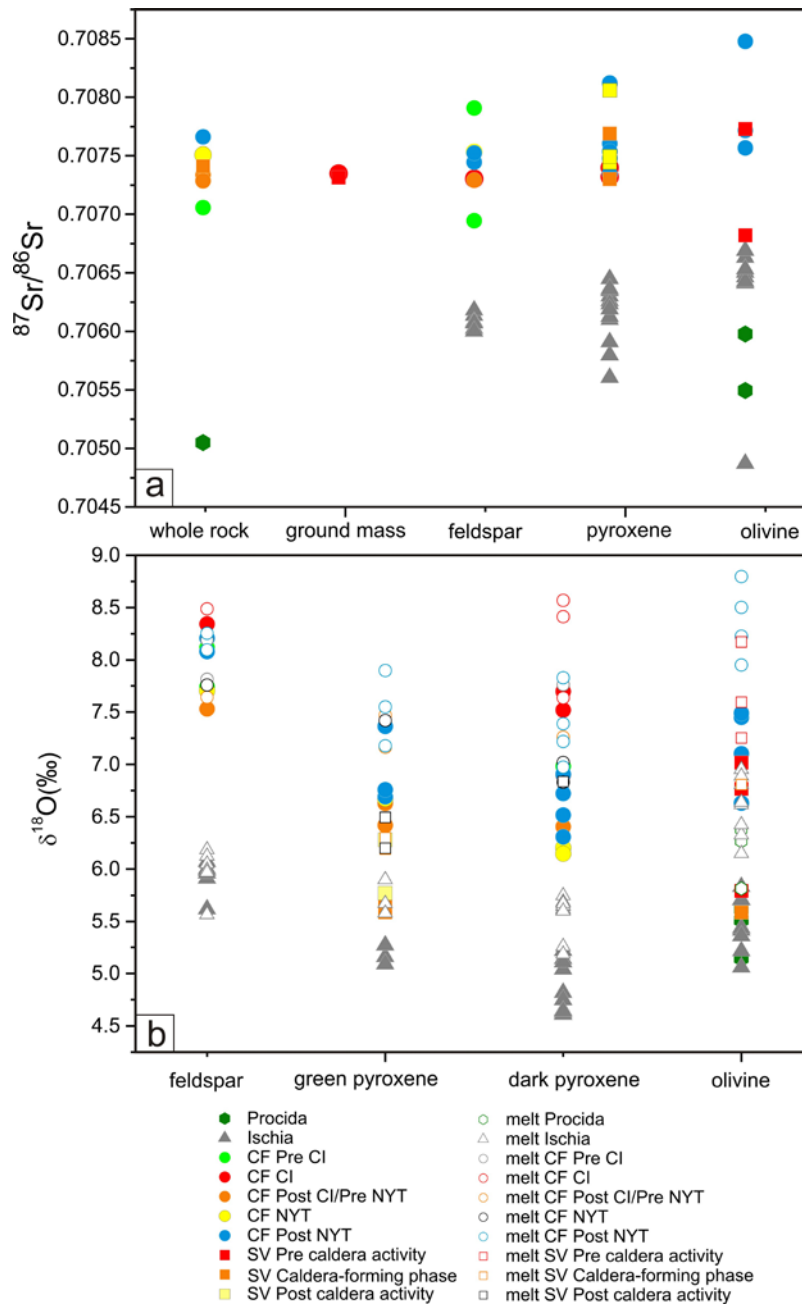


Fig. 3. a) $^{87}\text{Sr}/^{86}\text{Sr}$ isotopic data of groundmass and minerals taken from literature (for detail see Table 3 in electronic supplement) and partly analyzed in this work. All data were corrected using the recommended value of NIST SRM 987 $^{87}\text{Sr}/^{86}\text{Sr}$ ratio. The errors on the measured ratios are within the symbol; b) O-isotope compositions of minerals and calculated melt composition of Neapolitan rocks. $\delta^{18}\text{O}_{\text{melt}}$ is calculated using the Bindeman et al. (2004) approach. The error of each measurement is calculated as standard deviation of the San Carlos olivine standard and is $\sim 0.15\text{‰}$ (within the symbol). For duplicate analyses only the mean value has been plotted. Errors for calculated melt values were obtained by

measurement errors, calibration errors in the recalculation scheme (Bindeman et al. 2004) are not considered. Symbols as in Figure 2.

For the Pre CI activity, the range is between 7.76 and 8.19‰, while for the CI eruption the variability is wider ranging from 7.64 to 8.57‰. For the third period of magmatic activity, the $\delta^{18}\text{O}_{\text{melt}}$ is between 7.16 and 7.64‰. Between 6.95 and 7.81‰ is instead the isotopic variability for the NYT samples, while it is wider, from 7.11 to 8.80‰ considering Post NYT activity. $\delta^{18}\text{O}_{\text{melt}}$ of SV samples span from 6.19 (Caldera-forming phase) to 8.17‰ (Pre caldera activity). Compared to CF, SV products erupted during the last period have intermediate oxygen content from 6.20 to 6.84‰.

This new and expanded dataset compounds earlier evidence for isotopically distinct magma batches and derivation from isotopically highly variable precursor magmas contaminated by variable crystal cargo of distinct isotopic composition (e.g., Civetta et al. 1991; D'Antonio et al. 1999b, 2007, 2013; Pabst et al. 2008; Arienzo et al. 2016 and references therein; Di Renzo et al. 2007, 2011; Melluso et al. 2012; Iovine et al. 2017).

6.2 $\Delta^{17}\text{O}$ variations

$\Delta^{17}\text{O}$ values are plotted in Fig. 4 against $\delta^{18}\text{O}_{\text{melt}}$ together with reference values for the mantle and a range of crustal rocks to represent potential crustal assimilants. $\Delta^{17}\text{O}$ varies between -0.027 (colorless Post CI/ Pre NYT pyroxene from CF) and -0.094‰ (olivine from SV oldest period; Table 3, electronic supplement). Procida samples are all within analytical error (0.012 ‰). A wider $\Delta^{17}\text{O}$ range from -0.038 to -0.084‰ is shown by Ischia samples. The largest variation is found for the CF samples from -0.027 (colorless Post CI/ Pre NYT pyroxene) to -0.088‰ (Post NYT pyroxene). SV samples are between -0.051 (colorless pyroxene of the oldest period) and -0.094‰ (olivine crystals of the youngest period). To better understand the meaning of these variations we have analyzed some possible contaminants including pyroxenes from mantle serpentinized peridotite (Mazzeo et al. 2017), metasediments (Mazzeo et al. 2014) and minerals from skarns representing the local Mesozoic limestone (Table 4, electronic supplement). Altered pyroclastic rocks that potentially inhabit the deeper levels of the Campi Flegrei caldera are represented by altered and zeolitized pumices from PVD deposits. $\Delta^{17}\text{O}$ from these crustal rocks vary between -0.067 (altered NYT pumice) and -0.144‰ (zeolitized NYT pumice). This range includes all other potential contaminants (metapelites, serpentinized peridotite, minerals from SV skarn, Fig. 4). The separated pyroxene from the Mt. Pollino serpentinized harzburgite has $\delta^{18}\text{O}$ of 6.87‰ and $\Delta^{17}\text{O}$ of -0.098‰, while for the two metapelites $\delta^{18}\text{O}$ vary between 12.24‰ and 17.04 ‰ and $\Delta^{17}\text{O}$ from -

0.106‰ to -0.131‰. The triple oxygen composition of skarn hand-picked minerals (humite, vesuvian, phlogopite, grossular) vary between -0.071 and -0.142‰. Altered and zeolitized NYT pumices display highly variable oxygen isotope ratios ($\delta^{18}\text{O} = 10.87\text{‰}$; $\Delta^{17}\text{O} = -0.067\text{‰}$ for the altered pumice and $\delta^{18}\text{O} = 18.10\text{‰}$; $\Delta^{17}\text{O} = -0.144\text{‰}$ for the zeolitized one).

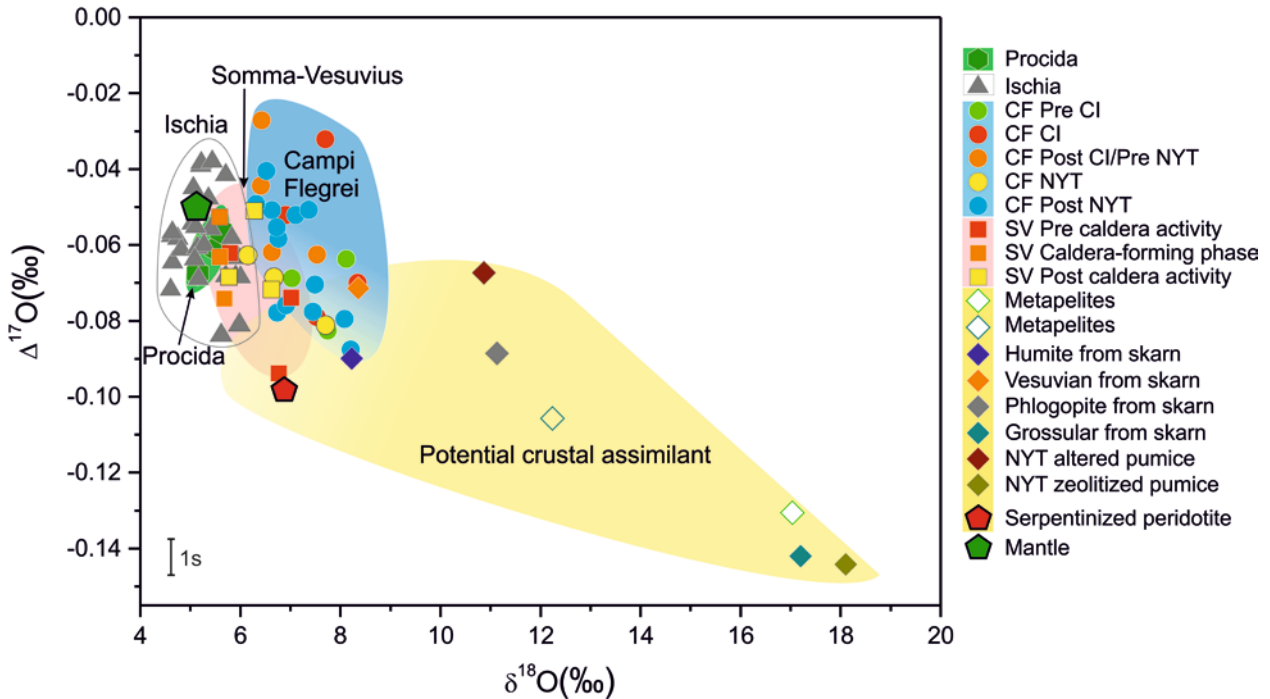


Fig. 4. $\Delta^{17}\text{O}$ variations in minerals from the Neapolitan volcanoes and in possible contaminants (metapelites, serpentinized peridotite, minerals from SV skarns and altered and zeolitized NYT pumices). For duplicate analyses only the mean value has been plotted. $\delta^{18}\text{O}$ in minerals is $\delta^{18}\text{O}_{\text{melt}}$. The error of each measurement is calculated as standard deviation of the S. Carlos olivine standard and is $\sim 0.012\text{‰}$. Symbols as in Figure 2.

7. Discussion

The principal questions that arise from our observations are: (1) what causes the striking isotopic and compositional disequilibrium between minerals and host magmas, (2) what is the nature and major element composition of the melts from which these isotopically distinct minerals have grown, and (3) how can we explain the large range and in particular the isotopically "heavy" compositions of $^{18}\text{O}/^{16}\text{O}$ isotope ratios. Relating to the last question, we specifically need to address the problem whether these heavy $^{18}\text{O}/^{16}\text{O}$ isotope ratios are the result of crustal assimilation processes or reflect unusual isotopic compositions of the mantle source. In a first step, and in order to assess the relation between isotopic composition represented by the minerals and degree of differentiation of their ("true") host magma, we calculated the Mg# of their host melt. To this

purpose, we used the Mg and Fe contents of olivine and clinopyroxene crystals that we analyzed for O and Sr isotopes using published $^{\text{Fe}/\text{Mg}}\text{Kd}_{\text{Ol-liq}}$ distribution coefficients of 0.27-0.33 (Matzen et al. 2011 and references therein) and $^{\text{Fe}/\text{Mg}}\text{Kd}_{\text{Cpx-liq}} = 0.27 \pm 0.03$ (Mollo et al. 2013 and references therein; see Table 5, electronic supplement). As shown in Figure 5a no systematic correlation between calculated $\delta^{18}\text{O}$ and their Mg# is recognized. A surprising result is that even olivines and clinopyroxenes which formed from rather mafic melts (calculated Mg# >64, see Table 5, electronic supplement) have elevated "crustal" $\delta^{18}\text{O}$ values > 8‰. Therefore, there must be rather mafic (close to primary) magmas at depth that host phenocrysts that are very heavy in $\delta^{18}\text{O}$. However, such mafic magmas have never been observed as eruptive products on the surface. When considering the Sr- and O-isotopic variation towards more evolved compositions, i.e. relating Mg# and $^{87}\text{Sr}/^{86}\text{Sr}$ ratios, (Fig. 5b) we observe a trend towards greater degree of homogenization from mafic to felsic compositions. Mafic minerals (Mg# > 45) analyzed here, and by implication their host melts, may cover the entire range of isotopic compositions observed in bulk rocks even within a single stratigraphic unit. Moreover, we observe that at similar major element composition (i.e. Mg#) Procida and Ischia magmas ($^{87}\text{Sr}/^{86}\text{Sr} < 0.707$) are clearly different from CF magmas ($^{87}\text{Sr}/^{86}\text{Sr} > 0.707$). Also for O-isotopes, melts in equilibrium with olivine and clinopyroxene from Ischia and Procida islands are quite similar to the typical mantle values ($5.2 \pm 0.2\%$; Matthey et al. 1994; Eiler, 2001) while the other samples show very different values and span a large range towards heavier $\delta^{18}\text{O}$ values, showing a positive correlation between $\delta^{18}\text{O}$ and $^{87}\text{Sr}/^{86}\text{Sr}$ (Fig. 5c). As general patterns, we observe (1) a rather large variation within and between mineral samples and their hosts, (2) even rather mafic magmas, close in composition to melts in equilibrium with peridotitic mantle, having elevated Sr isotope and crustal O-isotope compositions.

Mediterranean orogenic magmatism has been argued to be the result of partial melting of mantle sources modified by slab materials (fluids and/or melts from sediments and/or altered oceanic crust) during and/or after subduction event(s) that modified this pre-existing mantle composition (e.g., Mazzeo et al. 2014 and references therein). High $\delta^{18}\text{O}$ coupled with high $^{87}\text{Sr}/^{86}\text{Sr}$ values produce broad fields above the mantle enrichment trend (Figs. 5c and 6). The magma sources of Neapolitan volcanic products are clearly distinct for Procida and Ischia compared to Campi Flegrei and Vesuvius. Both groups form broad fields that are rooted (Ischia) or trending towards Sr isotope values of 0.7055 and roughly 0.7075, respectively, for mantle O-isotope compositions of 5.4‰. This suggests, by projecting down onto a mantle-sediment mixing curve, that the mantle source was modified by addition of subduction-derived sedimentary components (mostly likely pelagic clays), as was already suggested for Neapolitan volcanism in general (e.g., D'Antonio et al. 2007 and 2013; Mazzeo et al. 2014, and references therein; Iovine et al. 2017). Taking only our single

mineral data for Sr and O-isotopes, between <0.5 and 1.5% source contamination along a concave mixing curve explains well the initial mantle source composition of the Neapolitan magmas (Figs. 5c and 6c). Procida magmas are derived from a source that was less contaminated (~0.5%) by subducted sediments. CF and SV magma sources must have incorporated variable amounts from 1 to 1.5% of subducted sediments.

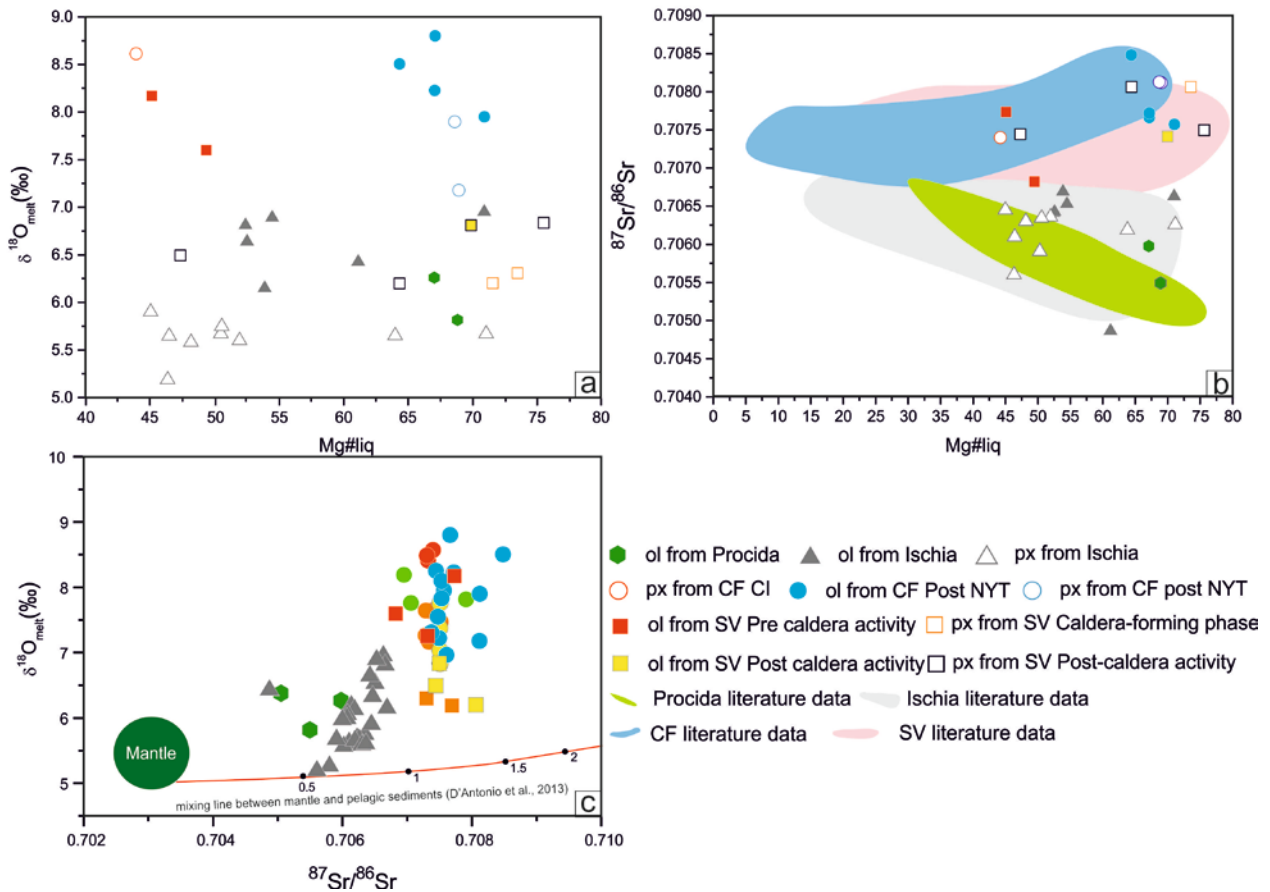


Fig. 5. Mg# liquidus (host rock) calculated based on the chemical composition of the analyzed olivine and clinopyroxene phenocrysts versus (a) $\delta^{18}\text{O}$ and (b) $^{87}\text{Sr}/^{86}\text{Sr}$. Full symbols represent calculated melt from olivine phenocrysts, empty symbols refer to pyroxene phenocrysts. See text for further details. In case of duplicate analyses we refer only to the mean value. Reference data and symbols as in Figure 2. (c) $\delta^{18}\text{O}$ versus $^{87}\text{Sr}/^{86}\text{Sr}$ for the analyzed samples compared to mantle values. The red curve represents a source enrichment process involving MORB mantle and pelagic sediments (see D'Antonio et al. 2013 for numerical parameters used in the modeling). Symbols as in Figure 2.

The important question then is, what causes the vertical displacement of magma compositions above the mantle-sediment mixing hyperbola, i.e. what component can increase the O-isotope composition without significantly affecting the Sr-isotopic values in the magmas, i.e. how to explain near-vertical trends on Sr-O-isotope diagrams. There are several scenarios that can explain these observations:

- (1) Assimilation of ascending magmas by a compositional component (bulk or partial melt) of metamorphic rocks within the lower to middle crust (e.g., Di Renzo et al. 2007 and 2011; D'Antonio et al. 2007 and 2013; Mazzeo et al. 2014),
- (2) Assimilation of Mesozoic carbonates in upper crustal reservoirs (Pappalardo et al. 2004, Piochi et al. 2006),
- (3) Digestion of hydrothermally altered, deposits of older CF pyroclastic rocks (Piochi et al. 2014). As we will show below, none of these models are fully consistent with our observations and therefore we will present, and argue for,
- (4) A combination between a mantle source unusually rich in heavy ^{18}O caused by mixing between mantle peridotite, probably partly serpentinized, and a 1:1 mixture of siliciclastic sediment and limestones.

7.1 Assimilation of silicic Hercynian crust

In order to quantify the potential role of magma assimilation within the crust, we have modeled energy-constrained assimilation + fractional crystallization (EC-AFC; Spera and Bohrsen, 2001). Modeling parameters are listed in Table 6 of the electronic supplement and results are shown in curves in Figures 6a and 6b. Our modeling can explain the Sr-O isotope features of CF products by a maximum of $\sim 12\%$ assimilation (curve 1 in Fig. 6b) of bulk continental crust into a mafic magma which already had inherited an enriched crustal isotopic signature in the mantle source by variable additions of 1 to 1.5% of subducted sediment. However, in order for the model to work and to explain the steep Sr-O-isotope trend we have to assume firstly an incompatible behavior for Sr ($D_0 = 0.5$), followed by compatible behavior ($D_0 = 2$). This is a reasonable assumption for differentiating mafic to intermediate alkaline magma, where feldspars appear late in the crystallization sequence. A second constraint is a rather low concentrations of 50 ppm Sr in the contaminant. Such a crustal end-member could be produced by low-P partial melting of silicic metamorphic rocks where K-feldspar remains on the solidus. For the SV products, we have modeled their Sr-O isotope variation assuming Hercynian basement as assimilant as suggested by Civetta et al. (2004), Paone (2006) and Di Renzo et al. (2007). Our modeling explains the Sr-O isotope features of SV products by a maximum of $\sim 21\%$ assimilation (curve 2 in Fig. 6b) of Hercynian crust into a mafic magma. Previous AFC modeling for Ischia magmas provided an estimate of 7% for the maximum amount of crustal assimilation needed to explain 3 ka old latitic products formed by a mafic magma, which already had inherited an enriched crustal isotopic signature in the mantle source by variable additions of <0.5 to 1% of subducted sediments (D'Antonio et al. 2013; Iovine et al. 2017). Procida magmas were not modeled due to the small

number of data. We conclude that our data and modeling of Neapolitan magmas is consistent (but not conclusive, see below) to have assimilated between 7 and 21% of Hercynian crust, the latter value being unrealistic. Prior to crustal assimilation, the magma source was already enriched by <0.5 to 1.5% of subducted sediments. The problem that exists with this model stems from our observation that olivines that originated from magmas with Mg# of 70 have O-isotope values as heavy as 9‰. The assimilation model already assumes rather extreme parameters and therefore the estimated 12% assimilation is a minimum value. 12 or more percent assimilation is associated with (a minimum of) 89% fractional crystallization in our EC-AFC model. At these conditions, magmas would become much more evolved than Mg# 70. Therefore assimilation cannot alone explain the observed high oxygen isotope ratios and the vertical Sr-O isotope trends.

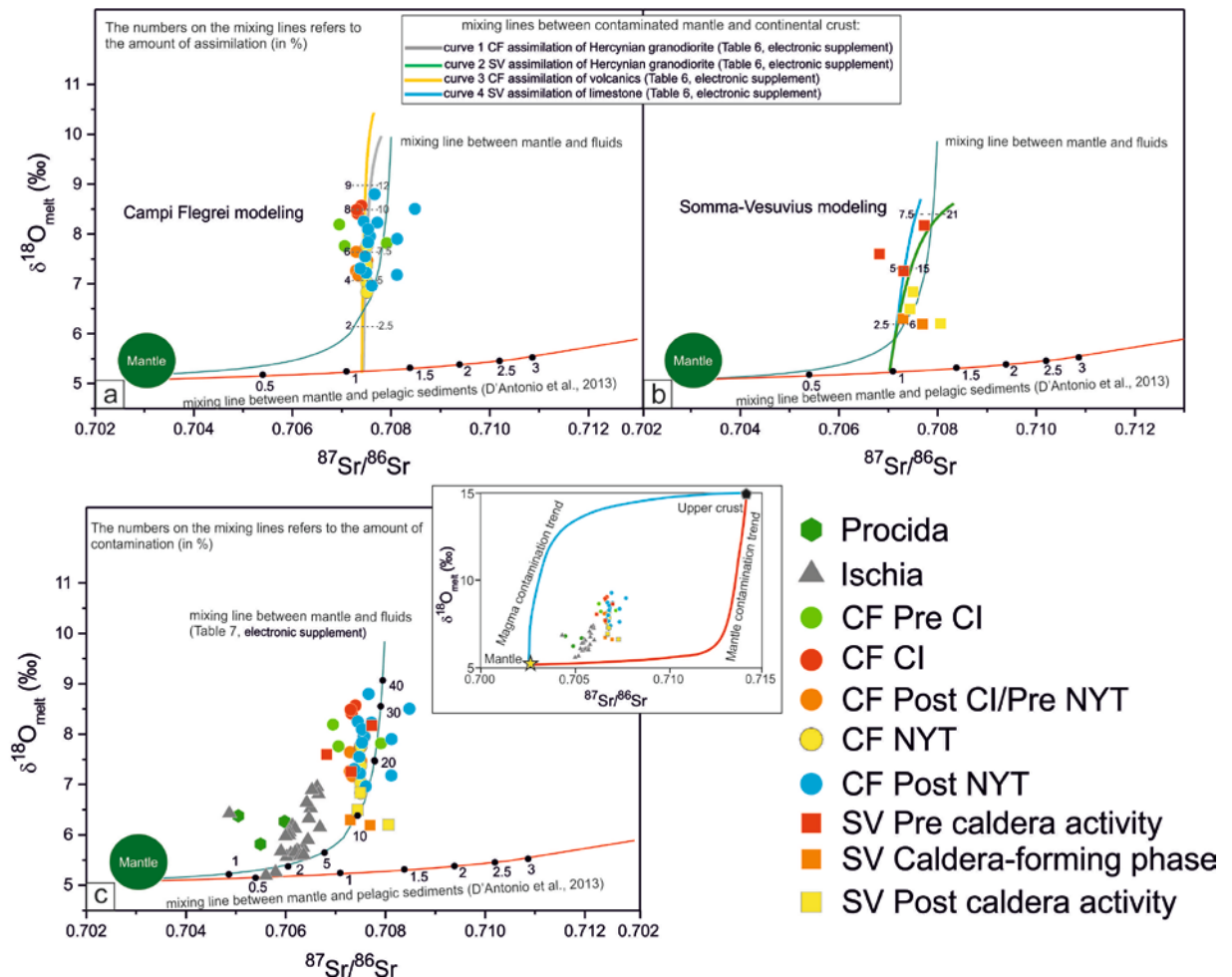


Fig. 6. $\delta^{18}\text{O}_{\text{melt}}$ versus $^{87}\text{Sr}/^{86}\text{Sr}$ binary diagram for the Neapolitan volcanoes. For duplicate analyses only the mean value has been plotted. Symbols as in Figure 2.

The red curve represents a source enrichment process involving MORB mantle and pelagic sediments (see D'Antonio et al. 2013 for numerical parameters used in the modeling). The (a) gray, yellow, (b) green and blue curves represent modeled AFC processes involving a primitive magma segregated by the subduction-modified mantle sector below Campi Flegrei and Somma Vesuvius, that crystallizes and assimilates continental crust, altered Campi Flegrei pyroclastic rock and carbonate, see Table 6 in electronic supplement

for numerical parameters used in the modeling). AFC models for Ischia are in D'Antonio et al. (2013) and Iovine et al. (2017). Procida samples are only three and therefore it is not possible to constrain a model. (c) The turquoise curve represents a magma contamination involving fluids from the subducted slab (Table 7 in electron supplement).

7.2 Assimilation of altered CF pyroclastic rock

Another possible assimilant for the CF would be altered pyroclastic rocks via cannibalization of earlier volcanic products. We explore this hypothesis by testing the use of $\Delta^{17}\text{O}$ values plotted against $\delta^{18}\text{O}$ (see Fig. 4). Assimilation processes would form straight mixing lines in such a diagram between the mantle source and possible crustal end-members. From this it would be straightforward to calculate the % of assimilation for hybrid products. Between possible contaminants analyzed in this work are altered and zeolitized NYT pumices. In fact, older and deeply altered pyroclastic rocks would equally well fulfill the decisive criteria to explain the vertical Sr-O isotope trends, i.e. Sr isotopes similar to the magmas themselves, heavy O isotope composition, and low Sr concentrations relative to the magmas. Indeed, a substantial portion ($\gg 50\%$ in volume) of the NYT was deposited inside the NYT caldera and subjected to pervasive zeolitization by hot hydrothermal fluids. The mean content of these authigenic phases generally exceeds 50 wt% and sometimes can reach 70 -80 wt.% (de'Gennaro et al. 2000 and references therein). Indeed, our samples (a pumice that was deeply modified by hot hydrothermal fluids and a zeolitized tuff) show heavy oxygen isotope compositions ($\delta^{18}\text{O} = 10.87$; $\Delta^{17}\text{O} = -0.067\text{‰}$ and $\delta^{18}\text{O} = 18.10$; $\Delta^{17}\text{O} = -0.144\text{‰}$, respectively; Fig. 4). With these characteristics, altered pyroclastic rocks are suitable contaminants. Such a contaminant could therefore have $\delta^{18}\text{O} = 18.10$ and $^{87}\text{Sr}/^{86}\text{Sr} = 0.7092$ (meteoric-hydrothermal fluids). Modeling of AFC processes provides a maximum of $\sim 9\%$ assimilation (curve 3 in Fig. 6b) of such altered volcanic rocks by a mafic parent magma which had inherited an isotopic signature from a mantle source variably modified by subduction. However, there is no evidence so far to argue that such rocks extend within the caldera to depth of > 4 km (De Vivo et al. 1989) where magma evolution and assimilation is thought to have taken place.

7.3 Assimilation of Mesozoic carbonate rocks

The elevated oxygen isotope values clearly indicate that crustal components are commonly involved in genesis and evolution of the Campanian magmatism. Magma-carbonate interaction, in particular, may be a relevant process and would be consistent with major constraints from the Sr-O vertical trend shown by our data: the assimilant should be high in ^{18}O compared to the magma,

and its Sr isotopic compositions should not be too different from the magmas themselves. Carbonates thus would be ideal candidates to explain the mixing trends. For the SV magmas, Civetta et al. (2004), Paone (2006), Di Renzo et al. (2007) and Piochi et al. (2007) proposed that contamination occurred within a Hercynian-like basement, similarly to what happens at the CF. Instead, Pappalardo et al. (2004) and Piochi et al. (2006), suggested that carbonate was the main contaminant. Further evidence for a magma-carbonate interaction is provided by (1) the abundance of high temperature metasomatised skarn xenoliths in the erupted products that have interacted to variable extent with magmatic components (e.g. Del Moro et al. 2001; Fulignati et al. 2005); (2) the generation of a CO_2 -rich fluid phases (e.g. Iacono-Marziano et al. 2008); and (3) the elevated $\delta^{18}\text{O}$ isotope composition of mafic SV minerals that interacted with sedimentary carbonate already prior to more extended magmatic differentiation (Dallai et al. 2011; this study). The calculated model could explain the vertical Sr-O isotope trends of SV products by a maximum of $\sim 7.5\%$ limestone assimilation (curve 4 in Fig. 6b) into a mafic magma. Jolis et al. (2013) have shown how this process will progressively enrich the host melt in CaO implying that $\delta^{18}\text{O}$ and CaO should correlate positively in case of extensive carbonate assimilation. Such correlation is indeed observed in magmatic rocks from Alban Hills with $\delta^{18}\text{O}$ and CaO trending towards maximum values of 13 ‰ and 24 wt% CaO, respectively (Peccerrillo et al. 2010). However, as shown by Figure 7, our data do not show any positive correlation between CaO and $\delta^{18}\text{O}$, clearly excluding assimilation of carbonates as a dominant process in elevating $\delta^{18}\text{O}$ at similar Sr isotope compositions. Moreover, addition of substantial carbonate would shift the composition towards stronger silica-undersaturation (e.g., Iacono-Marziano et al. 2008; Jolis et al. 2013), which is not observed for Ischia and the CF. In fact $\delta^{18}\text{O}$ is not correlated with any index of silica undersaturation. Finally, limestone fragments have never been found in any CF or Ischia volcanic products (D'Antonio, 2011 and references therein). Therefore, carbonate assimilation is ruled out here at least for Ischia and the CF. At Vesuvius, if crustal contamination with limestone occurred, it must have been operative mostly during the last few thousand years of its history. This is because, the Vesuvian rocks became strongly undersaturated only in the last 2 kyr (Di Renzo et al. 2007; Santacroce et al. 2008) but olivines "heavy" in $\delta^{18}\text{O}$ have been documented here already for less undersaturated lavas from the Pre caldera phase of Somma Vesuvius.

Based on these arguments, we conclude that none of the models presented so far can alone explain the observed relations between O-, Sr- isotopes and inferred mafic magma compositions. Therefore, we need to consider a combination of assimilation and $\delta^{18}\text{O}$ -enriched mantle source.

7.4 Source contamination by subducted components

The upper oceanic crust is characterized by ^{87}Sr enrichment, which strongly correlates with $\delta^{18}\text{O}$ (Staudigel et al. 1996). From these data, a maximum of $^{87}\text{Sr}/^{86}\text{Sr} = 0.70818$ and $\delta^{18}\text{O} = 12\text{‰}$ is assumed for the upper (low T) altered oceanic crust (Table 7, electronic supplement). A mantle-fluid mixing line suggests that the mantle source in the Neapolitan area was modified likely by maximum addition of $\sim 40\%$ of subduction-derived fluids (Fig. 6c). Beyond $\sim 10\%$ fluid addition, this process will cause a steep trend between Sr and O isotopes because of the relatively unradiogenic Sr isotope composition of the fluid. Anyway, the amount of fluid in the source (up to 40 wt %) is excessively high, possibly causing extensive and unrealistically high degrees of melting. It was already argued for the mantle source in the Neapolitan area that the enriched component is a hydrous melt rather than a hydrous fluid (Mazzeo et al. 2014).

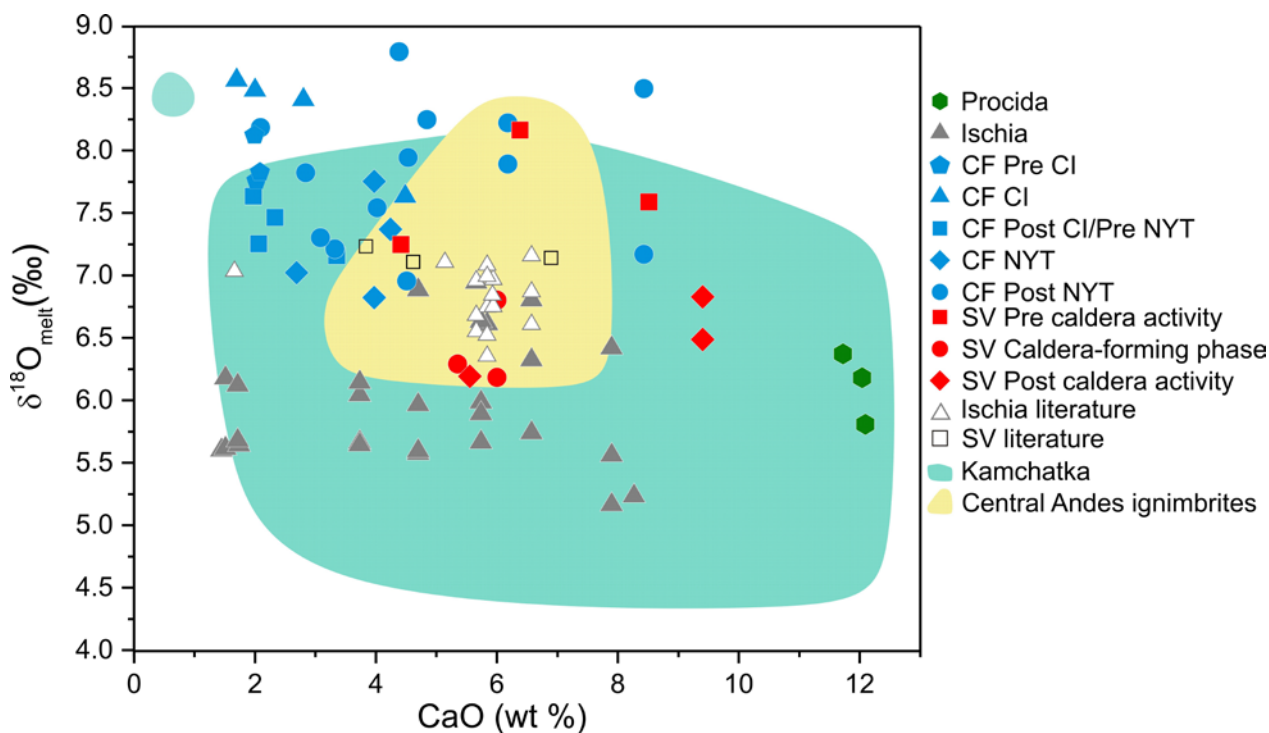


Fig. 7. $\delta^{18}\text{O}_{\text{melt}}$ versus CaO for the analyzed rocks compared to Kamchatka and Central Andean ignimbrites. For duplicate analyses we refer only to the mean value. Symbols as in Figure 2.

Kamchatka data are from Dorendorf et al. (2000) and Bindeman et al. (2004); Central Andean ignimbrites from Freymuth et al. (2015) and from the Central Andes Geochemical GPS Database (<http://andes.gzg.geo.uni-goettingen.de/maps3/>).

In order to understand how and to what extent the mantle source was enriched by subducted slab-derived components in such a way as to generate the magmas that feed the Neapolitan volcanoes, we will focus on a ternary mix, considering a mantle enriched by melt from pelagic sediment and limestone. It must be pointed out that the enrichment by pelagic sediments cannot explain alone

the Sr-O isotope values of our samples, especially the high $\delta^{18}\text{O}$ data. A contribution of a component, which is higher in $\delta^{18}\text{O}$ is implied. Such an enriched component could be provided by limestone, which has high concentrations of O and Sr. Therefore we modeled the addition of a mixture of shale and limestone to the mantle source. Modeling parameters are listed in Table 8 of the electronic supplement and results are shown in the curve of Figure 8. We assumed the $\delta^{18}\text{O}$ of the shale to be 17‰ (sampled TMG6, see Table 4, electronic supplement) and $^{87}\text{Sr}/^{86}\text{Sr}$ isotope ratio and Sr (ppm) as the average value of the shales analyzed in Mazzeo et al. (2014). For limestone, a value for $\delta^{18}\text{O}$ of 30‰ (Peccerillo et al., 2010), and a $^{87}\text{Sr}/^{86}\text{Sr}$ ratio of 0.7075, and 340 ppm Sr (Mazzeo et al., 2014 and references therein) were used in the model. This mixing model fits well the observed data (Fig. 8) with a mantle source (probably partly serpentinized) contaminated by 5.2% of sediment and 4.8% of limestone. This means a maximum of 10% of pelagic sediment + limestone added to the mantle source beneath the Neapolitan area. Based on the proposed models, we conclude that the most plausible scenario to explain the observed relations between O-, Sr- isotopes for mafic magmas ($\text{Mg}\# = 70$) is a mantle source contamination by subducted pelagic sediments and limestone. Additional assimilation of silicic Hercynian crust, however, can never be ruled out and may have additionally occurred in the more evolved magmas.

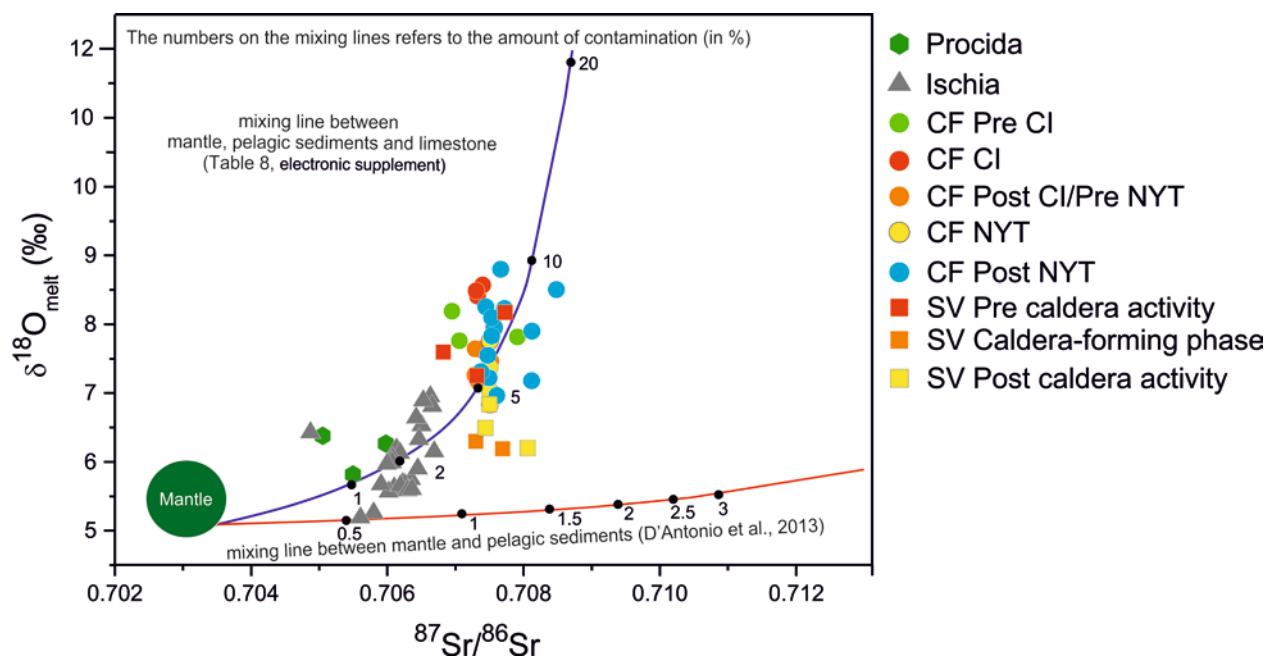


Fig. 8. $\delta^{18}\text{O}_{\text{melt}}$ versus $^{87}\text{Sr}/^{86}\text{Sr}$ binary diagram for the Neapolitan volcanoes. For duplicate analyses only the mean value has been plotted. Symbols as in Figure 2.

For the meaning of the red curve please refer to Figures 5c and 6. The blue curve is the result of a mixing between three components: the mantle source, pelagic sediments and limestone. See text for further details.

7.5 A comparison with Sr-O-isotope relations in magmas from subduction zones worldwide

Our results are compared in Figure 9 with compiled published $\delta^{18}\text{O}$ -isotope data from other Italian volcanic centers (Alban Hills, Mts. Ernici, Ischia, Aeolian Islands, Tuscany and Sardinia) and from subduction zones worldwide (Kamchatka, Lesser Antilles, Indonesia and Central Andes). All values have been calculated from minerals as melt-values.

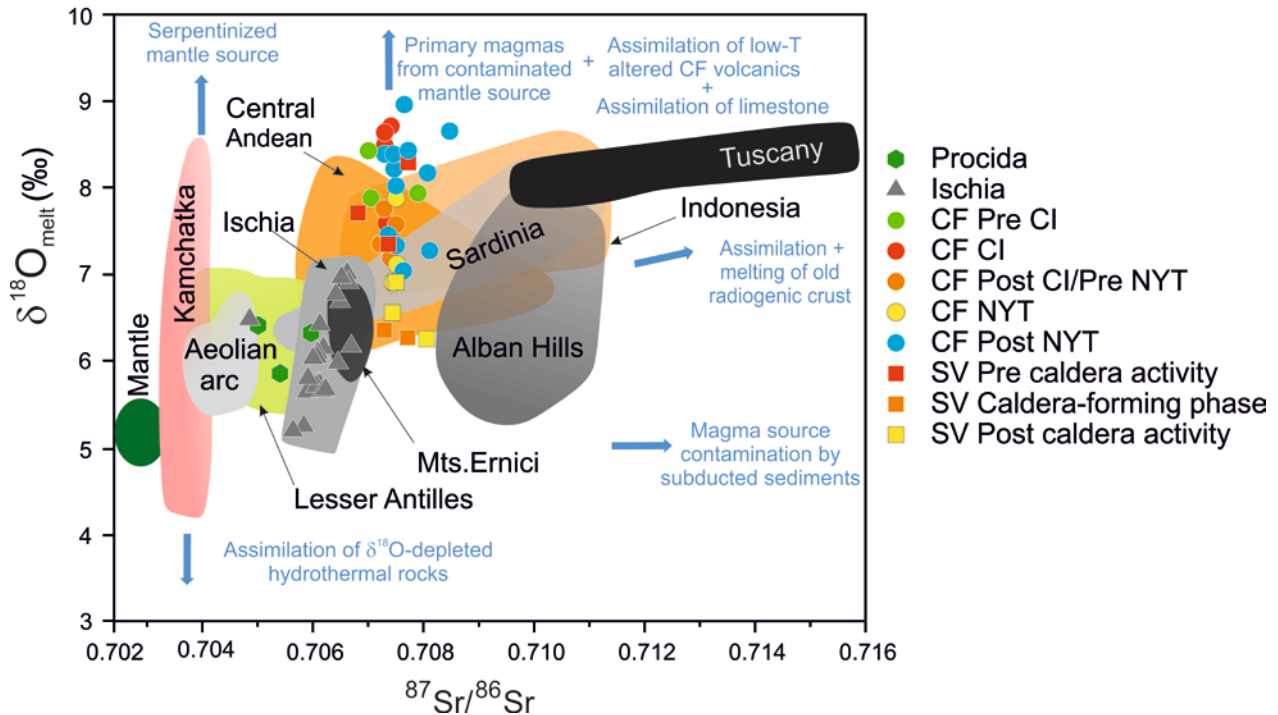


Fig. 9. $\delta^{18}\text{O}_{\text{melt}}$ versus $^{87}\text{Sr}/^{86}\text{Sr}$ binary diagram for the Neapolitan volcanic rocks compared with data from other volcanic centers from the Italian peninsula and subduction zones worldwide, after correction of $\delta^{18}\text{O}$ data. Symbols as in Figure 2.

See text for further details (Kamchatka data are from Dorendorf et al. 2000, Bindeman et al. 2004 and Portnyagin et al. 2007; Ischia, Ernici, Aeolian Arc (Alicudi and Filicudi), Indonesia and Lesser Antilles data are from D'Antonio et al. 2013 and references therein; Central Andean ignimbrites are from Freyemuth et al. 2015; Alban Hills are from Di Rocco et al., 2012 and D'Antonio et al. 2013 and references therein; Sardinia are from Downes et al. 2001; Tuscany are unpublished data; Mantle data are from Matthey et al. 1994 and Eiler, 2001).

This compilation (Fig. 9) shows vastly different magma types from different subduction zones worldwide with respect to their Sr-O-isotope systematics and identifies their different sources: (1) extreme vertical trend in the Kamchatka, (2) sediment-enrichment in the mantle source (e.g., Indonesia, Lesser Antilles, Aeolian arc), (3) assimilation or wholesale melting of old radiogenic continental crust affecting magmas derived from sediment-modified mantle sources (e.g., Tuscany, Sardinia), (4) assimilation of lower crustal lithologies (e.g., Central Andes, Alban Hills, Mts.

Ernici, Ischia). Procida samples fall within the trends for Lesser Antilles and Ischia. The only Ischia sample falling outside the trend number 4 is a mafic enclave of Zaro eruption (ZR3C; Table 1 in electronic supplement for reference). Sr-O-isotope values of CF and SV magmas together form one vertical trend in Sr-O isotope space that deviates profoundly from the compositional trends of other subduction-related magmas. Only basalt magmas from Kamchatka also show a distinct vertical trend and this was interpreted that the mantle source was probably serpentinized in the fore-arc by dehydration of oceanic crust. This serpentinite was subsequently dragged into the melting region by rifting and arc migration where the serpentinite dewatered to peridotite that was subsequently melted after fluxing by slab-derived fluids (Dorendorf et al. 2000). Such hydrated fore-arc serpentinite (derived fluid) as a potential source in arc magmatism has more recently gained support for the Kamchatka case (Bindemann et al. 2004) as well as other arc settings (e.g., Liu et al. 2014; Harris et al. 2015; Underwood and Clyne, 2017; Yogodzinski et al. 2017). Our preferred scenario that involves a mixture of mantle peridotite (at least partly serpentinized by fluids from the altered oceanic crust) and a mixture of different types of subducted sediments indicates an even more complex magma source. Such a scenario of mixing different components prior to melting has recently been developed by Nielsen and Marschall (2017), who argued that arc magmas in general are sourced by a mixture of lithologies in the subducted *mélange* that are melted subsequent to source mixing. We propose that combined Sr-O-isotopes in minerals from arc magmas are essential to identify this process.

8. Conclusions

In summary our data show that:

1. Oxygen isotope compositions are very different from typical mantle values, spanning a large range towards heavy $\delta^{18}\text{O}_{\text{melt}}$ values compared to other volcanoes of the Italian Peninsula and subduction zones worldwide (Fig. 9);
2. Magmas feeding the Neapolitan volcanoes derived from distinct sources generating different magma batches that change systematically through time and space: the CF magmatic system is quite distinct from the SV one although CF and SV magmas fall on the same vertical trend in O-Sr isotope space;
3. High $\delta^{18}\text{O}_{\text{melt}}$ values in mafic rocks with Mg# up to 70 cannot be explained by assimilation of crustal lithologies into the magmas. For these magmas we propose a mantle source that was modified by the addition of up to 10% of subducted sediments (pelagic sediments and limestone) similar to the *mélange* melting model of Nielsen and Marschall (2017).

4. Assimilation of Hercynian crust (at a maximum of 12 and 21%) is restricted to highly evolved trachytic to phonolitic magmas of the Campi Flegrei and Somma Vesuvius region, respectively.

Acknowledgements

This work has been financially supported by the DFG-project Wo 362/42-1 funded to G.W. We thank "Ricerca Dipartimentale 2016, Dipartimento di Scienze della Terra, dell'Ambiente e delle Risorse, University Federico II of Naples, Italy" for helping with some oxygen measurements at Göttingen.

References

- Arienzo, I., Moretti, R., Civetta, L., Orsi, G., Papale, P., 2010. The feeding system of Agnano-Monte Spina eruption (Campi Flegrei, Italy): dragging the past into the present activity and future scenarios. *Chemical Geology* 270, 135–147.
- Arienzo, I., Carandente, A., Di Renzo, V., Belviso, P., Civetta, L., D'Antonio, M., Orsi, G., 2013. Sr and Nd isotope analysis at the Radiogenic Isotope Laboratory of the Istituto Nazionale di Geofisica e Vulcanologia, Sezione di Napoli - Osservatorio Vesuviano. *Rapporti Tecnici INGV* 260, pp. 1–18 (available online at <http://istituto.ingv.it/lingv/produzionescientifica/rapporti-tecnici-ingv/archivio/rapporti-tecnici-2013/>).
- Arienzo, I., Mazzeo, F.C., Moretti, R., Cavallo, A., D'Antonio, M., 2016. Open-system magma evolution and fluid transfer at Campi Flegrei caldera (Southern Italy) during the past 5 ka as revealed by geochemical and isotopic data. The example of the Nisida eruption. *Chemical Geology* 427, 109–124.
- Belkin, H.E., De Vivo, B., 1993. Fluid inclusion studies of ejected nodules from plinian eruptions of Mt. Somma-Vesuvius. *Journal of Volcanology and Geothermal Research* 58, 89-100.
- Bindeman, I.N., Ponomareva, V.V., Bailey, J.C., Valley, J.W., 2004. Volcanic arc of Kamchatka: a province with high- $\delta^{18}\text{O}$ magma sources and large-scale $^{18}\text{O}/^{16}\text{O}$ depletion of the upper crust. *Geochimica et Cosmochimica Acta* 68, 841–865.
- Brown, R.J., Civetta, L., Arienzo, I., D'Antonio, M., Moretti, R., Orsi, G., Tomlinson, E.L., Albert, P.G., Menzies, M.A., 2014. Geochemical and isotopic insights into the assembly, evolution and disruption of a magmatic plumbing system before and after a cataclysmic caldera-collapse eruption at Ischia volcano (Italy). *Contributions to Mineralogy and Petrology* 168, 1-23.

- Capuano, P., Russo, G., Civetta, L., Orsi, G., D'Antonio, M., 2013. The active portion of the Campi Flegrei caldera structure imaged by 3-D inversion of gravity data. *Geochemistry, Geophysics, Geosystem* 14, 4681-4697.
- Chiodini, G., Vandemeulebrouck, J., Caliro, S., D'Auria, L., De Martino, P., Mangiacapra, A., Petrillo, Z., 2015. Evidence of thermal-driven processes triggering the 2005–2014 unrest at Campi Flegrei caldera. *Earth and Planetary Science Letters* 414, 58-67.
- Civetta, L., Gallo, G., Orsi, G., 1991. Sr- and Nd-isotope and trace-element constraints on the chemical evolution of the magmatic system of Ischia (Italy) in the last 55 ka. *Journal of Volcanology and Geothermal Research* 46, 213-230.
- Civetta, L., D'Antonio, M., de Lorenzo, S., Di Renzo, V., Gasparini, P., 2004. Thermal and geochemical constraints on the “deep” magmatic structure of Mt. Vesuvius. *Journal of Volcanology and Geothermal Research* 133, 1–12.
- Clayton, R.N., Grossman, L., Mayeda, T.K., 1973. A component of primitive nuclear composition in carbonaceous meteorites. *Science* 182, 485–488.
- Clayton, R.N., Mayeda T.K., 1983. Oxygen isotopes in eucrites, shergottites, nakhlites, and chassignites. *Earth and Planetary Science Letters* 62, 1–6.
- D'Antonio, M., Civetta, L., Di Girolamo, P., 1999a. Mantle source heterogeneity in the Campanian region (south Italy) as inferred from geochemical and isotopic features of mafic volcanic rocks with shoshonitic affinity. *Mineralogy and Petrology* 67, 163–192.
- D'Antonio, M., Civetta, L., Orsi, G., Pappalardo, L., Piochi, M., Carandente, A., de Vita, S., Di Vito, M.A., Isaia R., 1999b. The present state of the magmatic system of the Campi Flegrei caldera based on a reconstruction of its behavior in the past 12 ka. *Journal of Volcanology and Geothermal Research* 91, 247–268.
- D'Antonio, M., Tonarini, S., Arienzo, I., Civetta, L., Di Renzo, V., 2007. Components and processes in the magma genesis of the Phlegrean Volcanic District, southern Italy. *Geological Society of America* 418, 203–220.
- D'Antonio, M., 2011. Lithology of the basement underlying the Campi Flegrei caldera: volcanological and petrological constraints. *Journal of Volcanology and Geothermal Research* 200, 91–98.
- D'Antonio, M., Tonarini, S., Arienzo, I., Civetta, L., Dallai, L., Moretti, R., Orsi, G., Andria, M., Trecalli, A., 2013. Mantle and crustal processes in the magmatism of the Campania region: inferences from mineralogy, geochemistry, and Sr–Nd–O isotopes of young hybrid volcanics of the Ischia island (South Italy). *Contributions to Mineralogy and Petrology* 165, 1173–1194.

- D'Auria, L., Pepe, S., Castaldo, R., Giudicepietro F., Macedonio, G., Ricciolino, P., Tizzani, P., Casu, F., Lanari, R., Manzo, M., Martini, M., Sansosti, E., Zinno, I., 2015. Magma injection beneath the urban area of Naples: a new mechanism for the 2012–2013 volcanic unrest at Campi Flegrei caldera. *Scientific Reports* 5, 13100.
- Dallai, L., Ghezzo, C., Sharp, Z.D., 2003. Oxygen isotope evidence for crustal assimilation and magma mixing in the Granite Harbour Intrusives, Northern Victoria Land, Antarctica. *Lithos* 67, 135-151.
- Dallai, L., Cioni, R., Boschi, C., D'Oriano, C., 2011. Carbonate-derived CO_2 purging magma at depth: Influence on the eruptive activity of Somma-Vesuvius, Italy. *Earth and Planetary Science Letters* 310, 84-95.
- De Astis, G., Pappalardo, L., Piochi, M., 2004. Procida volcanic history: new insights into the evolution of the Phlegraean Volcanic District (Campania region, Italy). *Bulletin of Volcanology* 66, 622–641.
- De Gennaro, M., Cappelletti, P., Langella, A., Perrotta, A., Scarpati C., 2000. Genesis of zeolites in the Neapolitan Yellow Tuff: geological, volcanological and mineralogical evidence. *Contributions to Mineralogy and Petrology* 139, 17-35.
- De Vivo, B., Belkin, H.E., Barbieri, M., Chelini, W., Lattanzi, P., Lima, A., Tolomeo, L., 1989. The Campi Flegrei (Italy) geothermal system: a fluid inclusion study of the Mofete and San Vito fields. *Journal of Volcanology and Geothermal Research* 36, 303–326.
- Deino, A.L., Orsi, G., de Vita, S., Piochi, M., 2004. The age of the Neapolitan Yellow Tuff caldera-forming eruption (Campi Flegrei caldera, Italy) assessed by $^{40}\text{Ar}/^{39}\text{Ar}$ dating method. *Journal of Volcanology and Geothermal Research* 133, 157–170.
- Del Moro, A., Fulignati, P., Marianelli, P., Sbrana, A., 2001. Magma contamination by direct wall rock interaction: constraints from xenoliths from the walls of a carbonate-hosted magma chamber (Vesuvius 1944 eruption). *Journal of Volcanology and Geothermal Research* 112, 15-24.
- Di Renzo, V., Di Vito, M.A., Arienzo, I., Carandente, A., Civetta, L., D'Antonio, M., Giordano, F., Orsi, G., Tonarini, S., 2007. Magmatic history of Somma-Vesuvius on the basis of new geochemical and isotopic data from a deep borehole (Camaldoli della Torre). *Journal of Petrology* 48, 753–784.
- Di Renzo, V., Arienzo, I., Civetta, L., D'Antonio, M., Tonarini, S., Di Vito, M.A., Orsi, G., 2011. The magmatic feeding system of the Campi Flegrei caldera: architecture and temporal evolution. *Chemical Geology* 281, 227–241.

- Di Rocco, M., Freda, C., Gaeta, M., Mollo, S., Dallai, L., 2012. Magma Chambers Emplaced in Carbonate Substrate: Petrogenesis of Skarn and Cumulate Rocks and Implications for CO_2 Degassing in Volcanic Areas. *Journal of Petrology* 53, 2307–2332.
- Dorendorf, F., Wiechert, U., Wörner, G., 2000. Hydrated sub-arc mantle: a source for the Kluchevskoy volcano, Kamchatka/Russia. *Earth and Planetary Sciences Letters* 175, 69-86.
- Downes, H., Thirlwall, M.F., Trayhorn, S.C., 2001. Miocene subduction-related magmatism in southern Sardinia: Sr–Nd- and oxygen isotopic evidence for mantle source enrichment. *Journal of Volcanology and Geothermal Research* 106, 1-22.
- Eiler, J.M., 2001. Oxygen isotope variations of basaltic lavas and upper mantle rocks. In: Valley, J.W., Cole D.R., (Eds.), *Stable Isotope Geochemistry*. Mineralogical Society of America and *Reviews in Mineralogy and Geochemistry* 43, pp. 319–364.
- Fedele, L., Scarpati, C., Lanphere, M., Melluso, L., Morra, V., Perrotta, A., Ricci, G., 2008. The Breccia Museo formation, Campi Flegrei, southern Italy: geochronology, chemostratigraphy and relationship with the Campanian Ignimbrite eruption. *Bulletin of Volcanology* 70, 1189-1219.
- Freyduth, H., Brandmeier, M., Wörner, G., 2015. The origin and crust/mantle mass balance of Central Andean ignimbrite magmatism constrained by oxygen and strontium isotopes and erupted volumes. *Contributions to Mineralogy and Petrology* 169, 58.
- Fulignati, P., Panichi, C., Sbrana, A., Caliro, S., Gioncada, A., Del Moro, A., 2005. Skarn formation at the walls of the 79AD magma chamber of Vesuvius (Italy): Mineralogical and isotopic constraints. *Journal of Mineralogy and Geochemistry* 181, 53-66.
- Guidoboni, E., Ciuccarelli, C., 2011. The Campi Flegrei caldera: historical revision and new data on seismic crises, bradyseisms, the Monte Nuovo eruption and ensuing earthquakes (twelfth century 1582 ad). *Bulletin of Volcanology* 73, 655-677.
- Harris, C., le Roux, P., Cochrane, R., Martin, L., Duncan, A.R., Marsh, J.S., le Roex, A.P., Class, C., 2015. The oxygen isotope composition of Karoo and Etendeka picrites: High $\delta^{18}\text{O}$ mantle or crustal contamination. *Contributions to Mineralogy and Petrology* 170, 8. DOI.10.1007/s00410-015-1164-1.
- Iacono Marziano, G., Gaillard, F., Pichavant, M., 2008. Limestone assimilation by basaltic magmas: an experimental re-assessment and application to Italian volcanoes. *Contributions to Mineralogy and Petrology* 155, 719–738.
- Iovine, R.S., Mazzeo, F.C., Arienzo, I., D'Antonio, M, Wörner, G., Civetta, L., Pastore, Z., Orsi, G., 2017. Source and magmatic evolution inferred from geochemical and Sr-O-isotope data on hybrid lavas of Arso, the last eruption at Ischia island (Italy; 1302 AD). *Journal of Volcanology and Geothermal Research* 331, 1-15.

- Jolis, E.M., Freda, C., Troll, V.R., Deegan, F.M., Blythe, L.S., McLeod, C.L., Davidson, J.P., 2013. Experimental simulation of magma–carbonate interaction beneath Mt. Vesuvius, Italy. *Contributions to Mineralogy and Petrology* 166, 1335–1353.
- Jolis, E.M., Troll, V.R., Harris, C., Freda, C., Gaeta, M., Orsi, G., Siebe, C., 2015. Skarn xenolith record crustal CO_2 liberation during Pompeii and Pollena eruptions, Vesuvius volcanic system, central Italy. *Chemical Geology* 415, 17–36.
- Le Maitre, R.W., 2002. *Igneous rocks: a classification and glossary of terms: recommendations of the International Union of Geological Sciences, Sub-commission on the Systematics of Igneous Rocks*. Cambridge University Press, Cambridge, UK 1-236.
- Liu, C.Z., Wu, F.Y., Chng, S.L., Li, Q.L., Sun, W.D., Ji, W.Q., 2014. A 'hidden' ^{18}O -enriched reservoir in the sub-arc mantle. *Scientific Reports* 4, 4232. DOI. 10.1038/srep04232.
- Lustrino, M., Duggen, S., Rosenberg, C.L., 2011. The Central-Western Mediterranean: anomalous igneous activity in an anomalous collisional tectonic setting. *Earth-Science Reviews* 104, 1-40.
- Mangiacapra, A., Moretti, R., Rutheford, M., Civetta, L., Orsi, G., Papale, P., 2008. The deep magmatic system of the Campi Flegrei caldera (Italy), *Geophysical Research Letters* 35, L21304. DOI. 10.1029/2008GL035550.
- Mattey, D., Lowry, D., Macpherson, C., 1994. Oxygen isotope composition of mantle peridotite. *Earth and Planetary Science Letters* 128, 231-241.
- Matzen, A.K., Baker, M.B., Beckett, J.R., Stople, M., 2011. Fe–Mg Partitioning between Olivine and High-magnesian Melts and the Nature of Hawaiian Parental Liquids. *Journal of Petrology* 52, 1243-1263.
- Mazzeo, F.C., D'Antonio, M., Arienzo, I., Aulinas, M., Di Renzo, V., Gimeno, D., 2014. Subduction-related enrichment of the Neapolitan volcanoes (Southern Italy) mantle source: new constraints on the characteristics of the slab-derived components. *Chemical Geology* 386, 165–183.
- Mazzeo, F.C., Zanetti, A., Aulinas, M., Petrosino, P., Arienzo, I., D'Antonio M., 2017. Evidence for an intra-oceanic affinity of the serpentized peridotites from the Mt. Pollino ophiolites (Southern Ligurian Tethys): Insights into the peculiar tectonic evolution of the Southern Apennines. *Lithos* 284-285, 367-380.
- Melluso, L., de' Gennaro, R., Fedele, L., Franciosi, L., Morra, V., 2012. Evidence of crystallization in residual, Cl–F-rich, agpaitic, trachyphonolitic magmas and primitive Mg-rich basalt–trachyphonolite interaction, in the lava domes of the Phlegrean Fields (Italy). *Geological Magazine* 149, 532–550.

- Melluso, L., Morra, V., Guarino, V., de' Gennaro, R., Franciosi, L., Grifa, C., 2014. The crystallization of shoshonitic to peralkaline trachyphonolitic magmas in a H₂O–Cl–F-rich environment at Ischia (Italy), with implications for the feeder system of the Campania Plain volcanoes. *Lithos* 210-211, 242-259.
- Mollo, S., Putirka, K., Misiti, V., Soligo, M., Scarlato, P., 2013. A new test for equilibrium based on clinopyroxene–melt pairs: clues on the solidification temperatures of etnean alkaline melts at post-eruptive conditions. *Chemical Geology* 352, 92–100.
- Morabito, S., Petrosino, P., Milia, A., Sprovieri, M., Tamburrino, S., 2014. A multidisciplinary approach for reconstructing the stratigraphic framework of the last 40 ka in a bathyal area of the eastern Tyrrhenian Sea. *Global and Planetary Change* 123, 124-138.
- Nielsen, S.G., Marschall, H.R., 2017. Geochemical evidence for mélangé melting in global arcs. *Science Advances* 3, e1602402. Doi. 10.1126/sciadv.1602402.
- Orsi, G., Gallo, G., Zanchi A., 1991. Simple shearing block resurgence in caldera depressions. A model from Pantelleria and Ischia. *Journal of Volcanology and Geothermal Research* 47, 1–11.
- Orsi, G., de Vita, S., Di Vito, M.A., 1996. The restless, resurgent Campi Flegrei nested caldera (Italy): constraints on its evolution and configuration. *Journal of Volcanology and Geothermal Research* 74, 179–214.
- Orsi, G., Di Vito, M.A., Selva, J., Marzocchi, W., 2009. Long-term forecast of eruption style and size at Campi Flegrei caldera (Italy). *Earth and Planetary Science Letters* 287, 265-276.
- Pabst, S., Wörner, G., Civetta, L., Tesoro, R., 2008. Magma chamber evolution prior to the Campanian Ignimbrite and Neapolitan Yellow Tuff eruptions (Campi Flegrei, Italy). *Bulletin of Volcanology* 70, 961-976.
- Pack, A., Tanaka, R., Hering, M., Sengupta, S., Peters, S., Nakamura, E., 2016. The oxygen isotope composition of San Carlos olivine on the VSMOW2-SLAP2 scale. *Rapid Communications Mass Spectrometry* 30, 1495–1504.
- Paoletti, V., M. D'Antonio, A. Rapolla, 2013. The structural setting of the Ischia Island (Phlegrean Volcanic district, southern Italy): inferences from geophysics and geochemistry. *Journal of Volcanology and Geothermal Research* 249, 155-173.
- Paone, A., 2006. The geochemical evolution of the Mt. Somma-Vesuvius volcano. *Mineralogy and Petrology* 87, 53-80.
- Pappalardo, L., Piochi, M., Mastrolorenzo, G., 2004. The 3550 year BP-1944 A.D. magma-plumbing system of Somma-Vesuvius: constraints on its behaviour and present state through a review of Sr-Nd isotope data. *Annals of Geophysics, INGV* 47.

- Peccerillo, A., 2001. Geochemical similarities between the Vesuvius, Phlegraean Fields and Stromboli volcanoes: petrogenetic, geodynamic and volcanological implications. *Mineralogy and Petrology* 73, 93–105.
- Peccerillo, A., Federico, M., Barbieri, M., Brilli, M., Wu, T. W., 2010. Interaction between ultrapotassic magmas and carbonate rocks: evidences from geochemical and isotopic (Sr-Nd-O) compositions of granular lithic clasts from the Alban Hills Volcano (Central Italy). *Geochimica et Cosmochimica Acta* 74, 2999-3022.
- Perrotta, A., Scarpati, C., Luongo, G., Morra, V., 2010. Stratigraphy and volcanological evolution of the southwestern sector of Campi Flegrei and Procida Island, Italy. *The Geological Society of America Special Paper* 464, 171-191.
- Piochi, M., Bruno, P.P., De Astis, G., 2005. Relative roles of rifting tectonics and magma ascent processes: Inferences from geophysical, structural, volcanological, and geochemical data for the Neapolitan volcanic region (southern Italy). *Geochemistry, Geophysics, Geosystems* 6, Q07005.
- Piochi, M., Ayuso, R.A., De Vivo, B., Somma, R., 2006. Crustal contamination and crystal entrapment during evolution at Mt. Somma-Vesuvius volcano, Italy: geochemical and Sr isotopic evidence. *Lithos* 86, 303-329.
- Piochi, M., Kilburn, C.R.J., Di Vito, M.A., Mormone, A., Tramelli, A., Troise, C., De Natale, G., 2014. The volcanic and geothermally active Campi Flegrei caldera: an integrated multidisciplinary image of its buried structure. *International Journal of Earth Sciences* 103, 401-421.
- Portnyagin, M., Hoernle, K., Plechov, P., Mironov, N., Khubunaya, S., 2007. Constraints on mantle melting and composition and nature of slab components in volcanic arcs from volatiles (H_2O , S, Cl, F) and trace elements in melt inclusions from the Kamchatka Arc. *Earth and Planetary Science Letters* 255, 53-69.
- Rolandi, G., Barrella, A.M., Borrelli, A., 1993. The 1631 eruption of Vesuvius. *Journal of Volcanology and Geothermal Research* 58, 183–201.
- Rosi, M., Santacroce, R., 1983. The A.D. 472 ‘Pollena’ eruption, volcanological and petrological data for this poorly know Plinian-type event at Vesuvius. *Journal of Volcanology and Geothermal Research* 17, 249–271.
- Rosi, M., Sbrana, A., Vezzoli, L., 1988. Stratigrafia delle isole di Procida e Vivara. *Bollettino Gruppo Nazionale di Vulcanologia* 4, 500–525.
- Rosi, M., Principe, C., Vecchi, R., 1993. The 1631 eruption of Vesuvius reconstructed from the review of chronicles and study of deposits. *Journal of Volcanology and Geothermal Research* 58, 151–182.

- Santacroce, R., Cioni, R., Marianelli, P., Sbrana, A., Sulpizio, R., Zanchetta, G., Donahue, D.J., Joron J.L., 2008. Age and whole rock–glass compositions of proximal pyroclastics from the major explosive eruptions of Somma-Vesuvius: A review as a tool for distal tephrostratigraphy. *Journal of Volcanology and Geothermal Research* 177, 1–18.
- Scarpati, C., Perrotta, A., Lepore, S., Calvert, A., 2013. Eruptive history of Neapolitan volcanoes: constraints from ^{40}Ar – ^{39}Ar dating. *Geological Magazine* 150, 412-425.
- Schiano, P., Clocchiatti, R., Ottoline, L., Sbrana, A., 2004. The relationship between potassic, calc-alkaline and Na-alkaline magmatism in South Italy volcanoes: A melt inclusion approach. *Earth Planet Sci Lett* 220, 121-137.
- Smith, V.C., Isaia, R., Pearce, N.J.G., 2011. Tephrostratigraphy and glass compositions of post-15 kyr Campi Flegrei eruptions: implications for eruption history and chronostratigraphic markers. *Quaternary Science Reviews* 30, 3638–3660.
- Sparice, D., Scarpati, C., Mazzeo, F.C., Petrosino, P., Arienzo, I., Gisbert, G., Petrelli M., 2017. New proximal tephra at Somma-Vesuvius: evidences of a pre-caldera, large (?) explosive eruption. *Journal of Volcanology and Geothermal Research* 335, 71-81.
- Sparice, D., Scarpati, C., Perrotta, A., Mazzeo, F.C., Calvert, A.T., Lanphere, M.A., (in press). New insights on lithofacies architecture, sedimentological characteristics and volcanological evolution of pre-caldera (> 22ka), multi-phase, scoria-and spatter-cones at Somma-Vesuvius. *Journal of Volcanology and Geothermal Research*.
- Spera, F.J., Bohron, W.A., 2001. Energy-constrained open-system magmatic processes I: general model and energy-constrained assimilation and fractional crystallization (EC-AFC) formulation. *Journal of Petrology* 42, 999–1018.
- Staudigel, H., Plank, T., White, B., Schmincke, H.U., 1996. Geochemical fluxes during seafloor alteration of the basaltic upper oceanic crust; DSDP sites 417 and 418, in: G.E. Bebout, D.W. Scholl, S.H. Kirby, J.P. Platt (Eds.), *Subduction Top to Bottom*, American Geophysical Union, Washington,DC. Geophysical Monograph 96, pp. 19-38.
- Underwood, S.J., Clyne, M.A., 2017. Oxygen isotope geochemistry of mafic phenocrysts in primitive mafic lavas from the southernmost Cascade Range, California. *American Mineralogist* 102, 252-261.
- Yogodzinski, G.W., Kelemen, P., Hoernle, K., Brown, S.T., Bindemann, I., Vervoort, J.D., Sims, K.W.W., Portnyagin, M., Werner R., 2017. Sr and O isotopes in western Aleutian seafloor lavas: Implications for the source of fluids and trace element character of arc volcanic rocks. *Earth and Planetary Science Letters* 47, 169-180.

Zollo, A., D'Auria, L., de Matteis, R., Herrero, A., Virieux, J., Gasparini, P., 2002. Bayesian estimation of 2-D P-velocity models from active seismic arrival time data: imaging of the shallow structure of Mt Vesuvius (Southern Italy). *Geophysical Journal International* 151, 566–582.

Zollo, A., Maercklin, N., Vassallo, M., Dello Iacono, D., Virieux, J., Gasparini, P., 2008. Seismic reflections reveal a massive melt layer feeding Campi Flegrei caldera. *Geophysical Research Letters* 35, L12306.

Chapter 4: Timescales of magmatic processes prior to the 4.7 ka Agnano-Monte Spina eruption (Campi Flegrei caldera, Southern Italy) based on diffusion chronometry from sanidine phenocrysts

Raffaella Silvia Iovine¹ · Lorenzo Fedele² · Fabio Carmine Mazzeo² · Ilenia Arienzo³ · Andrea Cavallo⁴ · Gerhard Wörner¹ · Giovanni Orsi² · Lucia Civetta^{2,5} · Massimo D'Antonio^{2,3}

Received: 1 July 2016 / Accepted: 11 January 2017
© Springer-Verlag Berlin Heidelberg 2017

Abstract Barium diffusion chronometry applied to sanidine phenocrysts from the trachytic Agnano-Monte Spina eruption (~4.7 ka) constrains the time between reactivation and eruption of magma batches in the Campi Flegrei caldera. Backscattered electron imaging and quantitative electron microprobe measurements on 50 sanidine phenocrysts from representative pumice samples document core-to-rim compositional zoning. We focus on compositional breaks near the crystal rims that record magma mixing processes just prior to eruption. Diffusion times were modeled at a magmatic temperature of 930 °C using profiles based on quantitative BaO point analyses, X-ray scans, and grayscale swath profiles, yielding times ≤60 years between mixing and eruption. Such short timescales are consistent with volcanological and

geochronological data that indicate that at least six eruptions occurred in the Agnano-San Vito area during few centuries before the Agnano-Monte Spina eruption. Thus, the short diffusion timescales are similar to time intervals between eruptions. Therefore, the rejuvenation time of magma residing in a shallow reservoir after influx of a new magma batch that triggered the eruption, and thus pre-eruption warning times, may be as short as years to a few decades at Campi Flegrei caldera.

Keywords Diffusion chronometry · Pre-eruptive magmatic processes · Campi Flegrei caldera · Agnano-Monte Spina · EMP analysis · BSE imaging

Editorial responsibility: P. Wallace

Electronic supplementary material The online version of this article (doi:10.1007/s00445-017-1101-4) contains supplementary material, which is available to authorized users.

✉ Massimo D'Antonio
masdanto@unina.it

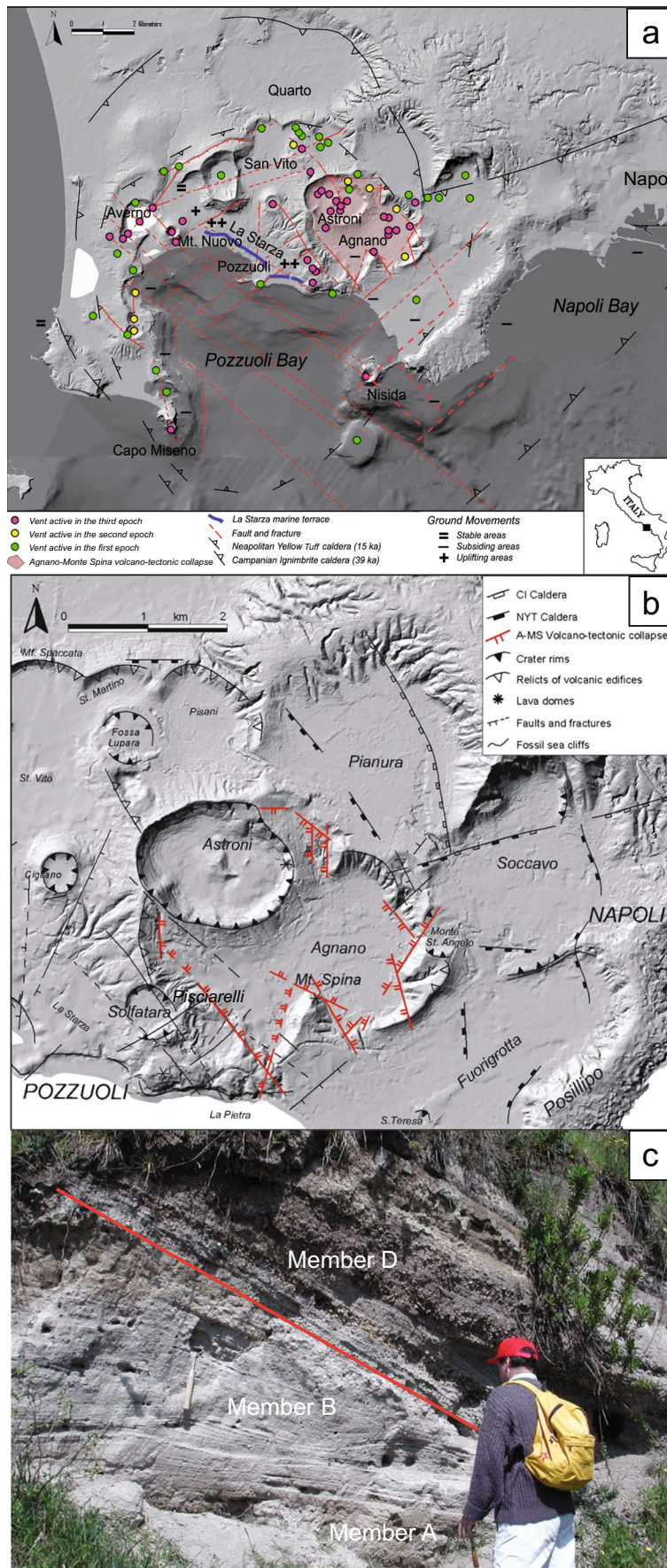
- ¹ Geowissenschaftliches Zentrum, Georg-August-Universität (GZG), Goldschmidtstrasse 1, 37077 Göttingen, Germany
- ² Dipartimento di Scienze della Terra, dell'Ambiente e delle Risorse (DiSTAR), University of Naples Federico II, Largo S. Marcellino 10, 80138 Naples, Italy
- ³ Istituto Nazionale di Geofisica e Vulcanologia (INGV)–Sezione di Napoli Osservatorio Vesuviano, Via Diocleziano 328, 80124 Naples, Italy
- ⁴ Istituto Nazionale di Geofisica e Vulcanologia (INGV)–Sezione Roma1, Via di Vigna Murata 605, 00143 Rome, Italy
- ⁵ Istituto Nazionale di Geofisica e Vulcanologia (INGV)–Sezione di Palermo, Via U. La Malfa 153, 90146 Palermo, Italy

Introduction

Knowing timescales of magmatic processes such as crystallization, mingling/mixing, and crystal mush rejuvenation in shallow plumbing systems is important for a better understanding of how these phenomena occur and how they relate to the compositional variety of igneous rocks (e.g., Costa et al. 2008; Costa and Morgan 2011; Schmitt 2011). Moreover, estimating the timescales of such magmatic processes is crucial for volcanic hazard assessment and risk mitigation at active volcanoes. In particular, for a dormant, though active and restless volcano, such as the Campi Flegrei caldera (CFC; Fig. 1a) (Orsi et al. 1996, 2004, 2009), an estimate of the time required for magma batches to become eruptible, either by coalescence of separate shallow reservoirs or magma mixing caused by deeper recharge, is important.

Two methods have been recently developed to estimate residence times of magmas and their crystals: (1) direct age determination by short-lived U-series isotopes (e.g., Cooper

Chapter 4: Timescales of magmatic processes prior to the 4.7 ka Agnano-Monte Spina eruption (Campi Flegrei caldera, Southern Italy) based on diffusion chronometry from sanidine phenocrysts



◀ **Fig. 1** **a** Schematic tectonic map of the Campi Flegrei caldera. The Agnano-San Vito area is located in the center, areas affected by volcano-tectonic collapse during the Agnano-Monte Spina eruption in pink. Colored dots indicate centers that have been active during the CFc activity of the past 15 kyr (Selva et al. 2012). **b** Detail of the Agnano-San Vito area. Red lines delineate areas collapsed during the A-MS eruption. Solfatara and Pisciarelli are areas of intense hydrothermal activity. **c** Deposits of the A-MS eruption, members A through D. Red line: unconformity related to the syn-eruptive collapse

and Reid 2008; Schmitt 2011) and (2) diffusion chronometry based on high spatial resolution element zoning in phenocrysts measured by electron microprobe (e.g., Turner and Costa 2007; Costa et al. 2008; Chakraborty 2008; Costa and Morgan 2011; Ruprecht and Cooper 2012; Chamberlain et al. 2014). These two approaches often yield different results (Cooper and Kent 2014) due to the fact that U-series chronology measures the absolute age, whereas diffusion chronometry only records times during which crystals reside at high temperature above the diffusion threshold. Thus, storage in relatively cold crystal mushes at or just below the solidus will not be recorded in diffusion times. For growth discontinuities at the outermost crystal rims that likely represent magma recharge and mixing events occurring just prior to eruption, the temperature histories can be well constrained by means of either crystal-liquid or crystal-crystal geothermometers; also, long storage is unlikely to have occurred when the compositional discontinuity is sharp. We use this approach in our study of deposits from the Agnano-Monte Spina eruption in the CFc (Fig. 1a).

Estimates of the timescales of pre-eruptive processes at the CFc have so far been based on two different approaches. U–Th mineral isochrons from pumice samples of the Campanian Ignimbrite (CI), the most energetic eruption of CFc, gave mineral ages that are 6.4 ± 2.1 kyr older than eruption age (Arienzo et al. 2011). A slightly older but still comparable (within analytical error) pre-eruptive age of 9.1 ± 2.5 kyr was determined for minerals from cognate syenite lithics from a crystallized carapace of the magma reservoir (Gebauer et al. 2014). However, such long timescales are probably related to pre-eruptive crystallization during magma rise from its source region (Arienzo et al. 2011) and/or to older crystal cargo and not to eruption-triggering mixing events. In the second approach, Perugini et al. (2015) argued that mixing takes place less than tens of minutes prior to eruption. However, their approach does not give meaningful time information on eruption-triggering processes because it compares compositional variation between lumps of pumice that represent samples of magmas that may have never been in diffusive contact with submillimeter compositional strips in experimentally mixed melts without crystals.

Here, we use diffusion chronometry on sanidine phenocrysts from representative trachytic pumice from the Agnano-Monte Spina explosive eruption (A-MS) that

occurred at 4.67 ± 0.09 cal ka at CFc (de Vita et al. 1999). In a probabilistic long-term forecast of the style and size of the next eruption at CFc, A-MS has been taken as the type-event for a large-size eruption in case of renewal of volcanism in short-mid terms (Orsi et al. 2009). Furthermore, the eruption, which was accompanied by a volcano-tectonic collapse, took place within the area today at the highest probability of opening of a new vent (Orsi et al. 2004; Selva et al. 2012) (Pisciarelli and Solfatara; Fig. 1a, b). A-MS products display clear evidence of mixing between trachytic magmas with different chemical compositions (de Vita et al. 1999; Arienzo et al. 2010) and are an ideal case study for determining timescales of magma mobilization prior to explosive volcanic events at CFc.

Geology and eruptive products

Volcanic history and petrology

Activity in the Campi Flegrei (CF) volcanic field (Fig. 1) began prior to 80 ka (Scarpato et al. 2013), with the last eruption occurring in 1538 AD. The caldera is inhabited by 500,000 people, making it a high-risk volcanic area (Orsi et al. 2009). Recent unrest started in the 1950s with faint seismicity, slow continuous uplift, and changes in the geochemical parameters of fumaroles and thermal springs (e.g., Saccorotti et al. 2007; Del Gaudio et al. 2010; Chiodini et al. 2015; D’Auria et al. 2015).

Volcanic deposits of the CF are mostly pyroclastic rocks and subordinate lavas, and volcanic activity has been dominantly explosive through time, with several volcano-tectonic collapse episodes that resulted in a nested resurgent caldera (Orsi et al. 1996). The most abundant volcanic rocks of the CF are trachytes and phonolites, but less abundant latites and shoshonites also occur. Two large-volume explosive eruptions accompanied by caldera collapse events, the Campanian Ignimbrite (CI; ~ 39 ka; De Vivo et al. 2001) and the Neapolitan Yellow Tuff (NYT; ~ 15 ka; Deino et al. 2004), are used as stratigraphic markers, allowing for subdivision of the CF history into three periods: period I, pre-CI; period II, between CI and NYT; and period III, post-NYT (Orsi et al. 1996).

In the past 15 kyr (period III), volcanic activity was characterized by at least 72 explosive eruptions of variable magnitude, fed by magma batches of less than 1 km^3 (Orsi et al. 2009; Smith et al. 2011). On the basis of the evaluation of the most important physical parameters (e.g., dispersal, volume, and density of the pyroclastic deposits; volume of erupted magma; total erupted mass; and eruption magnitude), Orsi et al. (2009) have performed a size classification of the explosive eruptions of the past 5 kyr at the CFc, which are grouped into three sizes: small, medium, and large. Two widespread,

well-developed paleosols separate products of period III (Di Vito et al. 1999). Recent geochronological data suggest that minor activity also occurred during the development of these paleosols (Fedele et al. 2011, 2012; Isaia et al. 2012).

During the past ~5 kyr, 22 generally low- to medium-magnitude explosive eruptions occurred from vents mostly located in the NE part of the NYT caldera in the Agnano-San Vito area (Di Vito et al. 1999; Orsi et al. 2004, 2009; Fig. 1a, b). The 12-km² Agnano-San Vito area, including the Astroni, Solfatara, and Agnano craters, is considered to be the site of highest probability for future eruptions (Orsi et al. 2004; Selva et al. 2012). This portion of the NYT caldera has been under extension since at least 5 ka (Capuano et al. 2013) through NW-SE- and NE-SW-trending regional faults, favoring the ascent of trachytic and latitic magmas which fed the eruptions. This caldera sector is currently affected by voluminous hydrothermal emissions (Chiodini et al. 2015 and references therein).

Mineralogical, geochemical, and isotopic variability of CF magmas results from source heterogeneity, crystal fractionation, and open-system mixing processes (e.g., D'Antonio et al. 1999, 2007; Pappalardo et al. 1999, 2002; Fedele et al. 2008, 2009, 2015, 2016; Pabst et al. 2008; Arienzo et al. 2009, 2015, 2016; Tonarini et al. 2009; Di Renzo et al. 2011; Di Vito et al. 2011; Fourmentraux et al. 2012; Melluso et al. 2012). Pressures estimated from melt inclusions in mafic minerals from <5 ka deposits indicate crystallization between ~9 and ~3–5 km (e.g., Mangiacapra et al. 2008; Arienzo et al. 2010, 2016). Therefore, the present CFc magmatic plumbing system likely comprises small, shallow reservoirs, where variably evolved magmas supplied from a deeper (~9 km) reservoir are stored, coalesce, and mix before and/or during eruptions (Pabst et al. 2008; Di Renzo et al. 2011; Arienzo et al. 2015, 2016).

The Agnano-Monte Spina eruption

The 4.67 ± 0.09 cal ka A-MS eruption occurred from a vent in the Agnano-San Vito area (Fig. 1b). The eruption, predated by at least three minor explosive events in the preceding hundred years from vents located in the same area, had a magnitude of 5.3 and has been classified as the only high-magnitude event of the past ~5 kyr at CFc (Orsi et al. 2004, 2009). Its distribution and thickness yield an estimate for the total volume of ejected magma of ~0.9 km³ (dense rock equivalent (DRE); Orsi et al. 2009). The well-studied A-MS sequence is composed of pyroclastic flow and fallout deposits subdivided into six members (A through F, Fig. 2). The upper part of member B is cut by an erosional unconformity (Fig. 1c) that marks a pause in the activity, followed by a ~6-km² collapse during a paroxysmal phase that deposited member D (de Vita et al. 1999). Eruptive phases were fed initially by a homogenous, evolved trachyte, followed by heterogeneous, less evolved

trachyte, likely resulting from mixing between two geochemical and isotopically distinct magmas (de Vita et al. 1999; Arienzo et al. 2010).

Samples and methods

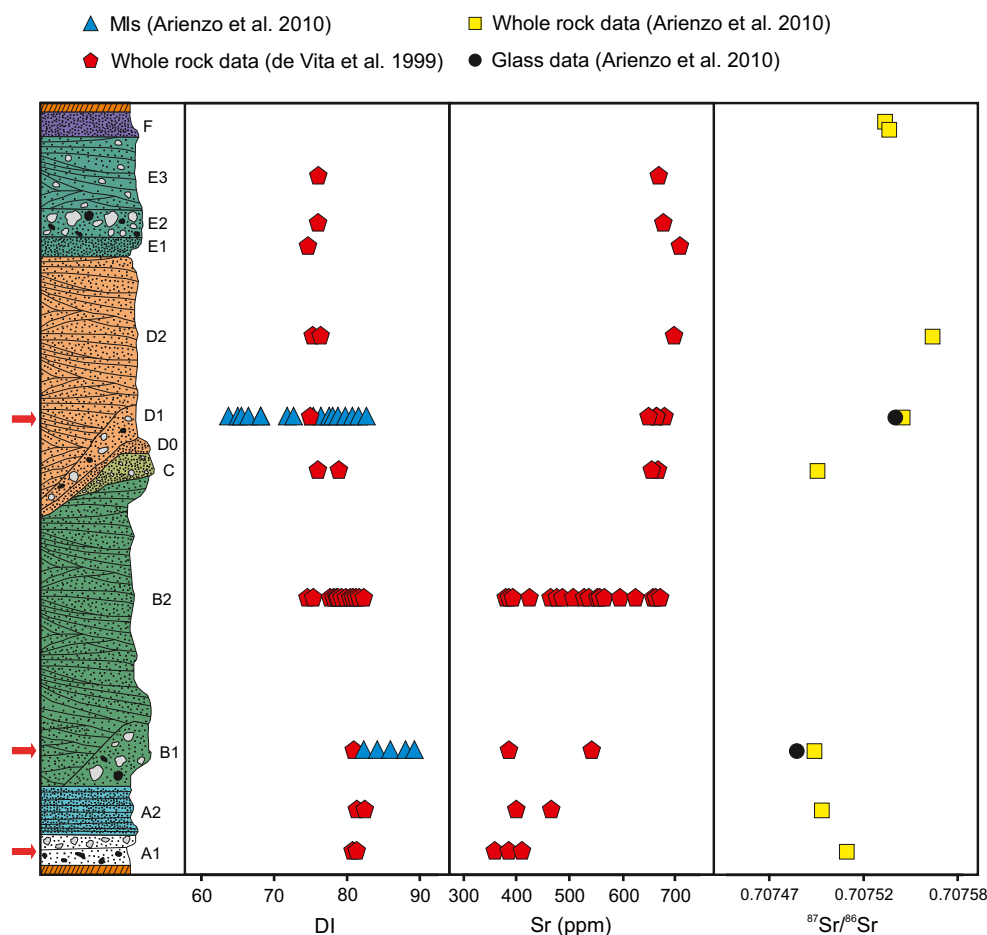
Representative pumice samples from A-MS members A, B, and D (Fig. 2; de Vita et al. 1999) are poorly porphyritic (5–10 vol%), with some large euhedral sanidine phenocrysts (2–5 mm, rarely ~7–8 mm). Clinopyroxene is generally more abundant, smaller, and strongly zoned from colorless cores to pale green rims. Plagioclase phenocrysts and microphenocrysts commonly display corroded margins and a “dusty” appearance due to abundant glassy inclusions. Biotite is sparse and mostly occurs as microphenocrysts <1 mm in size; a few phenocrysts range up to ~2 mm. Small monomineralic (clinopyroxene or plagioclase) and polymineralic (clinopyroxene + plagioclase ± biotite) aggregates are also observed. The groundmass is highly vesicular and glassy, with few microlites of opaques and apatite (both of which also occur as inclusions in clinopyroxene and biotite). Although pumices from all members are similar in texture and paragenesis, pumices from upper members D, E, and F have less sanidine (absent in the topmost F) compared to lower members A, B, and C, consistent with pumices becoming less evolved towards the top (de Vita et al. 1999; Arienzo et al. 2010).

Analytical methods

Representative samples from members A, B, and D were chosen to cover the observed range petrographic variability. Sanidine phenocrysts were handpicked from crushed pumice fragments under a binocular microscope, immersed in epoxy, polished, and carbon coated for electron microprobe analysis; minerals were also analyzed in polished slides from pumice fragments. A total of 50 sanidine phenocrysts were selected for core-to-rim compositional profiling. Figure 3 shows examples of the complex textural features of the investigated sanidine phenocrysts, highlighted by backscattered electron (BSE) images.

Major- and minor-element concentrations were determined through combined energy-dispersive and wavelength-dispersive electron microprobe (EDS-WDS-EMP) analyses. These were carried out on both single spots and core-to-rim transects crossing growth zones. Profiles are 200–300 μm long and commonly show a complex zoning pattern, with K₂O content (i.e., orthoclase component) decreasing first (normal zoning), then increasing (reverse zoning), then abruptly decreasing again, followed by oscillatory zoning, with frequent resorption surfaces (e.g., Fig. 4). Analyses (both BSE and quantitative measurements) were performed using a JEOL

Fig. 2 Chemostratigraphy of A-MS deposits subdivided in members A through F. Differentiation index (DI = normative quartz + orthoclase + albite + nepheline + leucite), Sr content, and $^{87}\text{Sr}/^{86}\text{Sr}$ values vs. stratigraphic position from de Vita et al. (1999) and Arienzo et al. (2010). Positions of samples analyzed in this work are indicated by red arrows



JXA-8200 Superprobe at Istituto Nazionale di Geofisica e Vulcanologia (INGV)–Sezione Roma1, Rome, and a JEOL JXA-8900R microprobe at GZG, Universität Göttingen. Both microprobes were equipped with five wavelength-dispersive system X-ray spectrometers, one energy-dispersive X-ray spectrometer, and a BSE detector for imaging and WDS profile analysis. Measurements at INGV were performed at 15-kV accelerating voltage, 20-nA beam current, and 10- μm beam size. Counting times were set to 10 s for the peak and 5 s for the background. For the determination of Ba, the counting time was increased to 60 s for the peak and 30 s for the background to minimize errors and detection limits. Data were treated using a ZAF correction procedure. Both natural and synthetic standards were employed to check the precision and accuracy of the instrument: jadeite for Si and Na, corundum for Al, forsterite for Mg, andradite for Fe, rutile for Ti, orthoclase for K, barite for Ba, celestine for Sr, fluorite for F, apatite for P and Cl, and spessartine for Mn. Typical analytical uncertainty was $\sim 1\%$ relative for major oxides and $\sim 10\%$ relative for minor oxides.

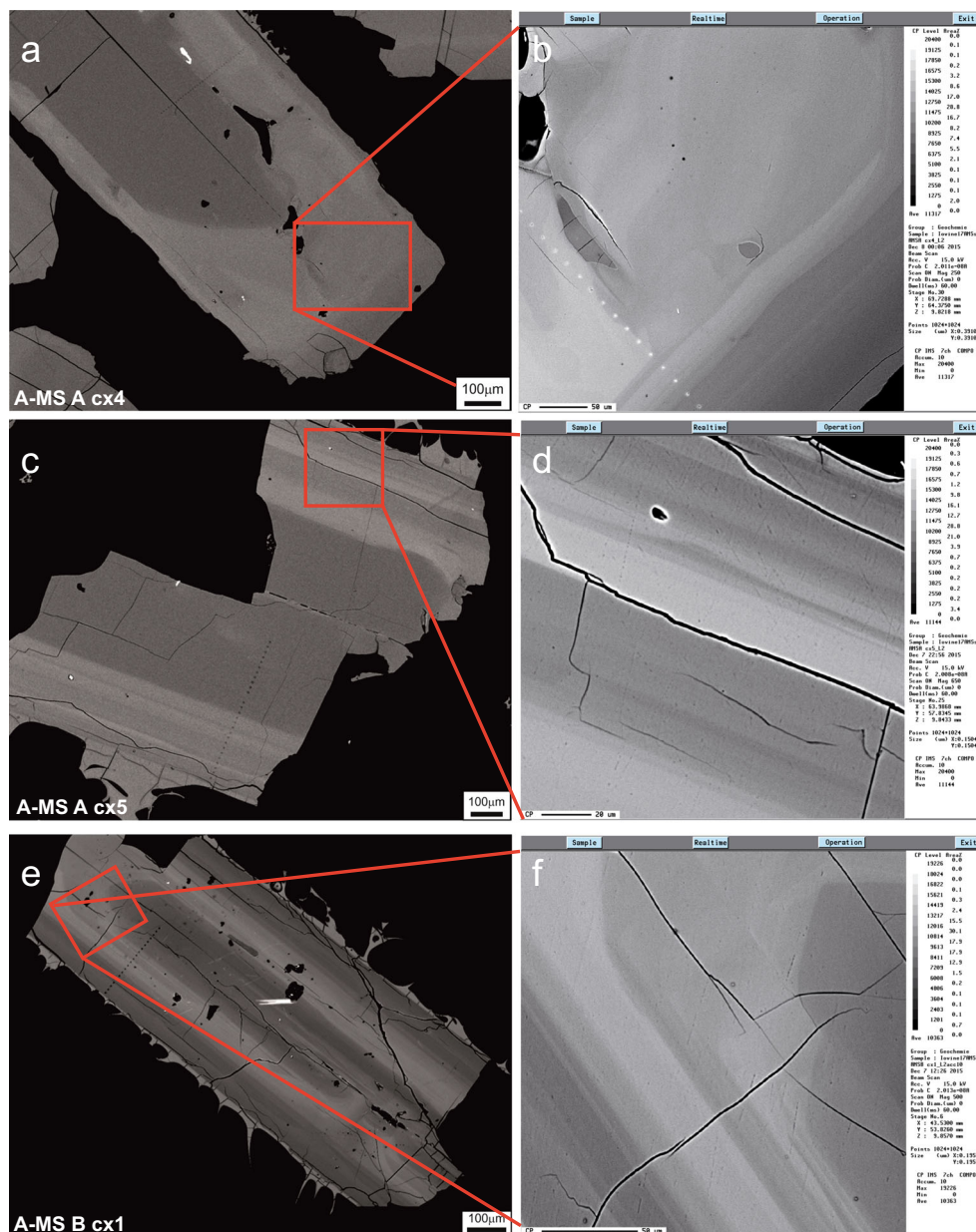
Measurements at GZG were done at 15-kV accelerating voltage, 15-nA beam current, and 10- μm beam size. Counting times were set to 15 s on the peak (60 s for Ba and Sr) and 5 s (30 s for

Ba and Sr) on the background. The following standards were used for calibration: albite for Na; anorthite for Si, Ca, and Al; sanidine for K; hematite for Fe; celsian for Ba; and SrTiO_3 for Sr. The relative standard deviation for major and minor elements, calculated using natural and synthetic standards, was below 2% for major oxides and $\sim 6\%$ for minor oxides. For the Ba, the absolute error (wt%) calculated is between 0.04 and 0.06 wt%.

Compositional discontinuities near the margins of sanidine crystals were mapped at GZG through accumulated BSE in COMPO-mode beam scans (accumulated BSE maps, Fig. 5a, b). Ten accumulations per image were successively acquired at 20-kV accelerating voltage and 20-nA beam current, with a slow scanning beam and acquisition time of 120 s per accumulation. The magnification was chosen based on zoning width and crystal size.

In addition, X-ray line scans for Ba were also acquired in COMPO-mode stage scan condition for selected crystals. Fifty accumulations per scan were acquired perpendicular to the outermost compositional break near the crystal rim at 10-kV accelerating voltage and 30-nA beam current, with an acquisition time of 2 s per pixel. Barium was analyzed simultaneously on three spectrometers using different types of Pentaerythritol (PETJ, normal sensitivity by JEOL, and

Fig. 3 Selected BSE (*left*) and detailed accumulated BSE (*right*) images (see “Analytical methods” section) of sanidine phenocrysts from A-MS eruption. **a** The crystal (AMS A cx5) has a darker (i.e., Ba-poorer) resorbed core and an inner rim with “swirly” zonation textures that indicate crystallization and dissolution. The outer rim is characterized by small-scale wavy oscillatory zoning that results from high-frequency growth and resorption events. Melt inclusions on the core-rim boundary of the crystal are evacuated (*black*), having been extruded by displacement due to vesicle formation inside the grain, demonstrating that the melt tubule was connected to the surrounding melt at the time of eruption. The zoomed image (**b**) shows remnant glass infiltrating along a cleavage plane crack in the *upper left*. **c** Crystal A-MS A cx5 shows an exceedingly complex oscillatory rim, more evident in the accumulated enlarged image (**d**). The oscillations are also documented in the grayscale profiles (Online Resource 1). **e, f** Crystal A-MS B cx1 is another example of spectacular complex zoning, more clearly visible in the zoomed image (**f**)



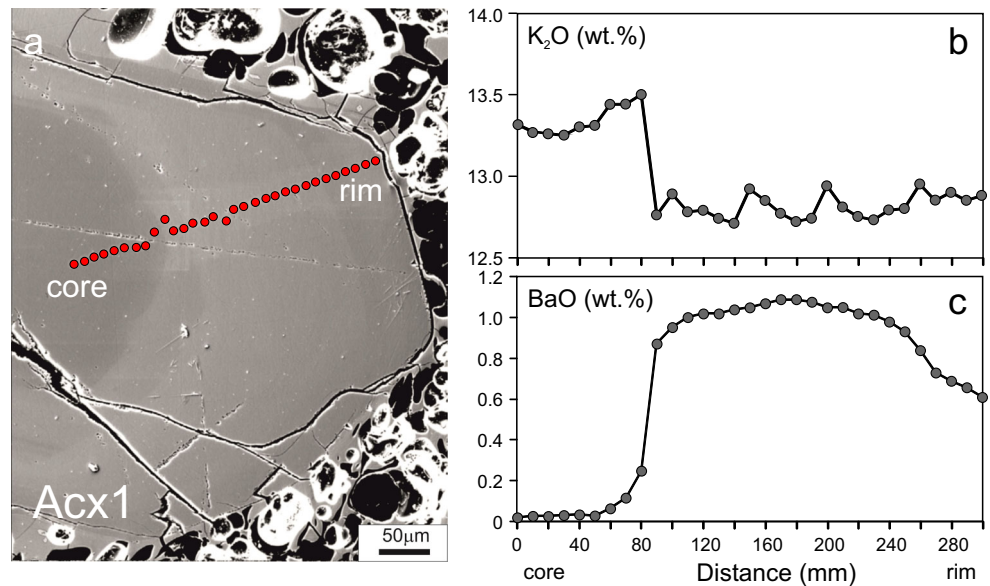
PETH, high sensitivity) crystals. Calculated diffusion times using Ba measured on each of the three spectrometers gave similar results; therefore, the results for Ba measured on channel 3 only will be utilized. X-ray line scans for K and Na were also measured to document their minor variation near the crystal rim. All EMP data, BSE images, accumulated maps, and X-ray scans are provided in Online Resources 1, 2, and 3.

Diffusion modeling and parameters

Barium diffusion modeling of zoning profiles across compositional discontinuities at the rim of selected phenocrysts followed methods previously described (Crank 1975; Morgan et al. 2004; Chamberlain et al. 2014). Three different

approaches were employed: (1) EMP quantitative analyses measured at 10-µm spatial resolution along a 100-µm transect across compositional profiles (Fig. 5c), (2) grayscale swath profiles extracted from accumulated BSE maps parallel to analytical traverses (red rectangle, Fig. 5b), and (3) X-ray line scans. The BSE grayscale profiles were processed using the ImageJ® software (Fig. 5d). The use of grayscale gradients assumes that grayscales are proportional to the Ba content of sanidine. We confirmed this relation between Ba contents and grayscale values quantitatively by a linear regression (R^2 of 0.975; Online Resource 4). All profiles were interpolated by a non-linear Boltzmann fit curve with the Mathematica® software. An initial Ba step function and a simple 1-D diffusion model for the relatively small diffusion length compared to the

Fig. 4 **a** Selected BSE image of an A-MS eruption sanidine (crystal A cx1) with trace of a compositional profile acquired by EMPA. **b** K₂O (wt%) and **c** BaO (wt%) variations along the core-rim profile



phenocryst size were assumed (Morgan et al. 2006). An angular correction ($<12^\circ$) was applied for a few traverses not crossing the interfaces at 90° , which is insignificant given other uncertainties involved. Diffusion constants and parameters are given in Fig. 5e, f.

Results

Composition of the analyzed sanidine phenocrysts

Sanidine phenocrysts from the A-MS pumice (members A, B, and D) are relatively homogeneous in composition ($An_{2-4}Ab_{16-25}Or_{71-82}$; Fig. 6; Online Resource 5), as previously described (de Vita et al. 1999). Sanidines from member D have a slightly wider compositional range and more K-rich ($An_{2-4}Ab_{16-19}Or_{78-82}$), less evolved compositions. On the other hand, sanidine from members A and B tend to be more evolved ($An_{2-4}Ab_{19-25}Or_{71-78}$; Figs. 4 and 6). Notwithstanding the overall major element homogeneity of these sanidines, core-to-rim BaO profiles commonly show normal-to-reverse-to-normal zoning and frequent resorption surfaces (Fig. 4b, c) that are ascribed to compositional and/or thermal variations or decompression-driven degassing in the magma during crystal growth (e.g., Ginibre et al. 2004; Blundy et al. 2006). Plagioclase with normal and reverse zoning was also analyzed ($An_{87-63}Ab_{12-32}Or_{1-6}$; Fig. 6; Online Resource 5) to calculate temperatures using the two-feldspar geothermometer.

Temperature constraints

Two-feldspar geothermometry (Putirka 2008) gave temperatures from 882 ± 26.5 to 973 ± 26.5 °C ($P = 100$ MPa; Online

Resource 5). This range is probably due to partial disequilibrium between minerals and glass caused by mixing between crystals of different origin and a slightly variable trachytic magma. Temperature estimates are also provided by phase equilibria experiments performed on A-MS samples by Roach (2005). The conditions that best reproduced the observed mineral assemblages, as well as melt and mineral compositions, are 900–950 °C at $P = 50$ –100 MPa and $fO_2 \sim NNO + 1.3$, assuming saturation with a 50:50 H₂O-CO₂ mixed fluid. Sanidine crystallization temperatures of less than 870 °C were observed only in a more evolved trachyte from the CI eruption (at $P = 20$ –200 MPa, $fO_2 = NNO + 0.8$ –1.0; Di Matteo et al. 2004; Fabbriozio and Carroll 2008; Fabbriozio et al. 2009). However, these low temperatures were found only for melts saturated with pure H₂O fluid. Since A-MS mineral-hosted melt inclusions have H₂O between 0.8 and 3.0 wt% and CO₂ from 150 to 500 ppm (Roach 2005; Arienzo et al. 2010), temperatures >870 °C are implied.

Another constraint for temperature may be provided by clinopyroxene, the most abundant phenocryst of A-MS rocks. Cpx-melt geothermometry (Putirka 2008 and references therein) on compositional data from the literature (de Vita et al. 1999) (Online Resource 5) yields temperatures in the range 1071–1156 °C, with an average uncertainty of ± 51 °C. These temperatures are much higher than those obtained on the feldspars, suggesting that clinopyroxene crystallized before the onset of sanidine crystallization, in agreement with textural evidence. Moreover, no clinopyroxene has passed the compositional test for equilibrium (Putirka 2008), implying that they grew in a more mafic melt and were subsequently introduced into the A-MS trachytic magma.

In summary, for the A-MS trachytes, temperatures are constrained by experiments to be between 870 and 950 °C, and by two-feldspar geothermobarometry to be between 882

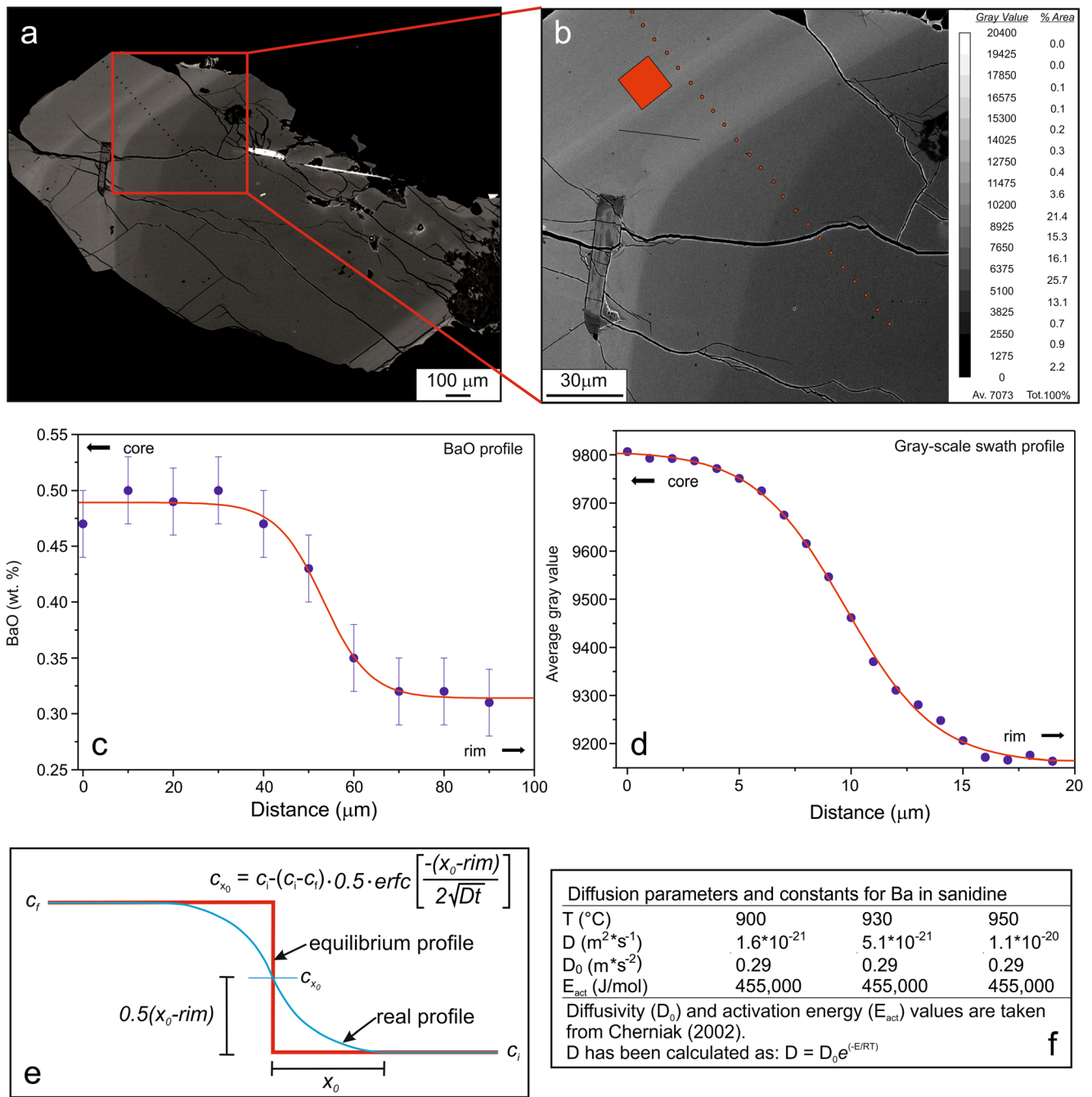


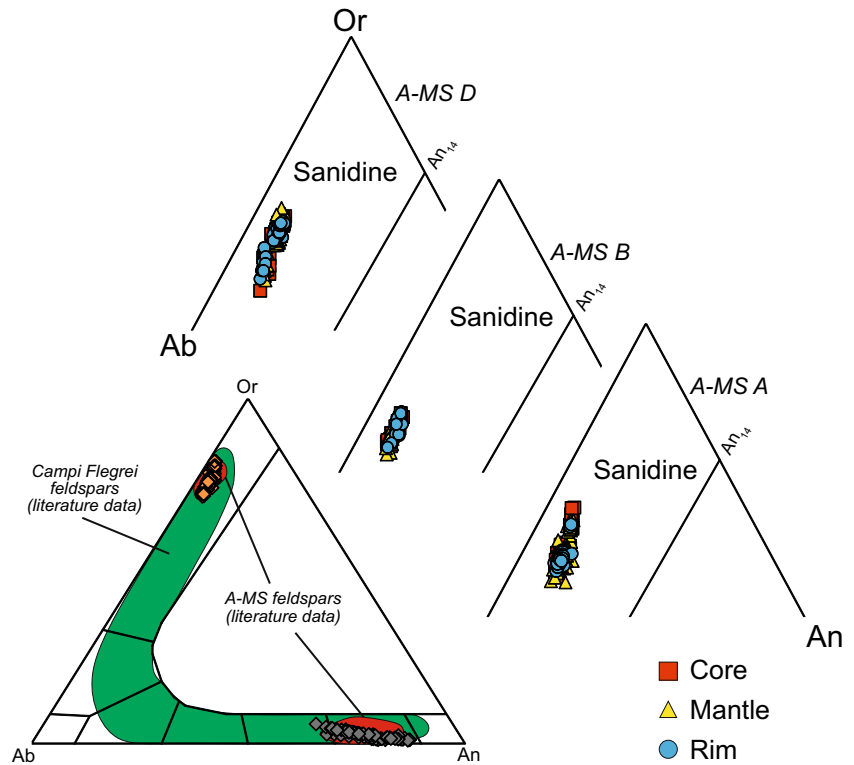
Fig. 5 **a** Accumulated BSE map of an A-MS sanidine (crystal B cx3). **b** Close-up view of **a**, showing in red the area on which the grayscale was determined. Profiles based on quantitative determination of BaO concentration (**c**) and swath profile based on gray scales (**d**) with interpolation obtained by Mathematica®. **e** Schematic diffusion profile showing

parameters of the equation used to extract timescales: c_i and c_f are initial and final BaO concentrations on each side of the interface, x_0 -rim is the half distance in micrometer along the profile, centered on the midpoint of the profile. **f** Diffusion constants (Cherniak 2002) and parameters for Ba in sanidine used in the modeling (see text for further details)

and 973 °C, with an average of 930 °C. Some of this range is probably caused by disequilibrium between minerals and glass, both of which are slightly variable in composition. A difference in temperature from 900 to 950 °C affects diffusion time estimates by 1–2 orders of magnitude. Given these uncertainties, we calculated diffusion timescales at temperatures of 900, 930, and 950 °C (Table 1), based on the range of

temperature recommended by Roach (2005) for A-MS trachytes. However, to facilitate the data presentation, we will refer in the subsequent discussion only to results of the 930 °C diffusion calculations, this intermediate value being also considered as the most reasonable crystallization temperature. Model results for 900 and 950 °C are presented in the Electronic Supplementary Material (Online Resource 7). Lower

Fig. 6 Classification diagram for A-MS sanidines (Online Resources 1, 2, and 3). Keys for end members: *Or* orthoclase, $K(Ba)AlSi_3O_8$; *An* anorthite, $CaAl_2Si_2O_8$; *Ab* albite, $Na(Sr)AlSi_3O_8$. *Green field*: feldspars from Campi Flegrei (Melluso et al. 2012). *Red field*: feldspars from A-MS (de Vita et al. 1999)



temperatures (<900 °C) yield unreasonably long timescales on the order of tens of thousands years and thus will not be presented because these are not consistent with the eruption history. Higher temperatures (950 °C) result in shorter diffusion times. In addition, other uncertainties, such as smoother profiles caused by geometric effects or compositional boundaries that may not have been completely vertical with respect to the thin section surface (see also discussion below), will result in higher apparent diffusion times in these cases. Thus, diffusion modeling at 930 °C should give maximum values.

Diffusion times

Calculations were carried out based on quantitative analysis of Ba concentrations, grayscale swath profiles, and X-ray scans (Online Resources 1, 2, and 3). The resulting times are listed in Table 1.

At 930 °C, BaO profiles yield diffusion time estimates in the range 8–980 years, whereas grayscale swath profiles provided time estimates in the range 1–171 years. Diffusion times extracted from X-ray line scans gave 2 to 20 years (Table 2). Comparison among results of the three different approaches shows that, for a given temperature, the timescales estimated from X-ray line scans and grayscale profiles are always much shorter than those derived from BaO profiles. The higher spatial resolution of grayscale and X-ray profiles results in steeper gradients, providing shorter values of diffusion time by almost an order of magnitude compared to profiles based on

quantitative point measurements at 10-µm spatial resolution. Because of this artifact, the shorter diffusion times derived from gray value swath profiles and X-ray profiles should be more reliable. There are examples where X-ray profiles are sharper than grayscale profiles. This is unexpected since the sample volume from which X-ray signals are derived should be larger than that of the BSE signal. The likely reason for some grayscale profiles being less sharp is that the grayscale profiles integrate an area over some distance along and across the compositional discontinuity, which could be uneven. In contrast, the X-ray profile crosses the boundary at a single point. In any case, the differences (in absolute years) of diffusion times calculated from the two types of profiles are small and the values reflect maximum times. For the discussion, we chose to refer only to diffusion times estimated from grayscale gradients.

Discussion

The results of the measured grayscale swath profiles can be subdivided into two groups (at 930 °C; Fig. 7a): about 80% of the profiles give short diffusion times of ≤60 years; the remaining 20% yield longer timescales up to 180 years. The first group of calculated ages, ≤60 years, is also the most likely, as illustrated by the cumulative frequency diagram (Fig. 7b); of these, about half are in the range of only 2–10 years, and the other half are in the range 10–60 years.

Chapter 4: Timescales of magmatic processes prior to the 4.7 ka Agnano-Monte Spina eruption (Campi Flegrei caldera, Southern Italy) based on diffusion chronometry from sanidine phenocrysts

Table 1 Timescale estimates for Agnano-Monte Spina sanidine phenocrysts derived from Ba diffusion models across selected transects, calculated at $T = 930$ °C

A-MS A	BaO profile	Grayscale profile	A-MS B	BaO profile	Grayscale profile	A-MS D	BaO profile	Grayscale profile
cx1	348		cx1	274		cx1	449	134
cx2	94		cx1_L1	130	4	cx3	1195	
cx3	62		cx1_L1 2°		2	cx3_L1	980	
cx4_L1	26		cx1_L2	997	23	cx3_L2		32
cx4_L2	897	16	cx1_L2 2°		4	cx4	35	
cx5	31	4	cx2_L1	192	5	cx5_L1	16	9
cx5_L2		9	cx2_L2	24	5	cx6_L1	15	151 ^a
cx5_L2 2°		1	cx3	267	33	cx6_L2	15	95 ^a
cx6	500	6	cx4_L1		57	cx7	38	8
cx10	609		cx4_L2	102		cx8_L1	164	1
cx12_L1	89	1	cx5_L1	22	31	cx8_L2	166	6
cx12_L1 2°		7	cx5_L2	39	8	cx8_L3	53	8
cx12_L2 2°		4	cx5_L3	29	7	cx9		13
cx12_L2 2°	104	8	cx7		45	cx10	49	101
cx13_L1	226	3	cx8_L1		2	cx11_L1		10
cx13_L1 2°		18	cx9_L1	31	123	cx11_L2	157	29
cx14_L1		5	cx9_L2	164		cx12_L1	41	3
cx14_L1 2°		4	cx9_L3	261		cx13_L1	102	44
cx14_L2	33	5	cx10_L1	44	15	cx13_L2	78	
cx15_L1	295	21	cx10_L1 2°		24	cx14	112	21
cx19_L1	45		cx10_L2		8			
cx19_L2	435	39	cx11	8				
cx20_L1	500	14	cx12		171			
cx20_L2		13	cx14	136				

^a Calculated on grayscale profile not close to the quantitative BaO profile. Numbers in italics indicate age estimates utilized for building the frequency histograms (Online Resource 6) and the cumulative frequency diagram of Fig. 7 and Online Resource 7 (see text for more details)

These age ranges have large errors due to temperature and diffusivity uncertainties. The five profiles that give longer timescales up to 180 years were likely not suitable for modeling because of non-vertical profile positions (Costa and Morgan 2011). We corrected for obliquely positioned profiles only in the horizontal plane of the crystals. Cutting the compositional interface obliquely to depth would also provide smoother profiles and longer timescales. Since it is impossible to rule out this case, these longer diffusion time estimates should be considered with caution.

It should be noted that the ages estimated from the A-MS feldspars are calculated based on the assumption that the shape of the initial profile was a sharp discontinuity (Fig. 5e). This assumption may not be correct, as it has been demonstrated in other cases (Till et al. 2012, 2015; Chamberlain et al. 2014) that an initially sharp profile is not consistent with the similarity of profiles (after diffusion) for elements with different diffusivities, such as Ba and Sr. If the starting profiles were not completely sharp, then our assumption of an initially sharp profile results in an overestimate of the timescale. Unfortunately, a better assessment of the initial

profile sharpness for the A-MS feldspars is not possible, given that the Sr content of these feldspars is too low and at the EMPA detection limit (Online Resources 1, 2, and 3). However, even though the high temperature for the A-MS feldspars implies Ba diffusion faster than in other silicic (e.g., rhyolitic) volcanic systems, we still obtain very short diffusion times, and if the gradients were not perfectly sharp initially, these short timescales are in fact maximum values.

The modeled compositional profiles relate to the last growth event highlighted by variable Ba content near the margin of the sanidine crystals that formed in response to the last recharge event before eruption, when crystallization effectively stopped. Thus, the calculated diffusion timescales relate only to processes that affected the last part of the sanidines, whereas the total “lifetime” of each crystal could be significantly older, as indicated by their complex textures (Figs. 3 and 4). For A-MS, there is no evidence for mixing magmas of vastly different major element compositions, and therefore—in agreement with earlier studies—we interpret these compositional profiles to result from mixing of more and less evolved trachytic magma, and that this mixing was the final

Table 2 Timescale estimates derived from X-ray scan profiles for selected Agnano-Monte Spina sanidine phenocrysts and comparison with time estimates derived from BaO and grayscale profiles, calculated at $T = 930\text{ }^{\circ}\text{C}$

	BaO profile	Grayscale profile	X-ray scan profile
Bcx1	274		5
Bcx2_L1	192	5	20
Bcx2_L1 2nd	192	5	23
Bcx9_L2	164		16
Bcx10_L1	44	15	4
Bcx10_L2		8	7
Dcx7	38	8	3
Dcx12_L1	41	3	2
Dcx12_L2			2

Numbers in italics indicate age estimates after eliminating multiple data on the same crystal (see text for more details)

event prior to the eruption and possibly its trigger. However, such mixing, sanidine resorption, and subsequent overgrowth prior to eruption could result from various processes: (i) recharge and mixing into a reservoir with a resident trachytic magma, likely crystal-rich and partially degassed, by a fresh, hotter, and volatile-rich trachytic magma; (ii) mixing of magmas within a compositionally-zoned reservoir during eruption; (iii) uptake of older cumulate crystals during intrusion and passage of a trachytic magma through a crystal mush pile. Cumulate sanidine crystals must be abundant within the CFc plumbing system as a result of fractional crystallization through time and during evolution of older magma batches (D’Antonio 2011). In all three scenarios, our calculated diffusion times relate to the interval between sanidine resorption after recharge/overtum/cumulate uptake and eruption.

Products of most CFc eruptions that occurred in the past ~5 kyr bear witness to magma mingling/mixing processes (e.g., de Vita et al. 1999; D’Antonio et al. 1999, 2007;

Tonarini et al. 2009; Arienzo et al. 2010, 2015, 2016; Di Renzo et al. 2011; Di Vito et al. 2011; Fourmentraux et al. 2012; Melluso et al. 2012). However, estimates for mixing times and ages of crystals based on direct U/Th mineral geochronology differ by orders of magnitude. Uranium-series isochrons show that some crystals in the large volume CI magma are more than 6 kyr older than the eruption age (Arienzo et al. 2011). Apparently, different approaches and different materials yield different ages, which cannot be directly compared. These old U–Th crystal ages possibly refer to a crystal cargo from a pre-eruptive crystallization event preceding the assembly and mixing of magmas, recorded by the bulk of the crystals. Our ages of a few tens up to 60 years (at 930 °C, Fig. 7) relate only to the time of diffusion after a mixing event (cases i and ii) or, possibly, the uptake of the older crystals (180 years). However, only clear-cut resorption interfaces with younger overgrowths are suitable for diffusion modeling since only these interfaces can be considered to represent initial condition of a distinct unconformity in the minerals’ composition. Complex oscillatory and reverse growth zonations throughout the crystal from core to rim, as interesting and informative as they may be for magma evolution, are poorly suited for extracting diffusion times that are related with processes that directly preceded the eruption. Thus, the apparent discrepancy between the old and young ages can be explained.

In order to put likely estimated timescales of tens of years into a geological context, the available volcanological and geochronological data on the activity of the Agnano-San Vito area need to be considered. Prior to the A-MS event and after a ~3.6-kyr-long quiescence marked by a thick, widespread paleosol (paleosol B; Di Vito et al. 1999), six low-energy eruptions occurred from vents located in this area (Figs. 1 and 8). According to available geochronological data, these events were clustered in two phases of activity separated by a ~300-year-long quiescence (Orsi et al. 2009 and references therein). The first phase lasted ~500 years and included three eruptions that emitted

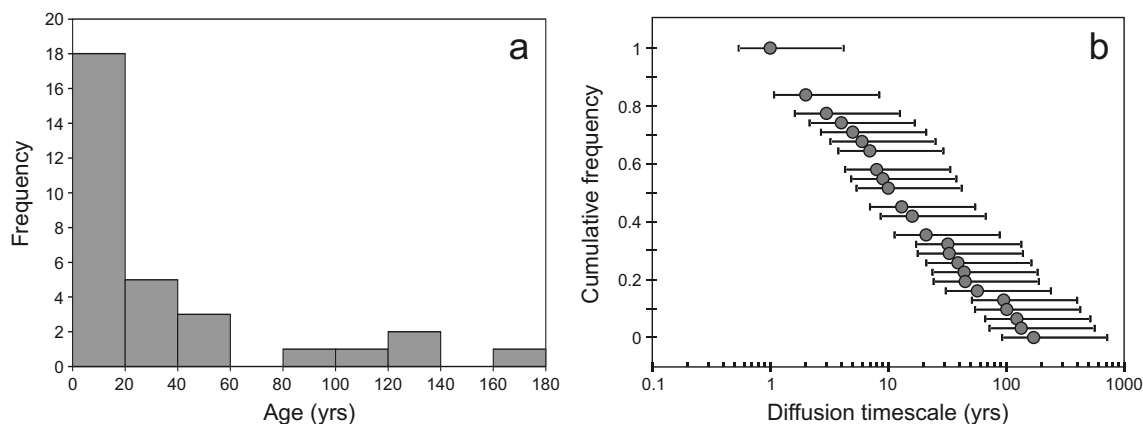


Fig. 7 Frequency histogram (a) and cumulative frequency diagram (b) for diffusion times estimated from 24 grayscale swath profiles at 930 °C (Table 1). The error bars consider an average temperature uncertainty of $\pm 26.5\text{ }^{\circ}\text{C}$ as resulting from two-feldspar geothermometry (Online Resource 5)

Fig. 8 Sketch of activity/ quiescence periods in the Agnano-San Vito area reconstructed on the basis of available volcanological and geochronological data. Magma volumes (DRE) and calibrated ^{14}C ages from Orsi et al. (2009). *N.a.* not available

eruption	volume (km ³ D.R.E.)	age (cal ka)	time span
Agnano-Monte Spina	0.854	4.67±0.09	
Palaeoastroni 2	0.010	4.71±0.07	~100 yr
Palaeoastroni 1	0.050	4.68±0.09	
Agnano 3	0.186	4.78±0.04	~300 yr
quiescence			
Monte Sant'Angelo	0.070	5.08±0.12	~500 yr
Agnano 2	0.014	n.a.	
Agnano 1	0.018	5.56±0.05	
Paleosol B			

altogether ~0.1 km³ of magma (DRE) (Agnano 1, Agnano 2, and Monte Sant'Angelo). The second phase of ~100-year duration was characterized by three eruptions (Agnano 3, Palaeoastroni 1, and Palaeoastroni 2) that emitted a total of ~0.25 km³ of magma (DRE). The three low-energy events in the second phase thus occurred in a time span of a few hundred years. Therefore, volcanological and geochronological data on the small-volume activity in the Agnano-San Vito area predating the Agnano-Monte Spina eruption suggest that the timescales estimated by diffusion chronology are similar to the average time interval between eruptions, and thus may represent the reactivation time of a magma that was residing in a shallow reservoir for some longer period of time. In this sense, reactivation times as measured here from diffusion modeling relate to the time between magma recharge and mixing and eventual eruption.

The volume of ~1 km³ of magma emitted by the A-MS eruption is relatively small compared to other larger eruptions in the area, such as the CI eruption, that emitted between 25 and >300 km³ of magma (DRE; Rosi et al. 1999; Fisher et al. 1993; Civetta et al. 1997; Fedele et al. 2007, 2016; Scarpati et al. 2014). The maximum age of crystal components that were involved in pre-eruptive mixing of the CI magmas has been estimated at 6.4 ± 2.1 kyr, based on U–Th isotope geochronology (Arienzo et al. 2011), indicating longer time spans for larger-volume eruptions. This is in agreement with recent studies showing that there is a relationship between the volume of magma and its residence time, well established in both plutonic and volcanic systems (e.g., Reid 2003; de Saint Blanquat et al. 2011). It should be noted, however, that magma residence times and crystal residence times are not necessarily the same. Even more important, an entire crystal must be older than its outer rim (which we study here). However, magmas and the bulk of the crystals may both have long residence times, whereas the process that rejuvenates the magma and triggers an eruption can be comparatively short and recorded in late overgrowths on older crystals. If a resident

magma with its old crystals becomes rejuvenated frequently within short time intervals, then the erupted volume of magma is likely to be small because small but frequent triggers are expected to give small and frequent eruptions. This is because small and infrequent recharges are likely to be unable to rejuvenate resident magma that has cooled and crystallized for a long time. So, no eruption occurs until a larger recharge arrives that would then cause a large (infrequent) eruption. A short timescale on the order of decades or centuries for the late overgrowth on older sanidines is therefore in agreement with the small magma volume erupted at A-MS.

Small magma batches that were erupted through time and space within the CF caldera also tend to have distinct major and trace elements (e.g., D'Antonio et al. 1999; Pappalardo et al. 1999, 2002; Pabst et al. 2008; Arienzo et al. 2009; Fourmentraux et al. 2012; Melluso et al. 2012). However, mixing components between distinct magma batches can be identified and traced to magmas that were erupted at different times from different craters (Pabst et al. 2008; Tonarini et al. 2009; Di Renzo et al. 2011; Di Vito et al. 2011; Arienzo et al. 2015, 2016). Therefore, there is likely to be some physical connection between the reservoirs from which magmas were evacuated. Moreover, there is evidence from zoning in sanidines that these crystals had a complex (and longer) history compared to the outermost zonation/resorption interfaces that we studied here (Fig. 3). Therefore, the history of individual magma batches should be longer than the time between eruptions. This implies that magma reservoirs should be larger in volume and longer lived than what is represented by individual eruptions. Thus, our diffusion times are shorter than the lifetime of magma in the reservoir. This excludes the possibility that erupted volumes represent reservoir size and that timescales extracted from our diffusion modeling simply reflect periods of filling and evacuation of the reservoir.

Conclusions

We applied diffusion chronometry to sanidine crystals from samples of the ~4.7 ka Agnano-Monte Spina eruption from the CF caldera, focusing on the last resorption and crystallization event prior to eruption. Profiles were measured by quantitative BaO point measurements, swath profiles based on BSE grayscale values, and Ba X-ray scans. Quantitative concentration profiles yield distinctly longer diffusion times due to their lower spatial resolution. Thus, diffusion time estimates from grayscale swath profiles are more reliable.

Diffusion times calculated at 930 °C (the most likely temperature) are mostly ≤ 60 years. Volcanological and geochronological data for the Agnano-San Vito area show that at least six eruptions occurred in a few centuries before the A-MS eruption. The available data suggest that the timescales estimated by diffusion chronology are similar to the inferred time intervals that occurred between eruptions, and thus, the diffusion timescales may represent the reactivation time of a magma that was residing in a shallow reservoir after the influx of a new magma batch that triggered the eruption. Such short timescales thus represent the final reactivation/remobilization of a magma from shallow depth in the A-MS plumbing system after longer residence. The range of estimated timescales is skewed to shorter values (see the cumulative frequency plot, Fig. 7b) and given the fact that our estimates are likely to be maximum values, the actual timescale between the recharge triggering event and eventual eruption may be within the lower part of the 2–60-year range. Our results suggest that pre-eruptive warning times of renewed activity, which may be expressed in deformation, gas discharge, and seismic events, could be relatively short.

Acknowledgments This study is part of the framework of “Project V2—Precursori di Eruzioni,” funded to M.D. by the Dipartimento per la Protezione Civile (DPC)—Istituto Nazionale di Geofisica e Vulcanologia (2013–2015), of DFG project Wo 362/42-1 funded to G.W., and of DAAD-MIUR Joint Mobility Program no. 57266092 funded to G.W. and M.D. This paper does not necessarily represent DPC official opinions and policies. T. Di Rocco, L. Francalanci, A. Kronz, D. Perugini, and M. Petrelli are thanked for analytical support and discussions. We are very grateful to the Associate Editor P.J. Wallace, as well as D. Morgan and a second anonymous reviewer, for their constructive comments and suggestions. D. Morgan is also acknowledged for his kind assistance in elaboration of the cumulative frequency plot.

References

Arienzo I, Civetta L, Heumann A et al (2009) Isotopic evidence for open system processes within the Campanian Ignimbrite magma chamber. *Bull Volcanol* 71:285–300

Arienzo I, Moretti R, Civetta L et al (2010) The feeding system of Agnano-Monte Spina eruption (Campi Flegrei, Italy): dragging the past into the present activity and future scenarios. *Chem Geol* 270(1–4):135–147

Arienzo I, Heumann A, Wörner G et al (2011) Processes and timescales of magma evolution prior to the Campanian Ignimbrite eruption (Campi Flegrei, Italy). *Earth Planet Sci Lett* 306:217–228

Arienzo I, D’Antonio M, Di Renzo V et al (2015) Isotopic microanalysis sheds light on the magmatic endmembers feeding volcanic eruptions: the Astroni 6 case study (Campi Flegrei, Italy). *J Volcanol Geotherm Res* 304:24–37

Arienzo I, Mazzeo FC, Moretti R et al (2016) Open-system magma evolution and fluid transfer at Campi Flegrei caldera (Southern Italy) during the past 5 ka as revealed by geochemical and isotopic data: the example of the Nisida eruption. *Chem Geol* 427:109–124

Blundy J, Cashman K, Humphreys M (2006) Magma heating by decompression-driven crystallization beneath andesite volcanoes. *Nature* 443:76–80

Capuano P, Russo G, Civetta L et al (2013) The active portion of the Campi Flegrei caldera structure imaged by 3D inversion of gravity data. *Geochim Geophys Geosys* 14:4681–4697

Chakraborty S (2008) Diffusion in solid silicates: a tool to track timescales of processes comes of age. *Annu Rev Earth Planet Sci* 36: 153–190

Chamberlain KJ, Morgan DJ, Wilson CJN (2014) Timescales of mixing and mobilisation in the bishop tuff magma body: perspectives from diffusion chronometry. *Contrib Mineral Petrol* 167:1034

Cherniak DJ (2002) Ba diffusion in feldspar. *Geochim Cosmochim Acta* 66:1641–1650

Chiodini G, Vandemeulebroeck J, Caliro S et al (2015) Evidence of thermal-driven processes triggering the 2005–2014 unrest at Campi Flegrei caldera. *Earth Planet Sci Lett* 414:58–67

Civetta L, Orsi G, Pappalardo L et al (1997) Geochemical zoning, mingling, eruptive dynamics and depositional processes—the Campanian Ignimbrite, Campi Flegrei Caldera, Italy. *J Volcanol Geotherm Res* 75:183–219

Cooper KM, Kent AJR (2014) Rapid remobilization of magmatic crystals kept in cold storage. *Nature* 506:480–483

Cooper KM, Reid MR (2008) Uranium-series crystal ages. *Rev Mineral Geochem* 69:479–544

Costa F, Morgan D (2011) Time constraints from chemical equilibration in magmatic crystals. In: Dosseto A, Turner SP, Van Orman JA (eds) *Timescales of magmatic processes: from core to atmosphere*. Blackwell Publishing Ltd, pp 125–159

Costa F, Dohmen R, Chakraborty C (2008) Time scales of magmatic processes from modeling the zoning patterns of crystals. *Rev Mineral Geochem* 69:545–594

Crank J (1975) *The mathematics of diffusion*, 2nd edn. Oxford University Press, Oxford, p 414

D’Antonio M (2011) Lithology of the basement underlying the Campi Flegrei caldera: volcanological and petrological constraints. *J Volcanol Geotherm Res* 200:91–98

D’Antonio M, Civetta L, Orsi G et al (1999) The present state of the magmatic system of the Campi Flegrei caldera based on a reconstruction of its behavior in the past 12 ka. *J Volcanol Geotherm Res* 91:247–268

D’Antonio M, Tonarini S, Arienzo I et al. (2007) Components and processes in the magma genesis of the Phlegrean Volcanic District, southern Italy. In: Beccaluva L, Bianchini G, Wilson M (eds.). *Cenozoic volcanism in the Mediterranean area*. *Geol Soc Am Spec Pap* 418, Geol Soc Am, Boulder, CO, pp 203–220

D’Auria L, Pepe S, Castaldo R et al (2015) Magma injection beneath the urban area of Naples: a new mechanism for the 2012–2013 volcanic unrest at Campi Flegrei caldera. *Sci Rep* 5:13100. doi:10.1038/srep13100

de Saint Blanquat M, Horsman E, Habert G et al (2011) Multiscale magmatic cyclicality, duration of pluton construction, and the paradoxical relationship between tectonism and plutonism in continental arcs. *Tectonophysics* 500:20–33

- de Vita S, Orsi G, Civetta L et al (1999) The Agnano–Monte Spina eruption (4100 years BP) in the restless Campi Flegrei caldera (Italy). *J Volcanol Geotherm Res* 91:269–301
- De Vivo B, Rolandi G, Gans PB et al (2001) New constraints on the pyroclastic eruptive history of the Campanian Volcanic Plain (Italy). *Mineral Petrol* 73:47–65
- Deino AL, Orsi G, de Vita S, Piochi M (2004) The age of the Neapolitan Yellow Tuff caldera-forming eruption (Campi Flegrei caldera—Italy) assessed by $^{40}\text{Ar}/^{39}\text{Ar}$ dating method. *J Volcanol Geotherm Res* 133:157–170
- Del Gaudio C, Aquino I, Ricciardi GP et al (2010) Unrest episodes at Campi Flegrei: a reconstruction of vertical ground movements during 1905–2009. *J Volcanol Geotherm Res* 195:48–56
- Di Matteo V, Carroll MR, Behrens H et al (2004) Water solubility in trachytic melts. *Chem Geol* 213:187–196
- Di Renzo V, Arienzo I, Civetta L et al (2011) The magmatic feeding system of the Campi Flegrei caldera: architecture and temporal evolution. *Chem Geol* 281:227–241
- Di Vito MA, Isaia R, Orsi G et al (1999) Volcanism and deformation since 12,000 years at the Campi Flegrei caldera (Italy). *J Volcanol Geotherm Res* 91:221–246
- Di Vito MA, Arienzo I, Braia G et al (2011) The Averno 2 fissure eruption: a recent small size explosive event at the Campi Flegrei caldera. *Bull Volcanol* 73:295–320
- Fabbrizio A, Carroll MR (2008) Experimental constraints on the differentiation process and pre-eruptive conditions in the magmatic system of Phlegraean Fields (Naples, Italy). *J Volcanol Geotherm Res* 171:88–102
- Fabbrizio A, Scaillet B, Carroll MR (2009) Estimation of pre-eruptive magmatic water fugacity in the Phlegraean Fields, Naples, Italy. *Eur J Mineral* 21:107–116
- Fedele FG, Giaccio B, Isaia R et al. (2007) The Campanian Ignimbrite factor: towards a reappraisal of the Middle to Upper Palaeolithic “transition”, in: Grattan J, Torrence R (eds) *Living under the shadow: the cultural impacts of volcanic eruptions*. One World Archaeology Series, 53, Left Coast Press, Walnut Creek, CA, pp 19–41
- Fedele L, Scarpati C, Lanphere M et al (2008) The Breccia Museo formation, Campi Flegrei, southern Italy: geochronology, chemostratigraphy and relationship with the Campanian Ignimbrite eruption. *Bull Volcanol* 70:1189–1219
- Fedele L, Zanetti A, Morra V et al (2009) Clinopyroxene/liquid trace element partitioning in natural trachytetrachyphonolite systems: insights from Campi Flegrei (southern Italy). *Contrib Mineral Petrol* 158:337–356
- Fedele L, Insinga DD, Calvert AT et al (2011) $^{40}\text{Ar}/^{39}\text{Ar}$ dating of tuff vents in the Campi Flegrei caldera (southern Italy): toward a new chronostratigraphic reconstruction of the Holocene volcanic activity. *Bull Volcanol* 73:1323–1336
- Fedele L, Insinga DD, Calvert AT et al (2012) Reply to the comment on the article “ $^{40}\text{Ar}/^{39}\text{Ar}$ dating of tuff vents in the Campi Flegrei caldera (southern Italy): toward a new chronostratigraphic reconstruction of the Holocene volcanic activity” by Isaia et al. *Bull Volcanol* 74:297–299
- Fedele L, Lustrino M, Melluso L et al (2015) Trace-element partitioning between plagioclase, alkali feldspar, Ti-magnetite, biotite, apatite, and evolved potassic liquids from Campi Flegrei (Southern Italy). *Am Mineral* 100:233–249
- Fedele L, Scarpati C, Sparice D et al (2016) A chemostratigraphic study of the Campanian ignimbrite eruption (Campi Flegrei, Italy): insights on magma chamber withdrawal and deposit accumulation as revealed by compositionally zoned stratigraphic and facies framework. *J Volcanol Geotherm Res* 324:105–117
- Fisher RV, Orsi G, Ort M, Heiken G (1993) Mobility of large-volume pyroclastic flow emplacement of the Campanian Ignimbrite, Italy. *J Volcanol Geotherm Res* 56:205–220
- Fourmentraux C, Métrich N, Bertagnini A, Rosi M (2012) Crystal fractionation, magma step ascent, and syn-eruptive mingling: the Averno 2 eruption (Phlegraean Fields, Italy). *Contrib Mineral Petrol* 163(6):1121–1137
- Gebauer SK, Schmitt AK, Pappalardo L et al (2014) Crystallization and eruption ages of Breccia Museo (Campi Flegrei caldera, Italy) plutonic clasts and their relation to the Campanian ignimbrite. *Contrib Mineral Petrol* 167:953
- Ginibre C, Wörner G, Kronz A (2004) Structure and dynamics of the Laacher See magma chamber (Eifel, Germany) from major and trace element zoning in sanidine: a cathodoluminescence and electron microprobe study. *J Petrol* 45(11):2197–2223
- Isaia R, Di Vito MA, de Vita S et al (2012) Comment on “ $^{40}\text{Ar}/^{39}\text{Ar}$ dating of tuff vents in the Campi Flegrei caldera (southern Italy): toward a new chronostratigraphic reconstruction of the Holocene volcanic activity” by Fedele et al. [*Bull Volcanol* 73:1323–1336]. *Bull Volcanol* 7:293–296
- Mangiaccapra A, Moretti R, Rutherford M et al (2008) The deep magmatic system of the Campi Flegrei caldera (Italy). *Geophys Res Lett* 35: L21304. doi:10.1029/2008GL035550
- Melluso L, De’ Gennaro R, Fedele L et al (2012) Evidence of crystallization in residual, Cl-F-rich, agpaitic, trachyphonolitic magmas and primitive Mg-rich basalt-trachyphonolite interaction in the lava domes of the Phlegraean Fields (Italy). *Geol Mag* 149(3):532–550
- Morgan DJ, Blake S, Rogers NW et al (2004) Time scales of crystal residence and magma chamber volumes from modelling of diffusion profiles in phenocrysts: Vesuvius 1944. *Earth Planet Sci Lett* 222: 933–946
- Morgan DJ, Blake S, Rogers NW et al (2006) Magma chamber recharge at Vesuvius in the century prior to the eruption of A.D. 79. *Geology* 34:845–848
- Orsi G, de Vita S, Di Vito MA (1996) The restless, resurgent Campi Flegrei nested caldera (Italy): constraints on its evolution and configuration. *J Volcanol Geotherm Res* 74:179–214
- Orsi G, Di Vito MA, Isaia R (2004) Volcanic hazard assessment at the restless Campi Flegrei caldera. *Bull Volcanol* 66:514–530
- Orsi G, Di Vito MA, Selva J, Marzocchi W (2009) Long-term forecast of eruption style and size at Campi Flegrei caldera (Italy). *Earth Planet Sci Lett* 287:265–276
- Pabst S, Wörner G, Civetta L, Tesoro R (2008) Magma chamber evolution prior to the Campanian ignimbrite and Neapolitan Yellow Tuff eruptions (Campi Flegrei, Italy). *Bull Volcanol* 70:961–976
- Pappalardo L, Civetta L, D’Antonio M et al (1999) Chemical and Sr–isotopic evolution of the Phlegraean magmatic system before the Campanian Ignimbrite and the Neapolitan Yellow Tuff eruptions. *J Volcanol Geotherm Res* 91:141–166
- Pappalardo L, Piochi M, D’Antonio M et al (2002) Evidence for multi-stage magmatic evolution during the past 60 kyr at Campi Flegrei (Italy) deduced from Sr, Nd and Pb isotopic data. *J Petrol* 43(8):1415–1434
- Perugini D, De Campos CP, Petrelli M, Dingwell DB (2015) Concentration variance decay during magma mixing: a volcanic chronometer. *Sci Rep* 5:14225. doi:10.1038/srep14225
- Putirka K (2008) Thermometers and barometers for volcanic systems. *Rev Mineral Geochem* 69:61–120
- Reid MR (2003) Timescales of magma transfer and storage in the crust. *Treatise on Geochemistry* 3:167–193
- Roach AL (2005) The evolution of silicic magmatism in the post-caldera volcanism of the Phlegraean Fields, Italy. Unpublished PhD Thesis, Department of Geological Sciences, Brown University, Providence, Rhode Island (USA), pp 171
- Rosi M, Vezzoli L, Grieco G (1999) Plinian pumice fall deposit of the Campanian ignimbrite eruption (Phlegraean Fields, Italy). *J Volcanol Geotherm Res* 91(2–4):179–198
- Ruprecht P, Cooper KM (2012) Integrating the uranium-series and elemental diffusion geochronometers in mixed magmas from Volcán Quizapu, Central Chile. *J Petrol* 53(4):841–871

Chapter 4: Timescales of magmatic processes prior to the 4.7 ka Agnano-Monte Spina eruption (Campi Flegrei caldera, Southern Italy) based on diffusion chronometry from sanidine phenocrysts

- Saccorotti G, Petrosino S, Bianco F et al (2007) Seismicity associated with the 2004–2006 renewed ground uplift at Campi Flegrei Caldera, Italy. *Phys Earth Planet Int* 165:14–24
- Scarpati C, Perrotta A, Lepore S, Calvert A (2013) Eruptive history of Neapolitan volcanoes: constraints from $^{40}\text{Ar}/^{39}\text{Ar}$ dating. *Geol Mag* 150:412–425
- Scarpati C, Sparice D, Perrotta A (2014) A crystal concentration method for calculating ignimbrite volume from distal ash-fall deposits and a reappraisal of the magnitude of the Campanian Ignimbrite. *J Volcanol Geotherm Res* 280:67–75
- Schmitt AK (2011) Uranium series accessory crystal dating of magmatic processes. *Annu Rev Earth Planet Sci* 39:321–349
- Selva J, Orsi G, Di Vito MA et al (2012) Probability hazard map for future vent opening at the Campi Flegrei caldera. *Italy Bull Volcanol* 74: 497–510
- Smith VC, Isaia R, Pearce NJG (2011) Tephrostratigraphy and glass compositions of post-15 kyr Campi Flegrei eruptions: implications for eruption history and chronostratigraphic markers. *Quat Sci Rev* 30:3638–3660
- Till CB, Vazquez JA, Boyce JW, Hitzman C (2012) Quantifying the interval between rejuvenation and eruption of rhyolite at Yellowstone caldera using high-resolution NanoSIMS geospeedometry. Abstract V43E-01 presented at 2012 Fall Meeting, AGU, San Francisco, California, 3–7 Dec
- Till CB, Vazquez JA, Boyce JW (2015) Months between rejuvenation and volcanic eruption at Yellowstone caldera, Wyoming. *Geology* 43:695–698. doi:10.1130/G36862.1
- Tonarini S, D’Antonio M, Di Vito MA et al (2009) Geochemical and isotopic (B, Sr, Nd) evidence for mixing and mingling processes in the magmatic system feeding the Astroni volcano (4.1–3.8 ka) within the Campi Flegrei caldera (South Italy). *Lithos* 107:135–151
- Turner S, Costa F (2007) Measuring timescales of magmatic evolution. *Elements* 3:267–272

5 Conclusions

5.1 Introduction

This work provides new information on the complex plumbing system beneath the Neapolitan region. One of the largest points that this study has hopefully raised is to constrain the time between reactivation and eruption of magma batches in the Campi Flegrei caldera, focusing on the type-event for a large-size eruption in case of renewal of volcanism in short-mid terms at the caldera. The other issue is the understanding of the role and the relative importance of sediment subduction versus crustal assimilation in magmatism of the Campanian volcanic district. The relationship between magma compositions and tectonic setting depends on reliably distinguishing among geochemical features that image the source region and those that resulted from magma evolution during transport. Processes affecting magmas after their genesis are important in characterizing the behaviour of the magmatic supply system. Such processes, for example, *fractional crystallization*, can produce highly evolved magmas, which when associated with long-lived magma storage in the crust can generate high magnitude explosive events. *Recharge* of distinct magma batches from deeper levels within the feeding reservoir may be required to trigger volcanic eruptions. *Crustal contamination* requires chemical exchange between magma and wall rocks that can lead to fluid enrichment, increasing the possibility of highly explosive eruptions or can induce quick cooling and/or crystallization of magma limiting its further mobility. Properly identifying the exact mechanism of magma evolution, i.e. magma mixing or crustal contamination, can be a useful tool for hazard assessment studies. For the Phlegrean magmas contamination processes by carbonate crustal rocks, still debated in the literature (e.g., D'Antonio, 2011) can now be safely excluded. The basic principles that should be conveyed to the people living in a volcanic area are about the nature of volcanic phenomena, their effects and the distance at which they are relevant. People should have knowledge of the area where they live and of the necessary measures that should be taken in case of unrest, not only by the Civil Protection, but also by individuals. They should know the forecast limits and be ready to adopt individual escape measures in case of failure of prediction. For many years scientists have warned the civil authorities of the potential risk of volcanic activity in the Neapolitan area, even if in their efforts they may have over-emphasized the true relevance of volcanic phenomena, thus creating a syndrome of an inescapable catastrophe and the need for strict measures to prevent it. Planning for emergency should be carried out by state agencies, which should clearly state the real effect of volcanic activity, and the measures that can be taken by individuals to reduce the risk. At the same time, the possible failure of emergency planning has to be presumed, and the rules for behavior be suggested for individuals who may find themselves

within an area already affected by volcanic phenomena. Apart from a deadly earthquake which hit the Italian island of Ischia in August, the Naples region has been relatively quiet for the past four decades, but this area hidden off the coast of Italy is so huge that it has the power to change life on Earth.

5.2 Findings

The key findings of this study are summarised in the subsections below.

5.2.1 Ischia plumbing system

The knowledge of the magmatic processes active during the evolution of the recent Ischia plumbing system is crucial to predict its future behavior. The overall petrochemical and Sr-O isotopic characteristics of the Arso eruption (the last one occurred on the Ischia island) products, along with those of the other known latitic products (Vateliero, Molaro and Cava Nocelle) emplaced at Ischia island about 3 ka BP in the same structural position, suggest a common history. The Sr-O isotopic variability support the hypothesis that mafic magmas of this period are generated in a mantle source region modified by addition of ~1% of subducted sediments and later modified by crustal assimilation of Hercynian metaplutonic rocks from the overlying continental crust (up to 7%). The recent latitic eruptions emplaced small volumes of products (<1 km³; de Vita et al., 2010). Thus, it is more likely that small batches of distinct magmas of deep provenance mixed during their ascent towards the surface, intercepting mineral residues left by previous eruptions. Such mixing and mingling processes are well recognizable through the Sr-isotopic signature of the endmembers, implying magma interaction rates much faster than the eruption rate. All this implies that, even during the present quiescence of the volcano, a small batch of magma coming from the source can reach the shallow plumbing system. Here, mixing of this fresh magma with either a resident magma residue, if any, or a crystal mush might induce ground deformation, seismicity and change in fumarole activity over short timescale, although still detectable at surface.

5.2.2 Neapolitan magmatic system

Data obtained in this work show compositions that are very different from typical mantle values and that span a very large range towards heavy $\delta^{18}\text{O}_{\text{melt}}$ values compared to other magmatic compositions from the Italian Peninsula and subduction zone worldwide. Distinct trends and sources are recognized in the compilation from global data: (1) serpentized mantle (Kamchatka), (2) sediment-enrichment in the mantle source (Indonesia, Lesser Antilles, Eolian arc), (3) assimilation of old radiogenic continental crust affecting magmas derived from sediment-modified

mantle sources (Tuscany, Sardinia), (4) assimilation of lower crustal lithologies (Central Andes, Alban Hills, Mts. Ernici, Ischia). Data suggest that all Neapolitan magmas, derived from distinct sources representing different magma batches that change systematically through time, have suffered crustal contamination to largely different extents and that the Campi Flegrei magma system is quite distinct also from Somma Vesuvius magmas. However, Campi Flegrei and Somma Vesuvius magmas at least fall on the same vertical trend in O-Sr isotope space that deviates profoundly from all other subduction-related magmas. Only a scenario that involves a mantle source that was modified by the addition of up to 10% of subducted sediments (pelagic sediments and limestone) could be an explanation for high $\delta^{18}\text{O}_{\text{melt}}$ values in mafic rocks with Mg# up to 70. Such a scenario of mixing different components prior to melting has recently been developed by Nielsen and Marschall (2017), who argued that arc magmatism is sourced by a mixture of lithologies in the subducted melange. Assimilation of Hercynian crust (at a maximum of 12 and 21%) is restricted to highly evolved trachytic to phonolitic magmas of Campi Flegrei and Somma Vesuvius, respectively.

5.2.3 Magma residence times from diffusion chronometry

The zoning patterns of crystals are a valuable tool to reconstruct processes occurred in a magmatic system prior to eruption. In particular detailed analyses of the mineral zoning and modeling based on chemical diffusion laws allow to determinate the durations of magmatic processes, providing important constraints for volcanic hazard of active volcanoes. Indeed evidence of magma recharge or mixing events is commonly preserved as complex zoning and/or resorption surfaces in crystals while they grow in a magma chamber. The study focused on the compositional break near the crystal rim because the most external rim of a phenocryst, relate to resorption and regrowth, is featured by variable Ba content at the final stage of crystallization just prior to eruption (the latest stage of mixing as a likely eruption triggering process). In order to test the best methodology for calculating Ba diffusion residence time three different approaches were employed for Agnano Monte Spina sanidine phenocrysts: (1) electron microprobe quantitative analyses measured at 10 μm spatial resolution along a short transect approximately 100 μm across compositional profiles, (2) numerical gray-scale swath profiles extracted from accumulated Back Scatter Electron (BSE) maps parallel to analytical traverses, and (3) X-ray line scans. BSE gray-scale profiles were processed using ImageJ® software. The higher spatial resolution of gray-scale and X-ray profiles results in steeper gradients, providing lower estimates of diffusion time by almost an order of magnitude compared to profiles based on quantitative point measurements at 10 μm spatial resolution. Because of this artefact, the shortest diffusion times derived from gray-value swath

profiles and X-ray line scans should be more reliable. Diffusion times calculated at 930°C are mostly ≤ 60 years. The results are strictly dependent on the temperature because a difference of 50°C affects diffusion time estimates by 1-2 orders of magnitude.

5.3 Outlook

$\Delta^{17}\text{O}$ variations have been studied for the first time in order to assess the role of limestone assimilation in the evolution of the Campi Flegrei magmatic system. To exclude unequivocally the carbonate nature of the Phlegrean assimilated oxygen measurements should be conducted on the limestone. The line used for oxygen extraction is equipped with suitable valves and traps for the efficient recovery of oxygen from the silicate minerals and reliable handling of hazardous oxidants (i.e., BrF_5 , etc.) that are used as fluorination agents to break Si=O bonds. This extraction system is interfaced with a continuous flow stable isotope ratio mass spectrometer and is being used successfully for the oxygen isotopic measurements in silicates but not in carbonates. Further development of this system is under progress to extend it for the measurements of carbonate rocks also.

While magma residence times have been constrained for sanidine phenocrysts, there are many gaps in the evolutionary sequence of the magmas. Due to uncertainties about temperature-time paths over long timescales, diffusional analysis of only sanidine is probably not fully informative. It will therefore be useful to i) obtain information on timescale of pre-eruptive magmatic processes by modelling the diffusion of Ba-Sr, Fe-Mg in feldspar and pyroxene crystals from the same eruption ii) combine this information with those on recharge and mixing/mingling events, highlighted by Sr-isotopic microanalysis study, and iii) eventually relate the recognized pre-eruptive magmatic processes and their timescales to precursor phenomena described in the available historical sources. This integrative study will permit a better understanding of the behavior of the magmatic systems feeding the Neapolitan volcanoes.

5.4 References

D'Antonio M (2011) Lithology of the basement underlying the Campi Flegrei caldera: volcanological and petrological constraints. *J Volcanol Geoth Res* 200: 91–98.

de Vita S, Sansivero F, Orsi G, Marotta E, Piochi M (2010) Volcanological and structural evolution of the Ischia resurgent caldera (Italy) over the past 10 k.y. In: Groppelli, G., Viereck-Goette, L. (Eds.), *Stratigraphy and Geology of Volcanic Areas: Boulder, CO. Geol Soc Am Spec Pap* 464: 193–241.

Nielsen SG, Marschall HR (2017) Geochemical evidence for mélangé melting in global arcs. *Sci Adv* 3(4): 1-7. Doi.10.1126/sciadv.1602402.

Appendix A: Curriculum vitae

Raffaella Silvia Iovine

Date of birth: 15.09.1988

Place of birth: Naples (Italy)

Scientific education

- 28/06/2007** **ABITUR** (Virgilio, Pozzuoli Naples)
- 24/02/2011** **BACHELOR OF SCIENCES** (Geological Sciences)
Thesis: ‘Geochimica isotopica dei prodotti dell’eruzione dell’Arso (1302 A.D.), isola d’Ischia; Isotopic geochemistry of the products of the Arso eruption (1302 AD), Ischia Island’.
Supervisors: Prof. Dr. Lucia Civetta, Prof. Dr. Giovanni Orsi and Dr. Ilenia Arienzo
- 24//10/2013** **DIPLOMA** (Geology and Applied Geology)
Thesis: ‘Geochemical and isotopic studies of the Popocatepetl’s (Mexico) Ochre Pumice eruption (4965 yr B.P.) to define processes and the structure of the magmatic feeding system’.
Supervisors: Prof. Dr. Lucia Civetta, Prof. Dr. Giovanni Orsi and Dr. Ilenia Arienzo
- 01/2014 – 02/2018** **DOCTORATE** at the Geoscience Center Göttingen.
Thesis: ‘Source and magmatic evolution of the Neapolitan volcanoes through time (Southern Italy)’.
Supervisors: Prof. Dr. Gerhard Wörner, Prof. Dr. Massimo D’Antonio and Prof. Dr. Andreas Pack

Scientific experience

- 05/2011-08/2011 Scholarship at the Istituto Nazionale di Geofisica e Vulcanologia sezione di Napoli Osservatorio Vesuviano, Naples, Italy to define the

structure and the evolution of the magmatic system of the Ischia volcano (South Italy), by performing geochemical and isotopic (Sr and Nd) investigations and melt inclusions studies. Supervisors: Prof. Dr. Lucia Civetta, Prof. Dr. Giovanni Orsi and Dr. Ilenia Arienzo

Short courses

- | | |
|---------|---|
| 08/2015 | Application of diffusion studies to the determination of timescales in geochemistry and petrology. Bochum |
| 02/2017 | MATLAB Recipes for Earth Sciences. Potsdam |

Appendix B: Articles

Published

Iovine RS, Mazzeo FC, Arienzo I, D'Antonio M, Wörner G, Civetta L, Pastore Z, Orsi G (2017) Source and magmatic evolution inferred from geochemical and Sr-O-isotope data on hybrid lavas of Arso, the last eruption at Ischia island (Italy; 1302 AD). *Journal of Volcanology and Geothermal Research*, 331. Doi:10.1016/j.jvolgeores.2016.08.008.

Iovine RS, Fedele L, Mazzeo FC, Arienzo I, Cavallo A, Wörner G, Orsi G, Civetta L, D'Antonio M (2016) Timescales of magmatic processes occurred prior to the ~4.7 ka Agnano-Monte Spina eruption (Campi Flegrei caldera, Southern Italy) based on diffusion chronometry on sanidine phenocrysts. *Bulletin of Volcanology*, 79(2). Doi: 10.1007/s00445-017-1101-4.

Mazzeo FC, De Vita P, Aulinas M, Arienzo I, Cirillo G, **Iovine RS**, Sparice D (2016). New constraints on the origin of the ophiolitic rocks within sinorogenic turbiditic sequences at Cilento region (southern Italy) *Geologica Acta*, vol. 14, n 3.

Submitted

Iovine RS, Mazzeo FC, Wörner G, Arienzo I, Pelullo C, Cirillo G, Pack A, D'Antonio M (16.12.2017) Coupled $\delta^{18}\text{O}$ - $\delta^{17}\text{O}$ and $^{87}\text{Sr}/^{86}\text{Sr}$ isotope compositions suggest a radiogenic and ^{18}O -enriched magma source for Neapolitan volcanoes (Southern Italy). *Lithos*.

In preparation

Iovine RS, Wörner G, Mazzeo FC, Fedele L, Arienzo I, D'Antonio M (2017). Magma residence times from diffusion chronology on zoned alkali feldspar phenocrysts from the Campanian Ignimbrite (39 ka), Campi Flegrei caldera (Napoli, southern Italy).

Pelullo C, Mazzeo FC, Cirillo G, **Iovine RS**, Arienzo I, Aulinas M, Turiel JLF, D'Antonio M (2017). Magmatic processes inferred from geochemical and Sr-Nd-O isotopic data on the Zaro lava complex (<5 ka), Ischia island (Southern Italy).

Arienzo I, Di Vito MA, D'Antonio M, Mazzeo FC, **Iovine RS**, Cavallo A, Carandente A, Orsi G, Civetta L. A 10.3 ka old stratigraphic marker: The Pomice Principali Plinian eruption in the Campi Flegrei caldera (Napoli, southern Italy).

Conference abstracts

Cirillo G, Arienzo I, Mazzeo FC, Paonita A, Rizzo A, Petrosino P, Pelullo C, **Iovine RS**, D'Antonio M (2017). Sr-He-O isotopes in mafic phenocrysts from products of the Neapolitan Volcanoes (Southern Italy): constraints on the geochemical features of the mantle sources. SIMP Congress 2017, Pisa, September 3-6. Poster

Iovine RS, Wörner G, Pack A, Sengupta S, Mazzeo FC, Arienzo I, D'Antonio M (2017). Triple oxygen isotope composition of the Campi Flegrei magma systems. General Assembly 2017, Vienna, Austria, April 23- 28, Geophys. Res. Abstr, 19, EGU2017-4479. Poster

Iovine RS, Wörner G, Fedele L, Mazzeo FC, Arienzo I, Civetta L, Orsi G, D'Antonio M (2017). Ba-zonation modelling on sanidine phenocrysts from the Agnano-Monte Spina Eruption (4.7ka), Campi Flegrei caldera (Napoli, southern Italy). IODP/ICDP Kolloquium 2017, Braunschweig, Germany, March 14-16, 2017. Poster

Iovine RS, Mazzeo FC, Arienzo I, D'Antonio M, Wörner G, Civetta L, Pastore Z, Orsi G (2016). Sr-O-isotopic data on hybrid volcanic rocks of Arso, the last eruption occurred at Ischia island (Italy; 1302 AD). INGV Naples, September 20. Talk

Iovine RS, Mazzeo FC, Arienzo I, D'Antonio M, Wörner G, Civetta L, Pastore Z, Orsi G (2016). Sr-O-isotopic data on hybrid volcanic rocks of Arso, the last eruption occurred at Ischia island (Italy; 1302 AD). SIMP Congress 2016, Naples, September 6-9. Talk

Iovine RS, Wörner G, Mazzeo FC, D'Antonio M, Arienzo I, Fedele L, Civetta L, Orsi G (2016). Magma residence times from diffusion chronology on zoned alkali feldspar phenocrysts from the Agnano-Monte Spina Eruption (4.7 ka), Campi Flegrei caldera (Napoli, southern Italy). SIMP Congress 2016, Naples, September 6-9. Poster

Wörner G, **Iovine RS**, Mazzeo FC, D'Antonio M, Arienzo I, Civetta L, Orsi G (2016). Sr-O isotope systematics in the Campi Flegrei magma systems. Naples, September 6-9. Talk

Iovine RS, Wörner G, Mazzeo FC, Arienzo I, Fedele L, Civetta L, D'Antonio M, Orsi G (2016). Residence times of alkali feldspar phenocrysts from the Agnano-Monte Spina Eruption (4.7 ka), Campi Flegrei caldera (Napoli, southern Italy) based on Ba-zonation modelling. EGU General Assembly 2016, Vienna, Austria, April 17- 22, Geophys. Res. Abstr, 18, EGU2016-5080. Talk

Wörner G, **Iovine RS**, Mazzeo FC, D'Antonio M, Arienzo I, Civetta L, Orsi G (2016). Sr-O isotope systematics in the Campi Flegrei magma systems. EGU General Assembly 2016, Vienna, Austria, April 17- 22, Geophys. Res. Abstr, 18, EGU2016-13463. Poster

Iovine RS, Wörner G, Mazzeo FC, Arienzo I, Civetta L, D'Antonio M, Orsi G (2016). The Campi Flegrei volcano (Napoli, southern Italy): $^{87}\text{Sr}/^{86}\text{Sr}$ - $\delta^{18}\text{O}$ systematics and magma residence times. IODP/ICDP Kolloquium 2016, Heidelberg, Germany, March 14-16, 2016. Poster

Iovine RS, Wörner G, Pabst S, Arienzo I, Civetta L, D'Antonio M, Orsi, G (2015). The history of the Campi Flegrei (Napoli, Italy) magma system through time: the key to understand present and future volcanic processes. IODP/ICDP Kolloquium 2015, Bonn, Germany, March 2-4, 2015. Poster

D'Antonio M, Arienzo I, Fedele L, **Iovine RS**, Mazzeo F.C, Civetta L, Orsi G, Wörner G (2015). Timescales of magma processes occurred prior to recent Campi Flegrei caldera eruptions: first results from diffusion profiles on plagioclase phenocrysts. EGU General Assembly 2015, Vienna, Austria, April 12- 17, Geophys. Res. Abstr, 17, EGU2015-9570. Talk

Mazzeo FC, Fedele L, **Iovine RS**, Arienzo I, Cavallo A, D'Antonio M (2015). Timescales of mixing from diffusion chronometry on alkali feldspar phenocrysts from the Agnano-Monte Spina Eruption (4.7 ka), Campi Flegrei (southern Italy). SIMP Congress 2015, Florence, September 2-5. Talk

Appendix C: Supplementary material

Supplementary material of the three papers is provided in digital form. The attached DVD contains .docx, .xlsx, .pdf and .jpeg files available online or submitted. An overview on file names and the respective content is given here:

[*Paper Arso, Supplementary material.xlsx*]: The complete dataset of chemical composition of analyzed minerals and mass balance modeling (available online at <http://dx.doi.org/10.1016/j.jvolgeores.2016.08.008>).

[*Paper Neapolitan volcanoes, Tables.xlsx*]: Tables of the paper including a list of analyzed samples, geochemical and Sr- O isotope results and modeling parameters (submitted to Lithos, 16.12.2017).

[*Paper Neapolitan volcanoes, References.xlsx*]: References related to the file "*Paper Neapolitan volcanoes, Tables.xlsx*" (submitted to Lithos 16.12.2017).

[*Paper Agnano Monte Spina, ESM_1.xlsx*]: EMP data, BSE images, accumulated maps, and X-ray scans for selected sanidines of Member A (available online at <https://doi.org/10.1007/s00445-017-1101-4>).

[*Paper Agnano Monte Spina, ESM_2.xlsx*]: EMP data, BSE images, accumulated maps, and X-ray scans for selected sanidines of Member B (available online at <https://doi.org/10.1007/s00445-017-1101-4>).

[*Paper Agnano Monte Spina, ESM_3.xlsx*]: EMP data, BSE images, accumulated maps, and X-ray scans for selected sanidines of Member D (available online at <https://doi.org/10.1007/s00445-017-1101-4>).

[*Paper Agnano Monte Spina, ESM_4.jpeg*]: A linear regression between Ba contents and grayscale values, showing the equation and its parameters (available online at <https://doi.org/10.1007/s00445-017-1101-4>).

[*Paper Agnano Monte Spina, ESM_5.xlsx*]: Temperature estimates obtained through two-feldspar geothermometry on plagioclase-sanidine pairs, and Cpx-melt geothermometry (available online at <https://doi.org/10.1007/s00445-017-1101-4>).

[*Paper Agnano Monte Spina, ESM_6.docx*]: Time estimates calculated for temperatures of 900, 930 and 950 °C (available online at <https://doi.org/10.1007/s00445-017-1101-4>).

[*Paper Agnano Monte Spina, ESM_7.pdf*]: Frequency histograms for all age estimates based on the three methodologies, calculated for temperatures of 900, 930 and 950 °C (available online at <https://doi.org/10.1007/s00445-017-1101-4>).